

University of New Mexico

UNM Digital Repository

Mechanical Engineering ETDs

Engineering ETDs

Spring 4-9-2021

Fundamental dislocation solutions for infinite and semi-infinite media

Luo Li Mr

University of New Mexico - Main Campus

Follow this and additional works at: https://digitalrepository.unm.edu/me_etds



Part of the [Materials Science and Engineering Commons](#), and the [Mechanical Engineering Commons](#)

Recommended Citation

Li, Luo Mr. "Fundamental dislocation solutions for infinite and semi-infinite media." (2021).
https://digitalrepository.unm.edu/me_etds/205

This Thesis is brought to you for free and open access by the Engineering ETDs at UNM Digital Repository. It has been accepted for inclusion in Mechanical Engineering ETDs by an authorized administrator of UNM Digital Repository. For more information, please contact disc@unm.edu.

Luo Li

Candidate

Mechanical Engineering

Department

This thesis is approved, and it is acceptable in quality and form for publication:

Approved by the Thesis Committee:

Tariq Khraishi

, Chairperson

Yu-Lin Shen

Pankaj Kumar

**FUNDAMENTAL DISLOCATION SOLUTIONS FOR INFINITE
AND SEMI-INFINITE MEDIA**

BY

LUO LI

B.S., Mechanical Engineering, Zhuhai, Beijing Institute of
Technology, 2016

THESIS

Submitted in Partial Fulfillment of the
Requirements for the Degree of

**Master of Science
Mechanical Engineering**

The University of New Mexico
Albuquerque, New Mexico

May, 2021

ACKNOWLEDGEMENTS

I heartily acknowledge Dr. Tariq Khraishi, my advisor and committee chair, for encouraging me through the years of classroom teachings and the long number of months writing and rewriting these chapters. His guidance and professional instruction will remain with me as I continue my career.

I also appreciate my committee members, Dr. Yu-Lin Shen and Dr. Pankaj Kumar for their valuable recommendations pertaining to this study and assistance in my professional development.

To Abu Bakar Siddique, for the verification results and guidance in my study, thank you.

And finally to my family, I am grateful to all your support.

FUNDAMENTAL DISLOCATION SOLUTIONS FOR INFINITE AND SEMI-INFINITE MEDIA

by

Luo Li

B.S., Mechanical Engineering, Zhuhai, Beijing Institute of Technology, 2016

M.S., Mechanical Engineering, University of New Mexico, 2021

ABSTRACT

Much research has gone into determining stress fields of dislocation, as the understanding of dislocations is fundamental to understanding metal or crystal plasticity. In this thesis, the stress field of a rectangular dislocation loop in an infinite isotropic solid is developed for a Volterra-type dislocation with three non-zero Burgers vector components. Also, the stress and strain fields of a rectangular dislocation loop in an isotropic solid, which is a semi-infinite medium, are obtained here for a Volterra-type dislocation. Moreover, analytical and numerical verifications of the developed stress/strain fields are performed. This is done by ensuring the satisfaction of the equilibrium equations and the strain compatibility equations. The results of this paper add to the knowledge base of elastic fields of dislocation loops and has its own application.

Table of Contents

FUNDAMENTAL DISLOCATION SOLUTIONS FOR INFINITE AND SEMI-INFINITE MEDIA.....	iv
Chapter 1 Introduction	1
Chapter 2 The Stress Field of a Rectangular Dislocation Loop in an Infinite Medium: Analytical Solution with Verification.....	2
ABSTRACT	2
INTRODUCTION	3
INTEGRATION OF THE PEACH-KOEHLER (PK) EQUATION.....	5
RESULTS AND DISCUSSION	9
Equilibrium Equations Verification.....	10
Strain Compatibility Equations Verification.....	12
Comparison with Devincere Formula.....	13
CONCLUSIONS.....	17
APPENDIX	18
REFERENCES	21
Chapter 3 The Strain/Stress Fields of a Subsurface Rectangular Dislocation Loop Parallel to the Surface of a Half Medium: Analytical Solution with Verification.....	24
ABSTRACT	24
INTRODUCTION	25
Elastic Fields of a Sub-Surface Rectangular Dislocation Loop.....	28
RESULTS AND DISCUSSION	32
Stress Traction on the Free Surface	32
Equations of Equilibrium	34
Strain Compatibility Equations.....	35
Comparison with the numerical “collocation point” method.....	37
CONCLUSIONS.....	40
APPENDICES	41
REFERENCES	48

Chapter 4 Strain Field Development of a Rectangular Dislocation Loop in a Semi-Infinite Medium with Verification.....	51
ABSTRACT	51
INTRODUCTION	52
METHODOLOGY	54
Development of the strains of the sub-surface rectangular dislocation loop	54
RESULTS AND DISCUSSION	58
Strain Compatibility Equations Verification.....	58
Equilibrium Equations Verification	60
Free-Traction Condition on the Free Surface	62
Normalized Plots for the Stress Field of a Subsurface Rectangular Dislocation Loop	62
CONCLUSIONS	69
APPENDIX	70
REFERENCES	78

Chapter 1 Introduction

Dislocations are line defects, around which the atoms of the crystal lattice are misaligned. For a rectangular dislocation closed loop, there are four linear dislocation segments composing the loop. The stress field of a rectangular dislocation loop in an infinite isotropic solid is developed in Chapter 2 for a Volterra-type dislocation with three non-zero Burgers vector components. In addition, the stress/strain fields of a rectangular dislocation loop in an isotropic solid, which is a semi-infinite medium, are obtained in Chapter 3 for a Volterra-type dislocation. To be specific, the stress field of the dislocation loop in an infinite isotropic material (Chapter 2) is obtained by integrating the Peach-Koehler equation over a rectangular perimeter. On the other hand, the stress field of the dislocation loop parallel and beneath to the free surface is developed by integrating the displacement equation of infinitesimal dislocation loops over a finite rectangular dislocation loop, then utilizing the tensorial small strain equation and Hooke's law for isotropic material (Chapter 3). Chapter 4 integrates the strain equation instead of the displacement equation for infinitesimal dislocation loops. Analytical and numerical verifications of the developed stress field are performed herein, which is done by ensuring the satisfaction of the equilibrium equations and the strain compatibility equations. Moreover, a comparison with the stress field of a Volterra-type dislocation loop composed of four dislocation segments, using DeVincre's formula, is presented in Chapter 2. In addition, the effect of the free surface on stresses is displayed versus depth from the surface in Chapter 4. Furthermore, a comparison with a new numerical method for the problem of dislocations near a free surface is performed in Chapter 3.

Chapter 2 The Stress Field of a Rectangular Dislocation Loop in an Infinite Medium: Analytical Solution with Verification

ABSTRACT

The stress field of a rectangular dislocation loop in an isotropic solid, which is in an infinite medium, is obtained here for a Volterra-type dislocation which has three non-zero Burgers vector components. Explicitly, the stress field of the dislocation loop in an infinite isotropic material is developed by integrating the Peach-Koehler equation over a finite rectangular dislocation loop. In this work, analytical/numerical verification of the stress field is demonstrated. To be specific, the verification is carried out to ensure that both the Equilibrium Equations and the Strain Compatibility Equations are satisfied. Moreover, a comparison with the stress field of a rectangular loop summed as four dislocation segments, using the DeVincre formula, is performed. Due to analytical verification, no error was detected in the presented solution. Also, comparing with the DeVincre formula presented identical results, qualitatively and quantitatively.

Keywords: Rectangular dislocation loop; infinite isotropic material; stress field; numerical/analytical verification.

INTRODUCTION

A rectangular dislocation loop is a closed loop formed by four linear dislocation segments. Dislocation lines cannot end inside a material. They have to end on free surfaces, grain boundaries, or form a close loop inside a material [1]. In this work, the development of the stress field of a Volterra-type rectangular dislocation loop is focused on.

The stress solution obtained in this paper facilitates in the development of three-dimensional dislocation dynamics codes [2-3]. The 3D discrete dislocation dynamics (DDD) simulation codes are able to capture the collective interaction of a whole population of curved dislocation lines in a mass of crystalline material on a mesoscopic scale, and to predict mechanical macroscopic behavior out of this interaction. In these codes, a contiguous and curved dislocation line in 3D is discretized in one form or another. One approach is to replace the dislocation line with straight finite-length segments of mixed character [3]. Another approach, followed by [4] is to decompose every segment into two perpendicular segments which are a screw segment and an edge segment. The stress field of the original dislocation curve is then approximated by the additive sum (from the principle of linear superposition) of the self-stresses of the segments composing the curve. Formulae for the self-stress of a straight dislocation segment of mixed character has been given by [5], and by [6].

Different kinds of dislocation problems in terms of material type, geometry and size have been investigated for decades. In the early years, research on infinite isotropic materials was focused on by different researchers. Derivations for the displacement, strain and stress fields of infinite screw and edge dislocations in an infinite medium, assuming material isotropy, were provided [6-8]. Moreover, integral equations for finding the displacement field (the Burgers equation) and the stress field (the Peach-Koehler equation) of a closed dislocation loop

(of any shape) in an infinite isotropic material have been provided by [6].

Several researchers have studied different kinds of the dislocation loop problems using various techniques. Initially, [9-10] investigated the prismatic circular loop. The circular glide loop was initially investigated by [11-12]. This solution was later corrected in [13-14]. In a more recent study of the displacement and stress fields of glide and prismatic circular dislocation loops, [15-16] corrected some earlier work. The displacement field, including the solid angle term, of a rectangular dislocation loop of the Volterra type in an infinite medium was developed by [17]. One utility for dislocation loops is its use in the “collocation point” method used to solve traction-free surface problems simulated with the 3-D method via a surface mesh of dislocation loops, see [18-21]. As for circular dislocation loops, they were used for modeling pile-ups around rigid cylindrical particles [22] and for modeling Frank sessile loops which result from irradiation damage in some metals [23, 24, 25].

If the Burgers vector is not constant in space, with respect to an inertial coordinate system, but rather varies along the dislocation line, the dislocation is then of the Somigliana type. Work on the ring Somigliana ring dislocation was performed by [26-27] for a radial Burgers vector, and by [28] for a tangential Burgers vector (i.e. a torsional dislocation loop).

In this chapter, the stress field of rectangular dislocation loop in an infinite isotropic material is developed by integrating the Peach-Koehler equation over a finite rectangular dislocation loop. Also presented are analytical and numerical verifications of the analytical solution obtained here. Furthermore, a comparison of the stress field developed here and the stress field obtained using the DeVincre Formula [5] is performed. The analytical results here add to the knowledge base of solutions for dislocations of different geometries. It has direct applications in Eigenstrain theory/computations [29] and the collocation-point method for capturing the effect of free surfaces on dislocation forces/motion [30].

INTEGRATION OF THE PEACH-KOEHLER (PK) EQUATION

The dislocation problem under consideration is shown in Fig. 1. The figure shows a rectangular dislocation loop (also described as a “finite-sized dislocation loop”) in an infinite isotropic medium. This Volterra-type dislocation loop has three Burgers vector components b_x , b_y and b_z , and has a dimension $2a$ in the x -direction and a dimension $2b$ in the y -direction. The line sense of the dislocation loop is shown by the arrow along the dislocation loop. The goal in this problem is to obtain the stress components for an arbitrary material field point P. Note that in this paper x_1 and x are used interchangeably, so are x_2 and y , and so are x_3 and z . Analogously for x'_1 and x' , and so on.

The PK Equation (1) is an integral equation for the stress field of any curved closed dislocation loop [6]. It is composed of three terms. They are all line integrals and they sum the contributions of infinitesimal line lengths (dl') along the line sense of the loop:

$$\sigma_{\alpha\beta} = -\frac{G}{8\pi} \oint_C b_m \epsilon_{im\alpha} \frac{\partial}{\partial x'_i} \nabla'^2 R dx'_\beta - \frac{G}{8\pi} \oint_C b_m \epsilon_{im\beta} \frac{\partial}{\partial x'_i} \nabla'^2 R dx'_\alpha - \frac{G}{4\pi(1-\nu)} \oint_C b_m \epsilon_{imk} \left(\frac{\partial^3 R}{\partial x'_i \partial x'_\alpha \partial x'_\beta} - \delta_{\alpha\beta} \frac{\partial}{\partial x'_i} \nabla'^2 R \right) dx'_k; \quad (1)$$

$$\sigma_{\alpha\beta} \text{term1} = -\frac{G}{8\pi} \oint_C b_m \epsilon_{im\alpha} \frac{\partial}{\partial x'_i} \nabla'^2 R dx'_\beta; \quad (2)$$

$$\sigma_{\alpha\beta} \text{term2} = -\frac{G}{8\pi} \oint_C b_m \epsilon_{im\beta} \frac{\partial}{\partial x'_i} \nabla'^2 R dx'_\alpha; \quad (3)$$

$$\sigma_{\alpha\beta} \text{term3} = -\frac{G}{4\pi(1-\nu)} \oint_C b_m \epsilon_{imk} \left(\frac{\partial^3 R}{\partial x'_i \partial x'_\alpha \partial x'_\beta} - \delta_{\alpha\beta} \frac{\partial}{\partial x'_i} \nabla'^2 R \right) dx'_k; \quad (4)$$

Where $\sigma_{\alpha\beta}$ is the $\alpha\beta^{\text{th}}$ component of the stress tensor σ , b_m is the m^{th} component of the displacement vector $\vec{b} = \mathbf{b} = (b_x, b_y, b_z)$, δ_{ij} is the ij^{th} component of the Kronecker delta, G is the shear modulus, ϵ is the permutation symbol, ν is Poisson's ratio, $R = \sqrt{(x' - x)^2 + (y' - y)^2 + (z' - z)^2}$ (see Fig. 1) and $\nabla'^2 R = 2/R$.

For integration of the Peach-Koehler Equation, some steps need to be considered for the rectangular loop in Figure 1 which is composed of four numbered segments/sides. First, the elevation of the dislocation loop above the xy -plane is fixed in the xyz global coordinate system, which means the value of z' is constant in this case or $dz' = 0$. Second, x' is a constant equal to $+a$ along segment 1, which means $dx' = 0$ along this segment. Analogously, $x' = -a$ and $dx' = 0$ along segment 3, $y' = +b$ and $dy' = 0$ along segment 2, $y' = -b$ and $dy' = 0$ along segment 4.

For the sake of illustration, only the integration for σ_{xz} for a non-zero b_z is shown as an example of the integration of the PK Equation:

$$\sigma_{xz} term1 = -\frac{G}{8\pi} \oint_C b_z \epsilon_{izx} \frac{\partial}{\partial x_i'} \frac{2}{R} dz' = 0; (dz' = 0) \quad (5)$$

$$\sigma_{xz} term2 = -\frac{G}{8\pi} \oint_C b_z \epsilon_{izz} \frac{\partial}{\partial x_i'} \frac{2}{R} dx' = 0; (\epsilon_{izz} = 0) \quad (6)$$

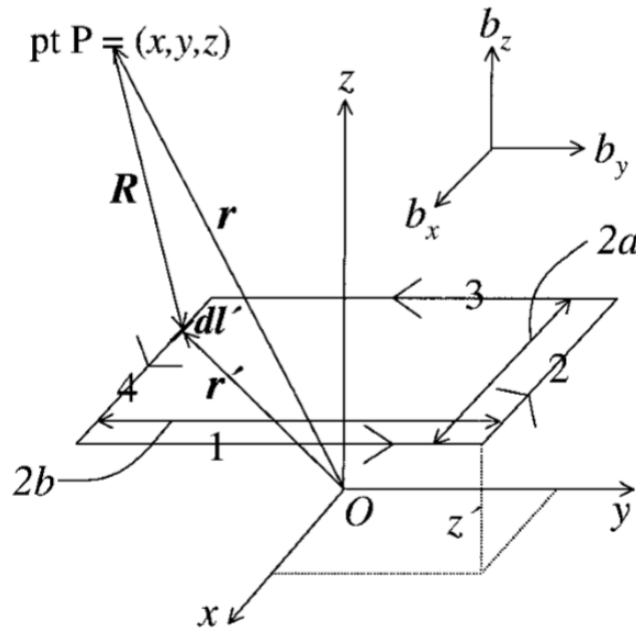


Fig. 1. The geometry of a rectangular dislocation loop in an infinite material. Here $\vec{r}' = r' = (x', y', z')$. The primed quantities belong to a differential length dl' on the dislocation loop

$$\begin{aligned} \sigma_{xz} term3 &= -\frac{G}{4\pi(1-\nu)} \oint_C b_z \epsilon_{xzy} \left(\frac{\partial^3 R}{\partial^2 x' \partial z'} - \delta_{xz} \frac{\partial}{\partial x'} \frac{2}{R} \right) dy' - \frac{G}{4\pi(1-\nu)} \oint_C b_z \epsilon_{yzx} \left(\frac{\partial^3 R}{\partial y' \partial x' \partial z'} - \right. \\ &\left. \delta_{xz} \frac{\partial}{\partial y'} \frac{2}{R} \right) dx' = \frac{G}{4\pi(1-\nu)} \oint_C b_z \left(\frac{\partial^3 R}{\partial^2 x' \partial z'} \right) dy' - \frac{G}{4\pi(1-\nu)} \oint_C b_z \left(\frac{\partial^3 R}{\partial y' \partial x' \partial z'} \right) dx'; (\epsilon_{xzy} = \\ &-1, \epsilon_{yzx} = 1, \delta_{xz} = 0) \quad (7) \end{aligned}$$

Hence,

$$\begin{aligned} \sigma_{xz} &= \sigma_{xz} term1 + \sigma_{xz} term2 + \sigma_{xz} term3 = \frac{G}{4\pi(1-\nu)} \oint_C b_z \left(\frac{\partial^3 R}{\partial^2 x' \partial z'} \right) dy' - \\ &\frac{G}{4\pi(1-\nu)} \oint_C b_z \left(\frac{\partial^3 R}{\partial y' \partial x' \partial z'} \right) dx' = \left\{ \frac{Gb_z}{4\pi(1-\nu)} \int_{-b}^{+b} \left[\left(\frac{\partial^3 R}{\partial^2 x' \partial z'} \right) dy' \right]_{x'=+a} \right\} + \\ &\left\{ \frac{Gb_z}{4\pi(1-\nu)} \int_{+b}^{-b} \left[\left(\frac{\partial^3 R}{\partial^2 x' \partial z'} \right) dy' \right]_{x'=-a} \right\} - \left\{ \frac{Gb_z}{4\pi(1-\nu)} \int_{+a}^{-a} \left[\left(\frac{\partial^3 R}{\partial y' \partial x' \partial z'} \right) dx' \right]_{y'=+b} \right\} - \\ &\left\{ \frac{Gb_z}{4\pi(1-\nu)} \int_{-a}^{+a} \left[\left(\frac{\partial^3 R}{\partial y' \partial x' \partial z'} \right) dx' \right]_{y'=-b} \right\}; \quad (8) \end{aligned}$$

Let's focus on the integral: $\frac{Gb_z}{4\pi(1-\nu)} \int_{-b}^{+b} \left[\left(\frac{\partial^3 R}{\partial^2 x' \partial z'} \right) dy' \right]_{x'=+a}$. For the integrand $\frac{\partial^3 R}{\partial^2 x' \partial z'}$, it is given by:

$$\frac{\partial^3 R}{\partial^2 x' \partial z'} = \frac{3(-x+x')^2(-z+z')}{((-x+x')^2+(-y+y')^2+(-z+z')^2)^{5/2}} - \frac{-z+z'}{((-x+x')^2+(-y+y')^2+(-z+z')^2)^{3/2}}$$

Hence, the integral $\frac{Gb_z}{4\pi(1-\nu)} \int_{-b}^{+b} \left[\left(\frac{\partial^3 R}{\partial^2 x' \partial z'} \right) dy' \right]_{x'=+a}$ is in actuality composed of two integrals:

$$\frac{Gb_z}{4\pi(1-\nu)} \int_{-b}^{+b} \left[\left(\frac{3(-x+x')^2(-z+z')}{((-x+x')^2+(-y+y')^2+(-z+z')^2)^{5/2}} \right) dy' \right]_{x'=+a}$$

and

$$- \frac{Gb_z}{4\pi(1-\nu)} \int_{-b}^{+b} \left[\left(\frac{-z+z'}{((-x+x')^2+(-y+y')^2+(-z+z')^2)^{3/2}} \right) dy' \right]_{x'=+a}.$$

If one is interested in integrating by hand or manually, one can use the integral tables in [31]. We only show how to integrate the second integral here, i.e.

$$-\frac{Gb_z}{4\pi(1-\nu)} \int_{-b}^{+b} \left[\left(\frac{-z+z'}{((-x+x')^2+(-y+y')^2+(-z+z')^2)^{3/2}} \right) dy' \right]_{x'=+a}.$$

According to [31], $\int \frac{dx}{\sqrt{R_1^3}} = \frac{2(2cx+b)}{(4ac-b^2)\sqrt{R_1}}$, (9)

Where $R_1 = a + bx + cx^2$; Note that the integrand $\frac{-z+z'}{((-x+x')^2+(-y+y')^2+(-z+z')^2)^{3/2}}$ can be

written as $\frac{-z+z'}{(y'^2-2y'y+y^2+(-x+x')^2+(-z+z')^2)^{3/2}}$.

In this example, $R_1 = y'^2 - 2y'y + y^2 + (-x + x')^2 + (-z + z')^2 = a + by' + cy'^2$, where

$$a = y^2 + (-x + x')^2 + (-z + z')^2, \quad b = -2y, \quad c = 1.$$

According to equation (9),

$$\begin{aligned} \int \frac{-z+z'}{(y'^2-2y'y+y^2+(-x+x')^2+(-z+z')^2)^{3/2}} dy' &= \int \frac{(-z+z')dy'}{\sqrt{R_1^3}} = \frac{2(2cy'+b)(-z+z')}{(4ac-b^2)\sqrt{R_1}} = \\ &= \frac{2(2y'-2y)(-z+z')}{(4(y^2+(-x+x')^2+(-z+z')^2)-4y^2)\sqrt{y'^2-2y'y+y^2+(-x+x')^2+(-z+z')^2}} = \\ &= \frac{(y'-y)(-z+z')}{((-x+x')^2+(-z+z')^2)\sqrt{(-y+y')^2+(-x+x')^2+(-z+z')^2}}; \end{aligned}$$

Hence finally,

$$\begin{aligned} &-\frac{Gb_z}{4\pi(1-\nu)} \int_{-b}^{+b} \left[\left(\frac{-z+z'}{((-y+y')^2+(-x+x')^2+(-z+z')^2)^{3/2}} \right) dy' \right]_{x'=+a} = \\ &-\frac{Gb_z}{4\pi(1-\nu)} \left\{ \left[\frac{(b-y)(-z+z')}{((-x+a)^2+(-z+z')^2)\sqrt{(-y+b)^2+(-x+a)^2+(-z+z')^2}} \right] - \right. \\ &\left. \left[\frac{(-b-y)(-z+z')}{((-x+a)^2+(-z+z')^2)\sqrt{(-y-b)^2+(-x+a)^2+(-z+z')^2}} \right] \right\}; \quad (10) \end{aligned}$$

Moreover, one can also use the mathematical software Mathematica, which has a very strong symbolic engine, to do the integration instead. This provides efficiency and time savings.

RESULTS AND DISCUSSION

The stress field terms for a rectangular dislocation loop in an infinite medium were integrated from the PK Equation using the software Mathematica. The full list of results for the stress components, based on the Burgers vector components, are supplied in the appendices. For a loop with more than one, or all three, of the Burgers vector components not being zero, then the stress component is simply the sum, from the principle of superposition, of the results for these different Burgers vector components (as in the appendices). Note that in the appendices, we have replaced the z' in Fig. 1 with c .

If one is interested in the strain field terms or components instead, which are not listed here for brevity, these could be obtained from the stresses in the appendices using the inverted Hooke's law for isotropic materials:

$$\epsilon_{ij} = \frac{1}{2G} \left(\sigma_{ij} - \frac{\lambda \delta_{ij}}{2G+3\lambda} \sigma_{kk} \right) \quad (11)$$

Where σ_{kk} is the first invariant of the stress tensor, $\lambda = \frac{E\nu}{(1+\nu)(1-2\nu)}$, $G = \frac{E}{2(1+\nu)}$, and E is Young's modulus.

Equilibrium Equations Verification

The partial differential equations of static equilibrium in a solid material can be written in indicial notation as:

$$\sigma_{ij,j} = \frac{\partial \sigma_{ij}}{\partial x_j} = 0 \quad (12)$$

If the last equation is expanded on the repeated indices then the resulting three equations are:

$$\frac{\partial \sigma_{xx}}{\partial x} + \frac{\partial \sigma_{xy}}{\partial y} + \frac{\partial \sigma_{xz}}{\partial z} = 0 \quad (13)$$

$$\frac{\partial \sigma_{yx}}{\partial x} + \frac{\partial \sigma_{yy}}{\partial y} + \frac{\partial \sigma_{yz}}{\partial z} = 0 \quad (14)$$

$$\frac{\partial \sigma_{zx}}{\partial x} + \frac{\partial \sigma_{zy}}{\partial y} + \frac{\partial \sigma_{zz}}{\partial z} = 0 \quad (15)$$

This is keeping in mind the symmetry of the stress tensor, i.e. $\sigma_{ij} = \sigma_{ji}$. These equations should be satisfied at every material point of a solid in equilibrium. To verify the developed stress solution $\sigma_{\alpha\beta}$ given by equation (1) and provide in the appendices, one can see if equations (13-15) are identically satisfied either using analytical or numerical methods. For the analytical method, the equations are all reduced to zero by utilizing Mathematica. Similarly if one considers any line in space. For such line, the three equilibrium equations also equate analytically, or exactly, to zero. Hence, analytical verification of the equilibrium equations is feasible.

Alternatively, numerical verifications can also be made by plotting equations (13-15) along any plane in the material to see if the equations show a zero result. Figure (2.1, 2.2, 2.3) shows such plotting for $b_x \neq 0$. The figure shows that the equilibrium equations are satisfied. Note that given the combination of Burgers vector components and equilibrium equations a total of nine plots are minimally generated. For this reason, only three plots for one of the Burgers vector components are shown here for brevity.

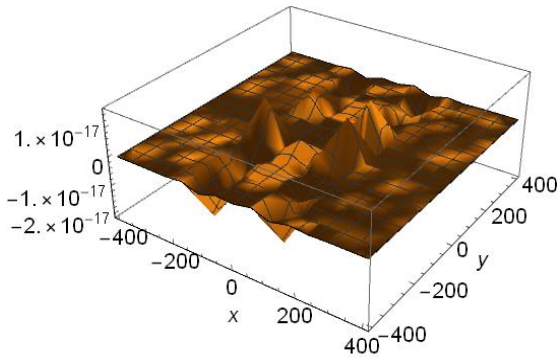


Fig. 2.1. Plot of equation (13)

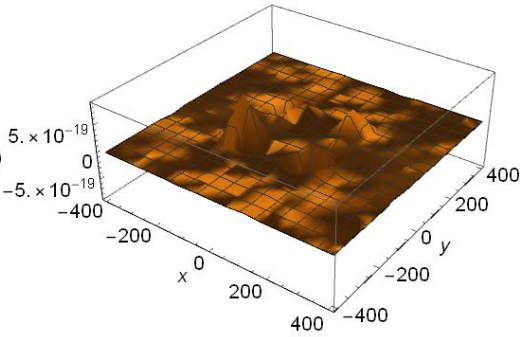


Fig. 2.2. Plot of equation (14)

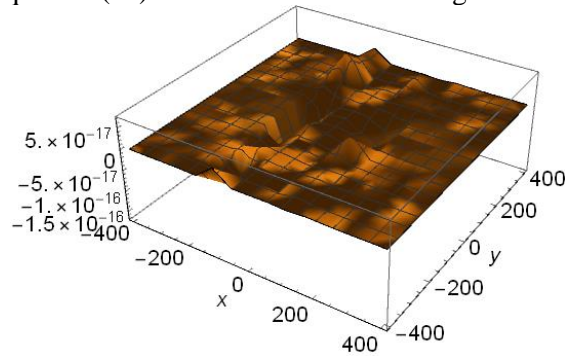


Fig. 2.3. Plot of equation (15). For these plots, the following values were chosen: $a = b = 100b_x$, $c = 10b_x$, $b_y = b_z = 0$, $b_x = 1$, $\nu = 0.3$, $\mu = 100$, $z = 11b_x$ $-4a \leq x \leq 4a$, $-4b \leq y \leq 4b$

Strain Compatibility Equations Verification

The equations of compatibility can be written in indicial notation as [32]:

$$\epsilon_{ij,kl} - \epsilon_{jl,ik} - \epsilon_{ik,jl} + \epsilon_{kl,ij} = 0 \quad (16)$$

This equation can be expanded over the repeated indices and written explicitly as six different/unique equations:

$$\frac{\partial^2 \epsilon_{xx}}{\partial y^2} + \frac{\partial^2 \epsilon_{yy}}{\partial x^2} = 2 \frac{\partial^2 \epsilon_{xy}}{\partial x \partial y} \quad (17)$$

$$\frac{\partial^2 \epsilon_{xx}}{\partial z^2} + \frac{\partial^2 \epsilon_{zz}}{\partial x^2} = 2 \frac{\partial^2 \epsilon_{xz}}{\partial x \partial z} \quad (18)$$

$$\frac{\partial^2 \epsilon_{zz}}{\partial y^2} + \frac{\partial^2 \epsilon_{yy}}{\partial z^2} = 2 \frac{\partial^2 \epsilon_{zy}}{\partial z \partial y} \quad (19)$$

$$\frac{\partial^2 \epsilon_{xx}}{\partial y \partial z} + \frac{\partial^2 \epsilon_{yz}}{\partial x^2} = \frac{\partial^2 \epsilon_{xz}}{\partial x \partial y} + \frac{\partial^2 \epsilon_{xy}}{\partial x \partial z} \quad (20)$$

$$\frac{\partial^2 \epsilon_{yy}}{\partial x \partial z} + \frac{\partial^2 \epsilon_{xz}}{\partial y^2} = \frac{\partial^2 \epsilon_{xy}}{\partial y \partial z} + \frac{\partial^2 \epsilon_{yz}}{\partial x \partial y} \quad (21)$$

$$\frac{\partial^2 \epsilon_{zz}}{\partial x \partial y} + \frac{\partial^2 \epsilon_{xy}}{\partial z^2} = \frac{\partial^2 \epsilon_{xz}}{\partial y \partial z} + \frac{\partial^2 \epsilon_{yz}}{\partial x \partial z} \quad (22)$$

These equations should be satisfied at every material point of a solid. To verify the developed stress solution, ϵ (the strain tensor) and its components are given by equation (11). One can then investigate if equations (17-22) are identically zero using either analytical or numerical methods. For the analytical method, the equations are so large that Mathematica is not able to reduce them to exactly 0. However, for any given line in space along the x -, y - or z -directions, Mathematica identically simplifies the compatibility equations to zero. Hence

analytical verification of the compatibility equations is possible.

Alternatively, numerical verifications can also be made by plotting equations (17-22) along any plane in the material to see if the equations give a zero result. Figure (3.1, 3.2, 3.3) shows such plotting for $b_y \neq 0$. The figure shows that the compatibility equations are satisfied. Note that given the combination of Burgers vector components and compatibility equations a total of eighteen plots are minimally generated. However, only three plots for one of the Burgers vector components are shown here for brevity.

Comparison with Devincere Formula

The DeVincere Formula [5] is an expression for the stress field of a straight or linear dislocation segment of finite length:

$$\sigma_{ij} = \frac{\mu}{\pi Y^2} \left\{ [\mathbf{b}'\mathbf{Y}\mathbf{t}']_{ij}^s - \frac{1}{1-\nu} [\mathbf{b}'\mathbf{t}'\mathbf{Y}]_{ij}^s - \frac{(\mathbf{b}'\mathbf{Y}\mathbf{t}')}{2(1-\nu)} [\delta_{ij} + t_i't_j' + \frac{2}{Y^2} [\rho_i Y_j + \rho_j Y_i + \frac{L'}{R} Y_i Y_j]] \right\} \quad (23)$$

Where \mathbf{b}' is the Burgers vector, $\mathbf{b}' = (b_x, b_y, b_z)$, \mathbf{t}' is the line sense vector or the line direction, $\mathbf{t}' = (t_x, t_y, t_z)$, σ_{ij} is ij^{th} component of the stress tensor, $\mathbf{Y} = \mathbf{R} + R\mathbf{t}'$, $\mathbf{R} =$

$((x' - x), (y' - y), (z' - z))$, $R = \sqrt{(x' - x)^2 + (y' - y)^2 + (z' - z)^2}$, δ_{ij} is the ij^{th}

component of the Kronecker delta, μ is shear modulus, ν is Poisson's ratio, $L' = \mathbf{R} \cdot \mathbf{t}'$, $\boldsymbol{\rho} =$

$\mathbf{R} - L'\mathbf{t}'$, $(\mathbf{b}', \mathbf{Y}, \mathbf{t}') = (\mathbf{b}' \times \mathbf{Y}) \cdot \mathbf{t}'$, and $[\mathbf{abc}]_{ij}^s = \frac{1}{2}((\mathbf{a} \times \mathbf{b})_i c_j + (\mathbf{a} \times \mathbf{b})_j c_i)$. Note that bold

lettering represents a vector(s) herein.

In this paper, the rectangular dislocation loop which is composed of four straight dislocation segments (or sides) is focused on here. Hence, the stress field of a rectangular dislocation can be obtained by adding up the contributions of four straight dislocation segments each obtained from the DeVincre Formula.

To compare with the stress field obtained from the DeVincre Formula, the following parameters are used for the plots in Figs. 4-9:

$$a = b = 100, c = 0, \nu = 0.3, b_x = b_y = 0; b_z = 1; y = 0, z = 20b_z, -2a \leq x \leq 2a,$$

The figures show perfect match between the analytical solution in this paper and the solution obtained from utilizing DeVincre Formula. This provides confidence in the presented analytical stress solution since it is matching the solution of four connected segments. Note that given the combination of Burgers vector components and stress components a total of eighteen plots are minimally generated. However, only six plots for one of the Burgers vector components are shown here for brevity.

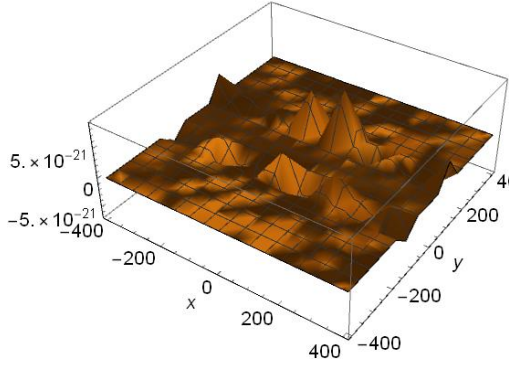


Fig. 3.1. Plot of equation (17)

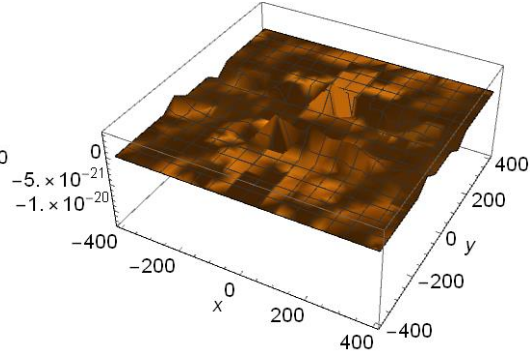


Fig. 3.2. Plot of equation (18)

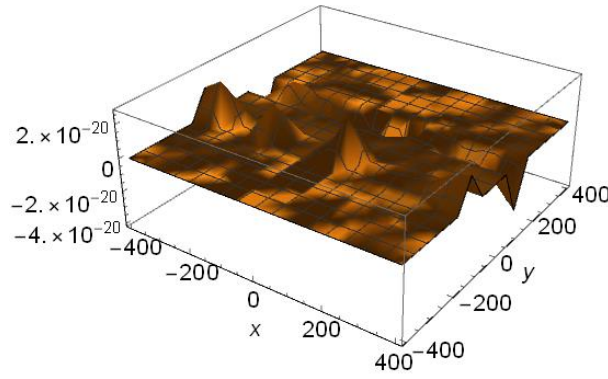


Fig. 3.3. Plot of equation (19). For these plots, the following values were chosen: $a = b = 100b_y$, $c = 10b_y$, $b_x = b_z = 0$, $b_y = 1$, $\nu = 0.3$, $\mu = G = 100$, $z = 11b_y$ $-4a \leq x \leq 4a$, $-4b \leq y \leq 4b$

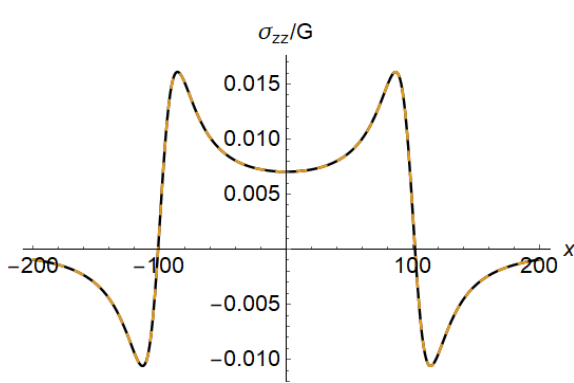


Fig. 4.

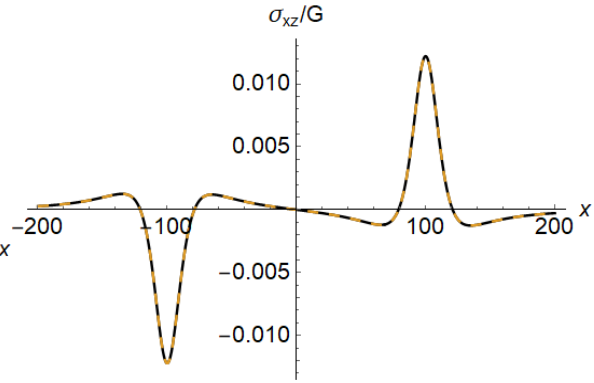


Fig. 5

Fig. 4. Comparison of $\frac{\sigma_{zz}}{G}$ analytical solutions in this paper (solid and black line) to the results of DeVincere Formula (dashed line) along x -direction for non-zero b_z

Fig. 5. Comparison of $\frac{\sigma_{xz}}{G}$ analytical solutions in this paper (solid and black line) to the results of DeVincere Formula (dashed line) along x -direction for non-zero b_z

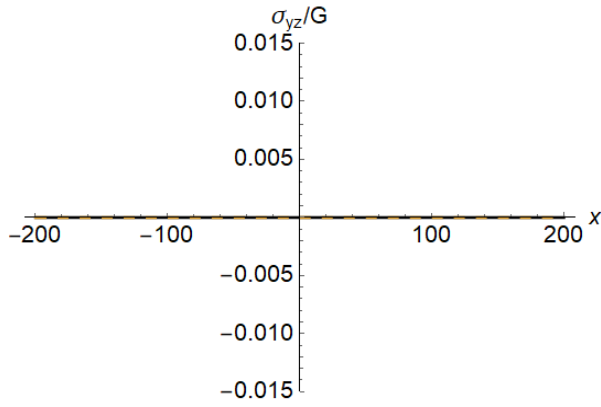


Fig. 6.

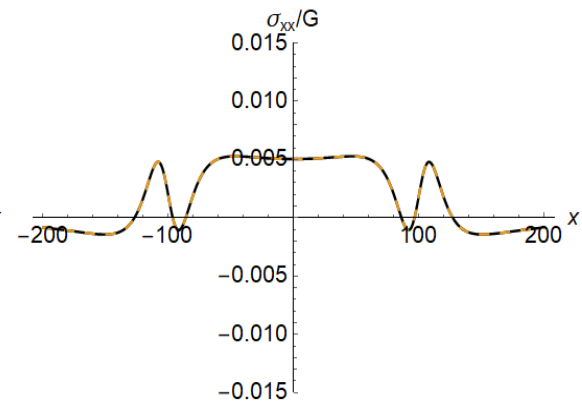


Fig. 7.

Fig. 6. Comparison of $\frac{\sigma_{yz}}{G}$ analytical solutions in this paper (solid and black line) to the results of DeVincere Formula (dashed line) along x -direction for non-zero b_z

Fig. 7. Comparison of $\frac{\sigma_{xx}}{G}$ analytical solutions in this paper (solid and black line) to the results of DeVincere Formula (dashed line) along x -direction for non-zero b_z

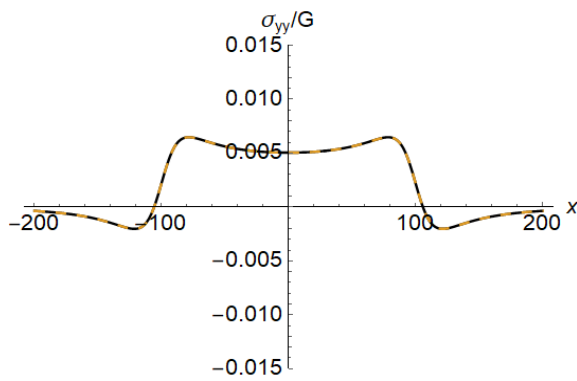


Fig. 8.

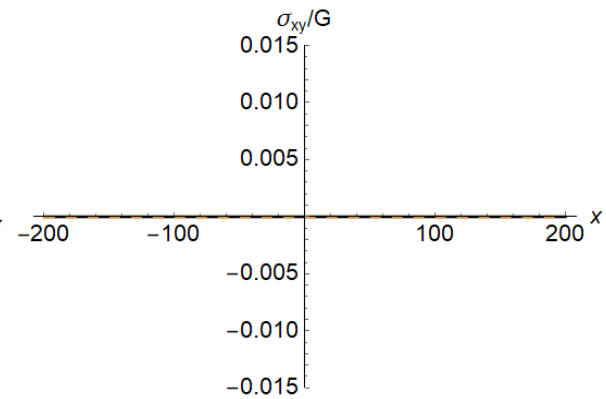


Fig. 9.

Fig. 8. Comparison of $\frac{\sigma_{yy}}{G}$ analytical solutions in this paper (solid and black line) to the results of DeVincere Formula (dashed line) along x -direction for non-zero b_z

Fig. 9. Comparison of $\frac{\sigma_{xy}}{G}$ analytical solutions in this paper (solid and black line) to the results of DeVincere Formula (dashed line) along x -direction for non-zero b_z

CONCLUSIONS

In conclusion, the stress field associated with a rectangular dislocation loop in an infinite medium has been developed. It is obtained by integrating the PK equation over a finite rectangular area. Also, the strain field can be developed by equation (11) if one is interested in it. The stress field obtained herein not only contributes to calculating the total stress fields of a rectangular dislocation loop in the isotropic half-medium, but also serves as a benchmarking tool for 3D dislocation dynamic codes which deal with generally-curved dislocations and need to properly quantify their elastic fields.

The developed field solutions were verified using both analytical equations and numerical calculations. The verifications were to ensure satisfaction of the equilibrium equations, satisfaction of the strain compatibility equations, and comparison against the stress field developed by DeVincre Formula for straight dislocation segments.

LIMITATIONS

The main limitation of the current work is that it deals with isotropic and not anisotropic materials. It also deals with infinite and not finite domains.

APPENDIX

Considering the Burgers vector component b_x :

$$\frac{\sigma_{xx}}{G} = \frac{b_x p}{2B1K\pi} \left(\frac{Q3}{\sqrt{A2}} - \frac{Q4}{\sqrt{A1}} \right) + \frac{b_x p}{2B2K\pi} \left(-\frac{Q3}{\sqrt{A4}} + \frac{Q4}{\sqrt{A3}} \right) + \frac{b_x p}{4B1^2K\pi} \left(\frac{B1Q1^2Q3}{A2^{3/2}} - \frac{(p^2-Q1^2)Q3}{\sqrt{A2}} - \frac{B1Q1^2Q4}{A1^{3/2}} + \frac{(p^2-Q1^2)Q4}{\sqrt{A1}} \right) + \frac{b_x p}{4B2^2K\pi} \left(-\frac{(B2Q2^2-A4(p^2-Q2^2))Q3}{A4^{3/2}} + \frac{(B2Q2^2-A3(p^2-Q2^2))Q4}{A3^{3/2}} \right);$$

$$\frac{\sigma_{yy}}{G} = \frac{b_x p}{4\pi} \left(\frac{1}{K} \left(-\frac{Q3}{A2^{3/2}} + \frac{Q4}{A1^{3/2}} \right) + \frac{2}{B1K} \left(\frac{Q3}{\sqrt{A2}} - \frac{Q4}{\sqrt{A1}} \right) + \frac{1}{K} \left(\frac{Q3}{A4^{3/2}} - \frac{Q4}{A3^{3/2}} \right) + \frac{2}{B2K} \left(-\frac{Q3}{\sqrt{A4}} + \frac{Q4}{\sqrt{A3}} \right) + 2 \left(\frac{1}{B1} \left(\frac{Q3}{\sqrt{A2}} - \frac{Q4}{\sqrt{A1}} \right) + \frac{1}{B2} \left(-\frac{Q3}{\sqrt{A4}} + \frac{Q4}{\sqrt{A3}} \right) \right) \right);$$

$$\frac{\sigma_{zz}}{G} = \frac{b_x p}{2B1K\pi} \left(\frac{Q3}{\sqrt{A2}} - \frac{Q4}{\sqrt{A1}} \right) + \frac{b_x p}{2B2K\pi} \left(-\frac{Q3}{\sqrt{A4}} + \frac{Q4}{\sqrt{A3}} \right) + \frac{b_x p}{4B1^2K\pi} \left(-\frac{(-B1p^2+A2(p^2+3Q1^2))Q3}{A2^{3/2}} + \frac{(-B1p^2+A1(p^2+3Q1^2))Q4}{A1^{3/2}} \right) + \frac{b_x p}{4B2^2K\pi} \left(\frac{(-B2p^2+A4(p^2+3Q2^2))Q3}{A4^{3/2}} - \frac{(-B2p^2+A3(p^2+3Q2^2))Q4}{A3^{3/2}} \right);$$

$$\frac{\sigma_{xy}}{G} = \frac{b_x p}{4K\pi} \left(\left(-\frac{1}{A1^{3/2}} + \frac{1}{A2^{3/2}} \right) Q1 + \left(-\frac{1}{A3^{3/2}} + \frac{1}{A4^{3/2}} \right) Q2 \right) + \frac{b_x p}{4\pi} \left(\frac{1}{C2} \left(-\frac{Q1}{\sqrt{A1}} - \frac{Q2}{\sqrt{A3}} \right) + \frac{1}{C1} \left(\frac{Q1}{\sqrt{A2}} + \frac{Q2}{\sqrt{A4}} \right) \right);$$

$$\frac{\sigma_{xz}}{G} = \frac{b_x Q1}{4B1^2K\pi} \left(-\left(-\frac{B1p^2}{A2^{3/2}} - \frac{(p^2-Q1^2)}{\sqrt{A2}} \right) Q3 + \left(-\frac{B1p^2}{A1^{3/2}} - \frac{(p^2-Q1^2)}{\sqrt{A1}} \right) Q4 \right) + \frac{b_x}{4\pi} \left(\frac{1}{C1} \left(\frac{Q1}{\sqrt{A2}} + \frac{Q2}{\sqrt{A4}} \right) Q3 - \frac{1}{C2} \left(\frac{Q1}{\sqrt{A1}} + \frac{Q2}{\sqrt{A3}} \right) Q4 \right) + \frac{b_x Q2}{4B2^2K\pi} \left(\left(\frac{B2p^2}{A4^{3/2}} + \frac{(p^2-Q2^2)}{\sqrt{A4}} \right) Q3 + \left(-\frac{B2p^2}{A3^{3/2}} - \frac{(p^2-Q2^2)}{\sqrt{A3}} \right) Q4 \right);$$

$$\frac{\sigma_{yz}}{G} = \frac{b_x}{4\pi} \left(\frac{1}{\sqrt{A1}} - \frac{1}{\sqrt{A2}} - \frac{1}{\sqrt{A3}} + \frac{1}{\sqrt{A4}} + \frac{1}{K} \left(-\frac{Q1^2+Q3^2}{A2^{3/2}} + \frac{Q2^2+Q3^2}{A4^{3/2}} + \frac{Q1^2+Q4^2}{A1^{3/2}} - \frac{Q2^2+Q4^2}{A3^{3/2}} \right) \right);$$

Considering the Burgers vector component b_y :

$$\frac{\sigma_{xx}}{G} = \frac{b_y p}{4\pi} \left(2 \left(\frac{1}{C2} \left(\frac{Q1}{\sqrt{A1}} + \frac{Q2}{\sqrt{A3}} \right) + \frac{1}{C1} \left(-\frac{Q1}{\sqrt{A2}} - \frac{Q2}{\sqrt{A4}} \right) \right) + \frac{1}{K} \left(-\frac{Q1}{A1^{3/2}} + \frac{Q1}{A2^{3/2}} - \frac{Q2}{A3^{3/2}} + \frac{Q2}{A4^{3/2}} + \frac{2}{C2} \left(\frac{Q1}{\sqrt{A1}} + \frac{Q2}{\sqrt{A3}} \right) + \frac{2}{C1} \left(-\frac{Q1}{\sqrt{A2}} - \frac{Q2}{\sqrt{A4}} \right) \right) \right);$$

$$\frac{\sigma_{yy}}{G} = \frac{b_y p}{2C2K\pi} \left(\frac{Q1}{\sqrt{A1}} + \frac{Q2}{\sqrt{A3}} \right) + \frac{b_y p}{2C1K\pi} \left(-\frac{Q1}{\sqrt{A2}} - \frac{Q2}{\sqrt{A4}} \right) + \frac{b_y p}{4C1^2K\pi} \left(-\frac{C1Q1Q3^2}{A2^{3/2}} - \frac{C1Q2Q3^2}{A4^{3/2}} + \frac{Q1(p^2-Q3^2)}{\sqrt{A2}} + \frac{Q2(p^2-Q3^2)}{\sqrt{A4}} \right) + \frac{b_y p}{4C2^2K\pi} \left(\frac{C2Q1Q4^2}{A1^{3/2}} + \frac{C2Q2Q4^2}{A3^{3/2}} - \frac{Q1(p^2-Q4^2)}{\sqrt{A1}} - \frac{Q2(p^2-Q4^2)}{\sqrt{A3}} \right);$$

$$\frac{\sigma_{zz}}{G} = \frac{b_y p}{2C_2 K \pi} \left(\frac{Q_1}{\sqrt{A_1}} + \frac{Q_2}{\sqrt{A_3}} \right) + \frac{b_y p}{2C_1 K \pi} \left(-\frac{Q_1}{\sqrt{A_2}} - \frac{Q_2}{\sqrt{A_4}} \right) + \frac{b_y p}{4C_1^2 K \pi} \left(-\frac{C_1 p^2 Q_1}{A_2^{3/2}} - \frac{C_1 p^2 Q_2}{A_4^{3/2}} + \frac{Q_1(p^2 + 3Q_3^2)}{\sqrt{A_2}} + \frac{Q_2(p^2 + 3Q_3^2)}{\sqrt{A_4}} \right) + \frac{b_y p}{4C_2^2 K \pi} \left(\frac{C_2 p^2 Q_1}{A_1^{3/2}} + \frac{C_2 p^2 Q_2}{A_3^{3/2}} - \frac{Q_1(p^2 + 3Q_4^2)}{\sqrt{A_1}} - \frac{Q_2(p^2 + 3Q_4^2)}{\sqrt{A_3}} \right);$$

$$\frac{\sigma_{xy}}{G} = \frac{b_y p}{4K\pi} \left(\left(-\frac{1}{A_2^{3/2}} + \frac{1}{A_4^{3/2}} \right) Q_3 - \left(-\frac{1}{A_1^{3/2}} + \frac{1}{A_3^{3/2}} \right) Q_4 \right) + \frac{b_y p}{4\pi} \left(\frac{1}{B_1} \left(-\frac{Q_3}{\sqrt{A_2}} + \frac{Q_4}{\sqrt{A_1}} \right) + \frac{1}{B_2} \left(\frac{Q_3}{\sqrt{A_4}} - \frac{Q_4}{\sqrt{A_3}} \right) \right);$$

$$\frac{\sigma_{xz}}{G} = \frac{b_y}{4\pi} \left(\frac{1}{\sqrt{A_1}} - \frac{1}{\sqrt{A_2}} - \frac{1}{\sqrt{A_3}} + \frac{1}{\sqrt{A_4}} + \frac{1}{K} \left(-\frac{Q_1^2 + Q_3^2}{A_2^{3/2}} + \frac{Q_2^2 + Q_3^2}{A_4^{3/2}} + \frac{Q_1^2 + Q_4^2}{A_1^{3/2}} - \frac{Q_2^2 + Q_4^2}{A_3^{3/2}} \right) \right);$$

$$\frac{\sigma_{yz}}{G} = \frac{b_y Q_3}{4C_1^2 K \pi} \left(\frac{C_1 p^2 Q_1}{A_2^{3/2}} + \frac{C_1 p^2 Q_2}{A_4^{3/2}} + \frac{Q_1(p^2 - Q_3^2)}{\sqrt{A_2}} + \frac{Q_2(p^2 - Q_3^2)}{\sqrt{A_4}} \right) - \frac{b_y Q_4}{4C_2^2 K \pi} \left(\frac{C_2 p^2 Q_1}{A_1^{3/2}} + \frac{C_2 p^2 Q_2}{A_3^{3/2}} + \frac{Q_1(p^2 - Q_4^2)}{\sqrt{A_1}} + \frac{Q_2(p^2 - Q_4^2)}{\sqrt{A_3}} \right) + \frac{b_y}{4\pi} \left(\frac{Q_1}{B_1} \left(\frac{Q_3}{\sqrt{A_2}} - \frac{Q_4}{\sqrt{A_1}} \right) + \frac{Q_2}{B_2} \left(\frac{Q_3}{\sqrt{A_4}} - \frac{Q_4}{\sqrt{A_3}} \right) \right);$$

Considering the Burgers vector component b_z :

$$\frac{\sigma_{xx}}{G} = \frac{Q_3 b_z}{4K\pi} \left(\frac{Q_1}{A_2^{3/2}} + \frac{Q_2}{A_4^{3/2}} \right) + \frac{Q_3 b_z}{2C_1 K \pi} \left(-\frac{Q_1}{\sqrt{A_2}} - \frac{Q_2}{\sqrt{A_4}} \right) - \frac{Q_4 b_z}{4K\pi} \left(\frac{Q_1}{A_1^{3/2}} + \frac{Q_2}{A_3^{3/2}} \right) - \frac{Q_4 b_z}{2C_2 K \pi} \left(-\frac{Q_1}{\sqrt{A_1}} - \frac{Q_2}{\sqrt{A_3}} \right) + \frac{Q_1 b_z}{2B_1 K \pi} \left(-\frac{Q_3}{\sqrt{A_2}} + \frac{Q_4}{\sqrt{A_1}} \right) + \frac{Q_2 b_z}{2B_2 K \pi} \left(-\frac{Q_3}{\sqrt{A_4}} + \frac{Q_4}{\sqrt{A_3}} \right) + \frac{b_z}{2\pi} \left(\frac{Q_3}{C_1} \left(-\frac{Q_1}{\sqrt{A_2}} - \frac{Q_2}{\sqrt{A_4}} \right) - \frac{Q_4}{C_2} \left(-\frac{Q_1}{\sqrt{A_1}} - \frac{Q_2}{\sqrt{A_3}} \right) \right) + \frac{Q_1 b_z}{4B_1^2 K \pi} \left(-\frac{Q_4(3B_1 p^2 + (3p^2 + Q_1^2)(b-y)^2)}{A_1^{3/2}} + \frac{Q_3(3B_1 p^2 + (3p^2 + Q_1^2)(b+y)^2)}{A_2^{3/2}} \right) + \frac{Q_2 b_z}{4B_2^2 K \pi} \left(-\frac{Q_4(3B_2 p^2 + (3p^2 + Q_2^2)(b-y)^2)}{A_3^{3/2}} + \frac{Q_3(3B_2 p^2 + (3p^2 + Q_2^2)(b+y)^2)}{A_4^{3/2}} \right);$$

$$\frac{\sigma_{yy}}{G} = \frac{b_z}{4\pi} \left(\frac{2Q_3}{C_1 K} \left(-\frac{Q_1}{\sqrt{A_2}} - \frac{Q_2}{\sqrt{A_4}} \right) - \frac{2Q_4}{C_2 K} \left(-\frac{Q_1}{\sqrt{A_1}} - \frac{Q_2}{\sqrt{A_3}} \right) + \frac{Q_1}{K} \left(\frac{Q_3}{A_2^{3/2}} - \frac{Q_4}{A_1^{3/2}} \right) + \frac{2Q_1}{B_1 K} \left(-\frac{Q_3}{\sqrt{A_2}} + \frac{Q_4}{\sqrt{A_1}} \right) + \frac{Q_2}{K} \left(\frac{Q_3}{A_4^{3/2}} - \frac{Q_4}{A_3^{3/2}} \right) + \frac{2Q_2}{B_2 K} \left(-\frac{Q_3}{\sqrt{A_4}} + \frac{Q_4}{\sqrt{A_3}} \right) + 2 \left(\frac{Q_1}{B_1} \left(-\frac{Q_3}{\sqrt{A_2}} + \frac{Q_4}{\sqrt{A_1}} \right) + \frac{Q_2}{B_2} \left(-\frac{Q_3}{\sqrt{A_4}} + \frac{Q_4}{\sqrt{A_3}} \right) \right) - \frac{Q_4}{C_2^2 K} \left(\frac{Q_1(3p^4 + a(3p^2 + Q_4^2)(a-2x) + (3p^2 + x^2)(b-y)^2 + 3p^2 x^2)}{A_1^{3/2}} + \frac{Q_2(3p^4 + a(3p^2 + Q_4^2)(a+2x) + (3p^2 + x^2)(b-y)^2 + 3p^2 x^2)}{A_3^{3/2}} \right) + \frac{Q_3}{C_1^2 K} \left(\frac{Q_1(3p^4 + a(3p^2 + Q_3^2)(a-2x) + (3p^2 + x^2)(b+y)^2 + 3p^2 x^2)}{A_2^{3/2}} + \frac{Q_2(3p^4 + a(3p^2 + Q_3^2)(a+2x) + (3p^2 + x^2)(b+y)^2 + 3p^2 x^2)}{A_4^{3/2}} \right) \right);$$

$$\begin{aligned} \frac{\sigma_{zz}}{G} = & \frac{Q3b_z}{2C1K\pi} \left(-\frac{Q1}{\sqrt{A2}} - \frac{Q2}{\sqrt{A4}} \right) - \frac{Q4b_z}{2C2K\pi} \left(-\frac{Q1}{\sqrt{A1}} - \frac{Q2}{\sqrt{A3}} \right) + \frac{Q1b_z}{2B1K\pi} \left(-\frac{Q3}{\sqrt{A2}} + \frac{Q4}{\sqrt{A1}} \right) + \\ & \frac{Q2b_z}{2B2K\pi} \left(-\frac{Q3}{\sqrt{A4}} + \frac{Q4}{\sqrt{A3}} \right) + \frac{Q3b_z}{4C1^2(-\pi K)} \left(-\frac{-C1p^2Q1-A2Q1(p^2-Q3^2)}{A2^{3/2}} + \right. \\ & \left. \frac{C1p^2Q2+A4Q2(p^2-Q3^2)}{A4^{3/2}} \right) - \frac{Q1b_z}{4B1^2(-\pi K)} \left(-\frac{B1p^2Q3+A2(p^2-Q1^2)Q3}{A2^{3/2}} + \right. \\ & \left. \frac{B1p^2Q4+A1(p^2-Q1^2)Q4}{A1^{3/2}} \right) + \frac{Q2b_z}{4B2^2(-\pi K)} \left(\frac{B2p^2Q3+A4(p^2-Q2^2)Q3}{A4^{3/2}} - \right. \\ & \left. \frac{B2p^2Q4+A3(p^2-Q2^2)Q4}{A3^{3/2}} \right) + \frac{Q4b_z}{4C2^2(-\pi K)} \left(\frac{-C2p^2Q1-A1Q1(p^2-Q4^2)}{A1^{3/2}} - \right. \\ & \left. \frac{Q2(p^4+p^2Q4^2+A3(p^2-Q4^2))}{A3^{3/2}} \right); \end{aligned}$$

$$\begin{aligned} \frac{\sigma_{xy}}{G} = & \frac{b_z}{2\pi} \left(-\frac{1}{\sqrt{A1}} + \frac{1}{\sqrt{A2}} + \frac{1}{\sqrt{A3}} - \frac{1}{\sqrt{A4}} \right) + \frac{b_z}{4K\pi} \left(\frac{B1}{A2^{3/2}} + \frac{B2}{A3^{3/2}} - \frac{B2}{A4^{3/2}} + \frac{C1}{A2^{3/2}} - \right. \\ & \left. \frac{C1}{A4^{3/2}} + \frac{C2}{A3^{3/2}} + \frac{-p^2-Q1^2}{A1^{3/2}} + \frac{-p^2-Q4^2}{A1^{3/2}} \right); \end{aligned}$$

$$\begin{aligned} \frac{\sigma_{xz}}{G} = & \frac{pQ3b_z}{4K\pi} \left(\frac{1}{A2^{3/2}} - \frac{1}{A4^{3/2}} \right) + \frac{pb_z}{4K\pi} \left(-\frac{Q4}{A1^{3/2}} + \frac{Q4}{A3^{3/2}} \right) + \\ & \frac{pb_z}{4B1^2K\pi} \left(-\frac{(p^2Q1^2+Q1^4-A2(p^2-Q1^2))Q3}{A2^{3/2}} + \frac{(p^2Q1^2+Q1^4-A1(p^2-Q1^2))Q4}{A1^{3/2}} \right) + \\ & \frac{pb_z}{4B2^2K\pi} \left(\frac{(B2Q2^2-A4(p^2-Q2^2))Q3}{A4^{3/2}} - \frac{(B2Q2^2-A3(p^2-Q2^2))Q4}{A3^{3/2}} \right); \end{aligned}$$

$$\begin{aligned} \frac{\sigma_{yz}}{G} = & \frac{b_z}{4K\pi} p \left(\left(\frac{1}{A1^{3/2}} - \frac{1}{A2^{3/2}} \right) Q1 + \left(\frac{1}{A3^{3/2}} - \frac{1}{A4^{3/2}} \right) Q2 + \right. \\ & \left. \frac{1}{C1^2} \left(-\frac{Q1(-C1Q3^2+A2(p^2-Q3^2))}{A2^{3/2}} - \frac{Q2(-C1Q3^2+A4(p^2-Q3^2))}{A4^{3/2}} \right) + \right. \\ & \left. \frac{1}{C2^2} \left(\frac{Q1(A1(p^2-Q4^2)+Q4^2(-p^2-Q4^2))}{A1^{3/2}} + \frac{Q2(A3(p^2-Q4^2)+Q4^2(-p^2-Q4^2))}{A3^{3/2}} \right) \right); \end{aligned}$$

$$p = c - z;$$

$$A1 = p^2 + (a - x)^2 + (b - y)^2;$$

$$A2 = p^2 + (a - x)^2 + (b + y)^2;$$

$$A3 = p^2 + (a + x)^2 + (b - y)^2;$$

$$A4 = p^2 + (a + x)^2 + (b + y)^2;$$

$$B1 = p^2 + (a - x)^2;$$

$$B2 = p^2 + (a + x)^2;$$

$$C1 = p^2 + (b + y)^2;$$

$$C2 = p^2 + (b - y)^2;$$

$$K = -1 + v;$$

$$Q1 = a - x;$$

$$Q2 = a + x;$$

$$Q3 = b + y;$$

$$Q4 = -b + y;$$

REFERENCES

1. Meyers MA, Chawla KK. Mechanical Behavior of Materials. 2nd edition. University of Cambridge, UK; 2009.
2. Rhee M, Zbib HM, Hirth JP, Huang H, De La Rubia T. Models for long/short range interactions in 3d dislocation simulation. *Modelling & Simulation in Material Science Engineering*. 1998;6(4):467-492.
3. Zbib HM, Rhee M, Hirth JP. On plastic deformation and the dynamics of 3d dislocations. *International Journal of Mechanical Engineering*. 1998;40(2-3):113-127.
4. Kubin LP, Canova G, Condat M, Devincere B, Pontikis V, and Brechet Y. Dislocation Microstructures and Plastic Flow: a 3D Simulation. *Solid State Phenomena*. 1992;23-24:455-472.
5. Devincere B. Three dimensional stress field expressions for straight dislocation segments. *Solid State Communication*. 1995;93(11):875-878.
6. Hirth JP, Lothe J. Theory of Dislocations. 5th edition. Krieger Publishing Company, Malabar, Florida; 1982.
7. Hull D, Bacon DJ. Introduction to Dislocations. University of Liverpool, UK; 2011.
8. Weertman J, Weertman JR. Elementary Dislocation Theory. Oxford University Press, Oxford; 1992.
9. Kroupa F. Circular edge dislocation loop. *Czechoslovak Journal of Physics B*. 1960; 1:284–293.
10. Bullough R, Newman RC. The spacing of prismatic dislocation loops. *Philosophical Magazine*. 1960; 2:921–926.
11. Keller JM. 1957; unpublished
12. Kröner E. *Kontinuumstheorie Der Versetzungen Und Eigenspannungen*. Springer-Verlag, Berlin; 1958.
13. Kroupa F. Interaction between prismatic dislocation loops and straight dislocations. *Philosophical Magazine*. 1962; 3:783–801.
14. Marcinkowski MJ, Sree Harsha KS. Properties of finite circular dislocation glide loops. *Journal of Applied Physics*. 1968; 4:1775–1783.

15. Khraishi TA, Hirth JP, Zbib HM, Khaleel MA. The displacement, and strain-stress fields of a general circular Volterra dislocation loop. *International Journal of Engineering Science*. 2000; 5:251–266.
16. Khraishi TA, Zbib HM, Hirth JP, De La Rubia TD. The stress field of a general circular Volterra dislocation loop: analytical and numerical approaches. *Philosophical Magazine Letters*. 2000; 6:95–105.
17. Khraishi TA, Zbib HM. The displacement field of a rectangular Volterra dislocation loop. *Philosophical Magazine Letters*. 2002; 7:265–277.
18. Khraishi TA, Zbib HM, De La Rubia TD. The Treatment of Traction-free Boundary Condition in Three-dimensional Dislocation Dynamics using Generalized Image Stress Analysis. *Materials Science and Engineering A*. 2001;309-310:283-287.
19. Khraishi TA, Zbib HM. Free Surface Effects in 3D Dislocation Dynamics: Formulation and Modeling. *Journal of Engineering Materials and Technology (JEMT)*. 2002;124(3):342-351.
20. Yan L, Khraishi TA, Shen Y-L, Horstemeyer MF. A distributed-dislocation method for treating free-surface image stresses in 3D dislocation Dynamics Simulations. *Modelling and Simulation in Materials Science and Engineering*. 2004;12(4): S289-S301.
21. Siddique AB, Khraishi T. Numerical methodology for treating static and dynamic dislocation problems near a free surface. *Journal of Physics Communications*. 2020;4(5): 055005. DOI 10.1088/2399-6528/ab8ff9
22. Khraishi TA, Zbib HM. Dislocation dynamics simulations of the interaction between a short rigid fiber and a glide circular dislocation pile-up. *Computational Materials Science*. 2002;24(3):310-322.
23. De La Rubia TD, Zbib HM, Khraishi TA, Wirth BD, Victoria M, Caturla MJ. Multiscale modelling of plastic flow localization in irradiated materials. *Nature*. 2000;406(6798):871-874.
24. Khraishi TA, Zbib HM, De La Rubia TD, Victoria M. Modeling of irradiation-induced hardening in metals using dislocation dynamics. *Philosophical Magazine Letters*. 2001;81(9):583-593.
25. Khraishi TA, Zbib HM, De La Rubia TD, Victoria M. Localized Deformation and Hardening in Irradiated Metals: Three-Dimensional Discrete Dislocation Dynamics Simulations. *Metallurgical and Materials Transactions B*. 2002;33(2):285-296.

26. Demir I, Hirth JP, Zbib HM. Extended stress field around a cylindrical crack using the theory of dislocation pile-ups. *International Journal of Engineering Science*. 1992; 8:829–845.
27. Demir I, Hirth JP, Zbib HM. The Somigliana ring dislocation. *Journal of Elasticity*. 1992;9: 223-246.
28. Demir I, Khraishi TA. The Torsional dislocation loop and mode III Cylindrical crack. *Journal of Mechanics*. 2005; 10:115-122.
29. Jesus Lerma, Tariq Khraishi, Sandeep Kataria, Yu-Lin Shen. Distributed dislocation method for determining elastic fields of 2D and 3D volume misfit particles in infinite space and extension of the method for particles in half space. *Journal of Mechanics*. 2015;31(3):249-260.
30. Siddique AB, Khraishi TA. Eigenvalues and Eigenvectors for 3×3 Symmetric Matrices: An Analytical Approach. *Journal of Advances in Mathematics and Computer Science*. 2020; 35(7):106-118. Available: <https://doi.org/10.9734/jamcs/2020/v35i730308>
31. Gradshteyn IS, Ryzhik IM. *Table of Integrals, Series, and Products*. 5th edition. Academic Press: San Diego, California; 1980.
32. Khraishi TA, Shen, YL. *Introductory Continuum Mechanics with Applications to Elasticity*. University Readers/Cognella, San Diego, California; 2011.

Chapter 3 The Strain/Stress Fields of a Subsurface Rectangular Dislocation Loop Parallel to the Surface of a Half Medium: Analytical Solution with Verification

ABSTRACT

The strain and stress fields of a rectangular dislocation loop in an isotropic solid that is a semi-infinite medium (half medium) are developed here for a Volterra-type dislocation. Specifically, the loop is parallel to the free surface of the solid. The elastic fields of the dislocation loop are developed by integrating the displacement equation of infinitesimal dislocation loops over a finite rectangular loop area below the free surface. The strains and stress then follow from the small strain tensor and Hooke's law for isotropic materials, respectively. In this paper, analytical verification and numerical verification for the elastic fields are both demonstrated. Equilibrium equations and strain compatibility equations are applied in the verification. Also, a comparison with a newly-developed numerical method for dislocations near a free surface is performed as well. The developed solution is a function of the loop depth beneath the surface and can be used as a fundamental solution to solve elasticity, plasticity or dislocation problems.

Keywords: dislocation loops, free surfaces, Volterra, image-stresses, semi-infinite medium

INTRODUCTION

The problem of finding analytical solutions for the elastic fields of dislocations in different material types, material geometry and sizes has occupied researchers for tens of years. Early on, researchers focused their research on infinite isotropic materials or mediums. They also focused their work on infinitely-long dislocations (i.e. two-dimensional problems). For example, [1-3], amongst other textbooks, provided older known derivations for the displacement, strain and stress fields of screw and edge dislocations in an infinite medium assuming material isotropy. However, [2] has also provided two integral equations for finding the displacement field (the Burgers equation) and another the stress fields of a closed dislocation loop (of any shape) in an infinite isotropic material.

Several researchers have studied different aspects of the dislocation loop problem using a variety of techniques. Initially, [4] and [5] investigated the prismatic circular loop (one whose Burgers vector is normal to its plane). The circular glide loop was initially investigated in [6] and given in [7]. The solution by Keller and Kröner was later corrected in [8] and [9]. In a more recent study of the displacement and stress fields of glide and prismatic circular dislocation loops, [10-11] corrected some earlier work. The displacement field, including the solid angle term, of a rectangular dislocation loop of the Volterra type in an infinite medium was developed by [12].

A Somigliana ring dislocation was investigated by [13-14]. A torsional dislocation loop of the Somigliana type was investigated by [15].

As for problems involving dislocations near a free surface, [16] derived the elastic fields of a dislocation meeting a surface in an angle for an arbitrary choice of Burgers vector. Baštecká [17] formulated the field stress due to a pure edge circular dislocation loop near a

free surface with Burgers vector normal to that free surface. The effects of free surfaces on a circular loop were also studied by [18] and [19]. [20-21] showed the field displacements due to an infinitesimal dislocation loop of arbitrary orientation and Burgers vector in a semi-infinite isotropic medium. The elastic field of a finite-sized closed dislocation loop can thus be obtained by means of area integration using the results for the infinitesimal loop. Jing et al. [22] used the last two references to find the displacement field of a rectangular dislocation loop parallel to a free surface. Maurissen and Capella [23-24] derived the field stress correction terms of a dislocation segment parallel and perpendicular to a free surface in a semi-infinite elastic medium. Comninou and Dundurs [25] presented the formulations of the elastic field of an angular dislocation segment in isotropic half-space. For an anisotropic medium, [26] derived an integral form of field stress for the case of a dislocation terminating at the free surface of an anisotropic half-space. Gosling and Willis [27] expressed the stresses due to an arbitrary dislocation in a semi-infinite medium as a line integral along the dislocation.

In [1-2], to treat the unphysical stress traction brought on the free surface by a screw dislocation line (parallel to the surface) whose fundamental solution is that of a screw dislocation in an infinite medium, an image screw dislocation with opposite Burgers vector is utilized. The image screw dislocation is a mathematical/un-crystal dislocation situated across from the surface at a distance equal to the crystal screw dislocation. The image solution does not satisfy the zero traction condition on the free surface when an edge dislocation parallel to the free surface is considered. In the case of an edge dislocation, [1] showed that extra term(s), called “surface correction terms” or stress surface correction terms, are needed to be added to the edge dislocation solution in an infinite medium plus the image edge dislocation solution (with opposite Burgers vector also treated as if it is in an infinite medium). With the

addition of these three terms, the correct stress field is obtained as it ensures zero traction on the free surface.

In recent years, several papers utilized the “collocation point” numerical method to solve the problem of dislocation near a flat free surface. These collocation point methods enforce zero traction on a select number of surface points and not infinite number of them as in analytical methods. For example, [28] and [29] utilized an image dislocation plus a stress correction term. The stress correction term(s) were obtained by meshing the large surface with prismatic contiguous “mathematical” dislocation loops. Yan et al. [30] and [31] dropped the use of the image dislocations in the collocation point method by instead utilizing a mesh of generally-prismatic dislocation loops.

In this paper, the strain-stress field of the correction terms due to a rectangular Volterra dislocation loop parallel to a free surface are developed by building on the corrective displacement field solution (using [21] and [22]). Also, strain-stress fields of the infinite medium term and the image term due to a rectangular dislocation loop are obtained by deriving the displacement field solution presented by [12]. Furthermore, analytical verification and numerical verification of the result will be presented.

Elastic field solutions for dislocation problems as presented herein, are beneficial for several reasons: 1- They serve as fundamental solutions, similar to a Green’s function, for other elasticity, plasticity or dislocation problems (e.g. for fracture problems, or general eigenstrain problems [32-33]), and 2- They serve as verification problems for numerical methods like the collocation-point method or different dislocation dynamic simulation codes.

Elastic Fields of a Sub-Surface Rectangular Dislocation Loop

First off, the problem configuration under consideration is given in Figure 1. The figure shows a free surface (labelled as such) of a half isotropic medium (i.e. semi-infinite medium) that is below the surface (i.e. lies in the positive z or x_3 direction). Beneath the free surface is a rectangular dislocation loop (labelled as “Finite-sized crystal dislocation loop”) that is parallel to free surface. This Volterra-type dislocation loop has a Burgers vector \mathbf{b} , which has three components b_x , b_y and b_z , and has a dimension $2a$ in the x -direction and a dimension $2b$ in the y -direction. The line sense of the loop is shown with the arrow going around the loop. The loop is below the surface a distance c . The goal is to determine the strain and stress tensors or components for an arbitrary field material point P. Note that in this paper, x_1 and x are used interchangeably, so are x_2 and y , and so are x_3 and z . Similarly for x'_1 and x' , and so forth.

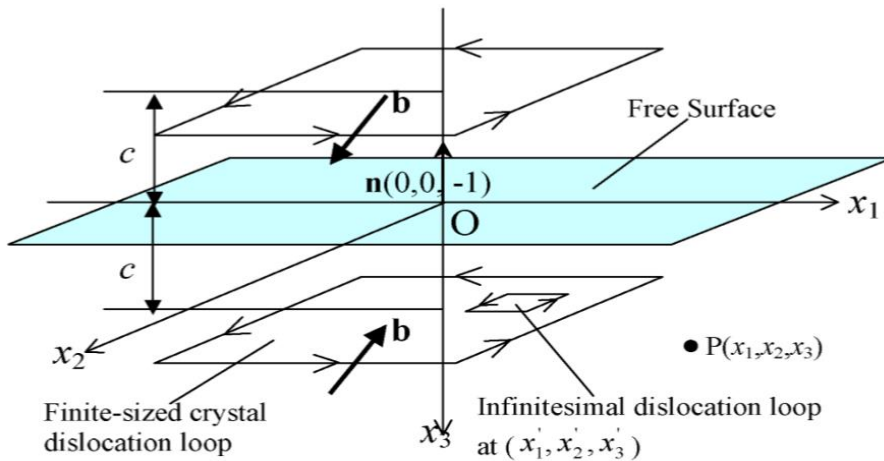


Fig.1. A finite-sized dislocation loop with an arbitrary Burgers vector, \mathbf{b} , below (by c) a free surface. Also shown an image dislocation loop with opposite Burgers vector above the surface. Lastly, an infinitesimal dislocation loop located at a point in the plane of the subsurface finite-sized loop is also shown.

To find the displacement, strain or stress fields (\vec{u} , ϵ or σ respectively) due to the subsurface dislocation loop, such fields are the sum of three terms:

$$\vec{u} = \vec{u}^{inf} + \vec{u}^{image} + \vec{u}^s \quad (1)$$

$$\epsilon = \epsilon^{inf} + \epsilon^{image} + \epsilon^s \quad (2)$$

$$\sigma = \sigma^{inf} + \sigma^{image} + \sigma^s \quad (3)$$

where the superscript “*inf*” refers to the field solution of a rectangular dislocation loop *as if* it was in an *infinite* medium and not in a half medium as shown in Figure 1, the superscript “*image*” refers to the field solution of an *image* rectangular dislocation loop which is also shown as the top loop in Figure 1 (also *as if* this image loop lied in an infinite medium), and finally the “*s*” superscript refers to surface correction terms needed to ensure a zero traction condition on the free surface.

Let’s focus first on the infinite term in the above equations. The Burgers equation [2] is an integral equation for the displacement field of a closed Volterra dislocation loop of any shape or curvature and lying in an infinite medium. It is composed of three integrals: the first of which is an area integral representing the solid angle of a rectangle, the second and third are line integrals summing the contributions of infinitesimal line lengths (dl') composing the loop along its line sense:

$$u_m(\mathbf{r}) = -\frac{1}{8\pi} \int_A b_m \frac{\partial}{\partial x'_j} \nabla'^2 R dA_j - \frac{1}{8\pi} \oint_c b_i \epsilon_{mik} \nabla'^2 R dx'_k - \frac{1}{8\pi(1-\nu)} \oint_c b_i \epsilon_{ijk} \frac{\partial^2 R}{\partial x'_m \partial x'_j} dx'_k \quad (4)$$

, where u_m is the m^{th} component of the displacement vector \vec{u} , b_m is the m^{th} component of the displacement vector $\vec{b} = \mathbf{b} = (b_x, b_y, b_z)$, ϵ is the permutation symbol, ν is Poisson’s ratio, $R = \sqrt{(x' - x)^2 + (y' - y)^2 + (z' - z)^2}$ (see Figure 2) and $\nabla'^2 R = 2/R$.

The integration of the above equation for the displacement field of the rectangular dislocation loop shown in Figure 2 was done in [12]. It is not re-produced here. This displacement field represents the “*inf*” and “*image*” terms in equation (1). To find the strain field associated with this rectangular dislocation loop in an infinite material, the tensorial small strain definition is invoked here:

$$\epsilon_{ij} = \frac{1}{2} \left(\frac{\partial u_i}{\partial x_j} + \frac{\partial u_j}{\partial x_i} \right) \quad (5)$$

This provides the “*inf*” and “*image*” terms in equation (2). Finally, to find the stress field of this loop, one invokes Hooke’s law for an isotropic material:

$$\sigma_{ij} = \lambda \epsilon_{kk} \delta_{ij} + 2\mu \epsilon_{ij} \quad (6)$$

where $\lambda = \frac{E\nu}{(1+\nu)(1-2\nu)}$, $\mu = \frac{E}{2(1+\nu)}$

Here, δ_{ij} is the ij^{th} component of the Kronecker delta, μ is shear modulus, ϵ_{kk} is the dilatation or the volumetric strain, and E is Young’s modulus. Finding the stresses using equation (6), will provide the “*inf*” and “*image*” terms in equation (3). The strain and stress fields have been obtained here using the mathematical software Mathematica which has a very strong symbolic engine. However, they are not provided here for brevity for they will take several pages to list.

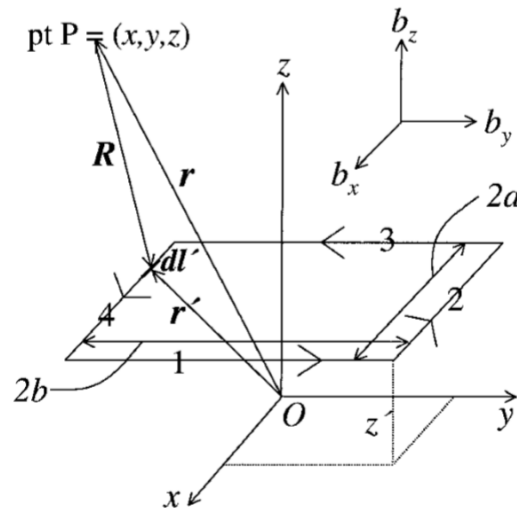


Fig.2. The geometry of a rectangular dislocation loop in infinite material. Here $\vec{r}' = \mathbf{r}' = (x', y', z')$.

As for the displacement surface correction term in equation (1), it can be obtained as follows:

$$\bar{u}^s = \int_A d\bar{u}^s \quad (7)$$

, where $d\bar{u}^s$ is the displacement vector at any field material point caused by an infinitesimal dislocation loop shown in Figure 1. By integrating the displacements caused by infinitesimal dislocation loops over a finite-sized area, one can obtain the displacement field associated with the sub-surface rectangular dislocation loop.

Bacon and Groves [21] provided a formula for the surface correction displacement term of a sub-surface infinitesimal dislocation loop, of area dS :

$$du_i^s = -kx'_3(1 - 2\delta_{j3})[A_{i3} \left(\frac{1}{R}\right)_{,ij} - \left(\frac{x_3}{R}\right)_{,ij3}] \quad (8)$$

where, $k = b_j dS/4\pi(1 - \nu)$, $A_{ij} = 2\nu + 4(1 - \nu)\delta_{ij}$, $dS = dx'_1 dx'_2$, $R^2 = (x_1 - x'_1)^2 + (x_2 - x'_2)^2 + (x_3 + x'_3)^2$. The integration for the sub-surface rectangular dislocation loop was done by [22] and won't be re-produced here for brevity. Using such solution, the surface correction term for the strain field in equation (2), can be obtained from equation (5). Once this strain field is developed, the surface correction term for the stress field in equation (3) can be obtained from equation (6).

RESULTS AND DISCUSSION

The surface correction terms for the strain and stress fields were obtained using the mathematical software Mathematica which has a very strong symbolic engine. Only the stress results are listed in the appendices (Appendix A for the b_x component, Appendix B for the b_y component, and Appendix C for the b_z component). If one is interested in the surface corrections terms for strain, which are not listed here brevity, these could be obtained from the stresses in the appendices using:

$$\epsilon_{ij} = \frac{1}{2\mu} \left(\sigma_{ij} - \frac{\lambda \delta_{ij}}{2G+3\lambda} \sigma_{kk} \right) \quad (9)$$

, where σ_{kk} is the first invariant of the stress tensor.

To verify the results, the authors embarked on several verifications: i- ensuring that the stress traction on the free surface is zero, ii- ensuring that the equilibrium equations are satisfied inside the half medium, iii- ensuring that the strain compatibility equations are satisfied inside the half medium, and iv- comparing the analytical results with numerical results from the collocation-point method described above.

Stress Traction on the Free Surface

The stress traction \vec{T} at the free surface is defined as:

$$\vec{T} = \boldsymbol{\sigma} \vec{n} \quad (10)$$

which should be $\vec{0}$ at the free surface. Here, $\boldsymbol{\sigma}$ is given by equation (3). However, the unit normal vector at the free surface is $\{0 \ 0 \ -1\}$, see Figure 1. This means from equation (10) that σ_{xz} σ_{yz} and σ_{zz} should all be zero at the surface points. To check that these three

stress components are zero on the surface, one could do one of two things. First, use equation (3) and specify $z = 0$ in it and see if it reduces to exactly 0 for each of the three stress components. Unfortunately, since the final results of equation (3) are a few pages in length, Mathematica was not able to simplify these stress components at $z = 0$ down to 0 value even if one waited more than 24 hours for the simplification. Alternatively, one can consider arbitrary lines along the x and y directions on the free surface and see if these reduce to zero. They indeed all identically reduced to zero. In addition to this analytical verification, surface or carpet plots of the three stress components on the free surface were created. This is a numerical verification as all such stress values should be zero. The plots in Figure 3 show just that.

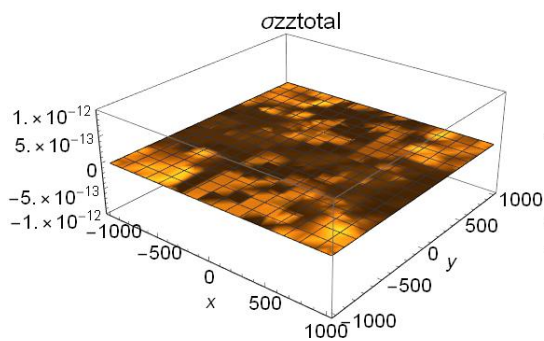


Fig.3.1. Plot of σ_{zz}

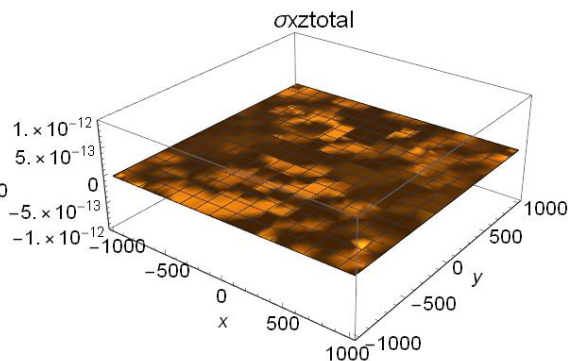


Fig.3.2. Plot of σ_{xz}

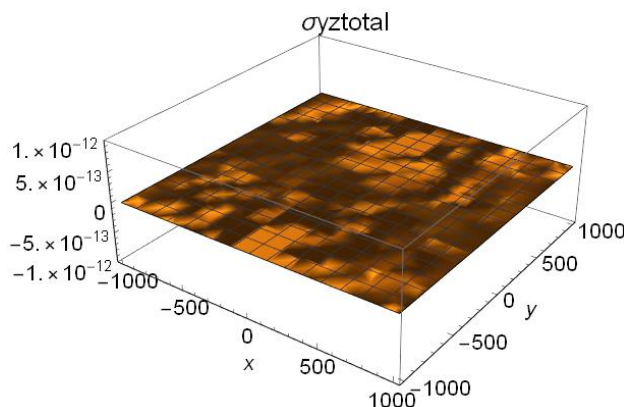


Fig.3.3. Plot of σ_{yz} .

For these plots, the following values were chosen: $a = b = 100b_z$, $c = 10b_z$, $b_x = b_y = 0$, $b_z = 1$, $\nu = 0.3$, $\mu = 100$, $z = 0$, $-10a \leq x \leq 10a$, $-10b \leq y \leq 10b$

Equations of Equilibrium

The partial differential equations of static equilibrium in a solid material are given in indicial notation by:

$$\sigma_{ij,i} = \frac{\partial \sigma_{ij}}{\partial x_i} = 0 \quad (11)$$

If one expands the last equation on the repeated indices then the resulting three explicit equations are:

$$\frac{\partial \sigma_{xx}}{\partial x} + \frac{\partial \sigma_{xy}}{\partial y} + \frac{\partial \sigma_{xz}}{\partial z} = 0 \quad (12)$$

$$\frac{\partial \sigma_{yx}}{\partial x} + \frac{\partial \sigma_{yy}}{\partial y} + \frac{\partial \sigma_{yz}}{\partial z} = 0 \quad (13)$$

$$\frac{\partial \sigma_{zx}}{\partial x} + \frac{\partial \sigma_{zy}}{\partial y} + \frac{\partial \sigma_{zz}}{\partial z} = 0 \quad (14)$$

These equations should be satisfied at every material point of a solid in equilibrium. To verify the developed stress solution σ given by equation (3), one can see if equations (12-14) are identically zero either using analytical or numerical methods. For the analytical method, the equations are so humungous that Mathematica is not able to simplify them to 0. However, for any given line in space along the x -, y - or z -directions, Mathematica identically simplifies the equilibrium equations to zero. Hence analytical verification of the equilibrium equations is possible. Alternatively, numerical verifications can also be made by plotting equations (12-14) along any plane in the material to see if the equations give a zero result. Figure 4 shows such plotting for $b_y \neq 0$ right below the sub-surface dislocation loop. The figure shows that the equilibrium equations are satisfied. Note that given the combination of Burgers vector components and equilibrium equations a total of nine plots are minimally generated. However, only three plots for one of the Burgers vector components are shown here for brevity.

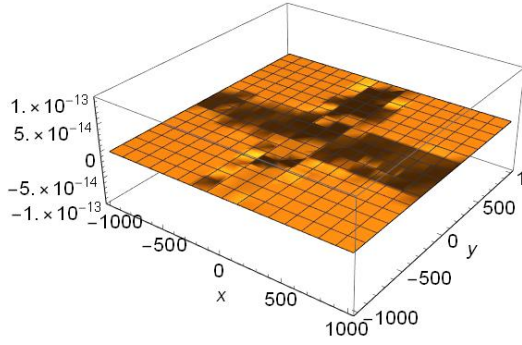


Fig. 4.1. Plot of equation (12)

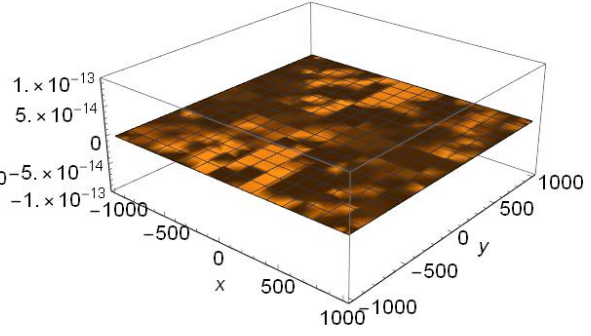


Fig. 4.2. Plot of equation (13)

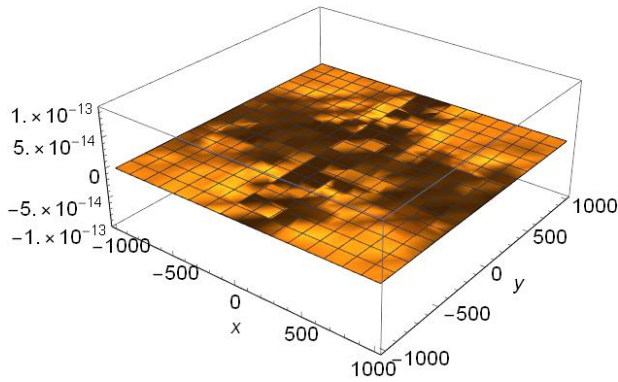


Figure. 4.3. Plot of equation (14). For these plots, the following values were chosen: $a = b = 100b_y$, $c = 10b_y$, $b_x = b_z = 0$, $b_y = 1$, $\nu = 0.3$, $\mu = 100$, $z = 11b_y$ $-10a \leq x \leq 10a$, $-10b \leq y \leq 10b$

Strain Compatibility Equations

The equations of compatibility can be written in indicial notation as [34]:

$$\epsilon_{ij,kl} - \epsilon_{jl,ik} - \epsilon_{ik,jl} + \epsilon_{kl,ij} = 0 \quad (15)$$

This equation can be expanded over the repeated indices and written explicitly as six different/unique equations:

$$\frac{\partial^2 \epsilon_{xx}}{\partial y^2} + \frac{\partial^2 \epsilon_{yy}}{\partial x^2} = 2 \frac{\partial^2 \epsilon_{xy}}{\partial x \partial y} \quad (16)$$

$$\frac{\partial^2 \epsilon_{xx}}{\partial z^2} + \frac{\partial^2 \epsilon_{zz}}{\partial x^2} = 2 \frac{\partial^2 \epsilon_{xz}}{\partial x \partial z} \quad (17)$$

$$\frac{\partial^2 \epsilon_{zz}}{\partial y^2} + \frac{\partial^2 \epsilon_{yy}}{\partial z^2} = 2 \frac{\partial^2 \epsilon_{zy}}{\partial z \partial y} \quad (18)$$

$$\frac{\partial^2 \epsilon_{xx}}{\partial y \partial z} + \frac{\partial^2 \epsilon_{yz}}{\partial x^2} = \frac{\partial^2 \epsilon_{xz}}{\partial x \partial y} + \frac{\partial^2 \epsilon_{xy}}{\partial x \partial z} \quad (19)$$

$$\frac{\partial^2 \epsilon_{yy}}{\partial x \partial z} + \frac{\partial^2 \epsilon_{xz}}{\partial y^2} = \frac{\partial^2 \epsilon_{xy}}{\partial y \partial z} + \frac{\partial^2 \epsilon_{yz}}{\partial x \partial y} \quad (20)$$

$$\frac{\partial^2 \epsilon_{zz}}{\partial x \partial y} + \frac{\partial^2 \epsilon_{xy}}{\partial z^2} = \frac{\partial^2 \epsilon_{xz}}{\partial y \partial z} + \frac{\partial^2 \epsilon_{yz}}{\partial x \partial z} \quad (21)$$

These equations should be satisfied at every material point of a solid. To verify the developed stress solution ϵ given by equation (2), one can see if equations (16-21) are identically zero either using analytical or numerical methods. For the analytical method again, the equations are so large that Mathematica is not able to simplify them to 0. However, for any given line in space along the x -, y - or z -directions, Mathematica identically simplifies the compatibility equations to zero. Hence analytical verification of the compatibility equations is possible. Alternatively, numerical verifications can also be made by plotting equations (16-21) along any plane in the material to see if the equations give a zero result. Figure 5 shows such plotting for $b_x \neq 0$ right below the sub-surface dislocation loop. The figure shows that the compatibility equations are satisfied. Note that given the combination of Burgers vector components and compatibility equations a total of eighteen plots are minimally generated. However, only three plots for one of the Burgers vector components are shown here for brevity.

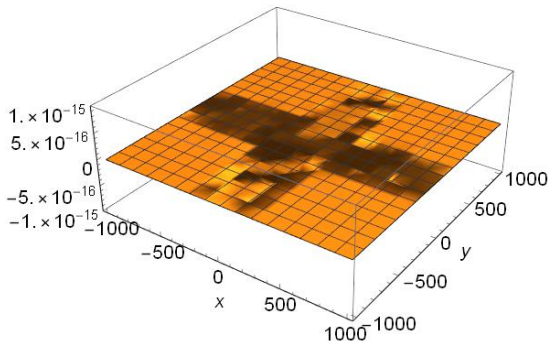


Fig. 5.1. Plot of equation (16)

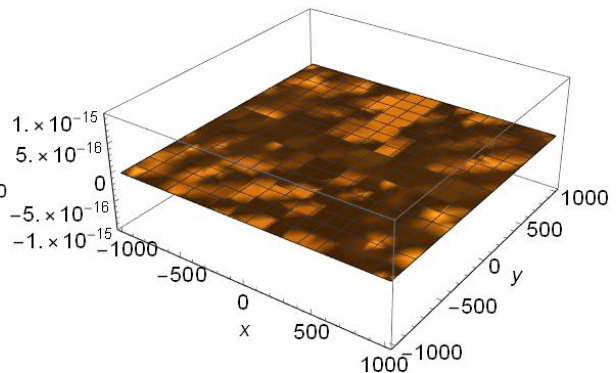


Fig. 5.2. Plot of equation (17)

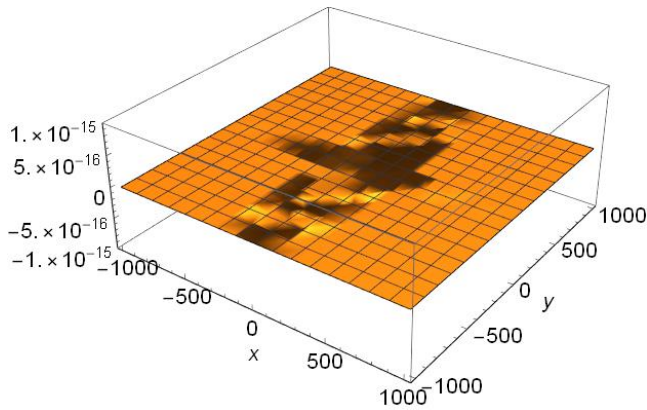


Fig. 5.3. Plot of equation (18). For these plots, the following values were chosen: $a = b = 100b_x$, $c = 10b_x$, $b_y = b_z = 0$, $b_x = 1$, $\nu = 0.3$, $\mu = G = 100$, $z = 11b_x$, $-10a \leq x \leq 10a$, $-10b \leq y \leq 10b$

Comparison with the numerical “collocation point” method

As mentioned above, the “collocation point” method is a numerical method that can work in tandem with the infinite stress/strain terms to find the strain and stress fields in equations (2) and (3). This numerical method works for any sub-surface dislocation geometry or inclination and not just horizontal dislocations or loops. To compare with this method, the following parameters were taken followed by stress components comparison between analytical and numerical solutions in Figures 6-15:

$$a = b = 100, c = 400|\mathbf{b}|, \nu = 0.3, z = 200|\mathbf{b}|, -10a \leq x \leq 10a, -10b \leq y \leq 10b$$

The figures show perfect match between the analytical and numerical solutions.

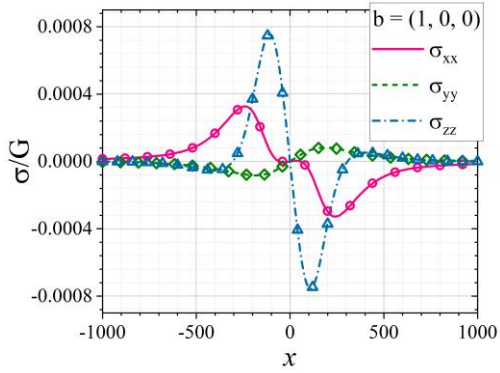


Fig.6.

Fig.6. Comparison of analytical solutions (solid and dashed lines) to the results of the numerical “collocation point” method (symbols) along x -direction for non-zero b_x

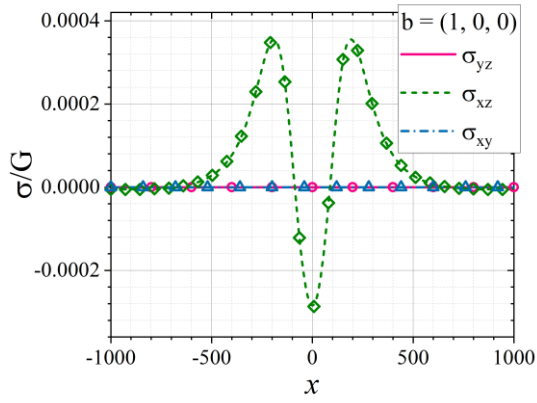


Fig.7.

Fig.7. Comparison of analytical solutions (solid and dashed lines) to the results of the numerical “collocation point” method (symbols) along x -direction for non-zero b_x

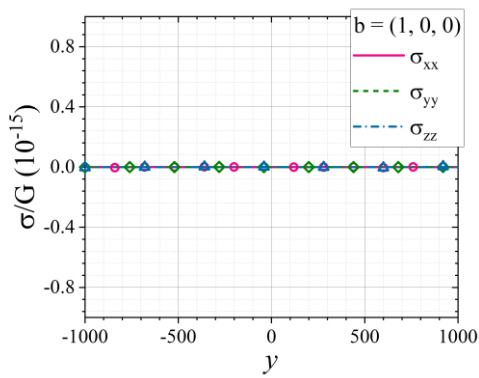


Fig.8.

Fig.8. Comparison of analytical solutions (solid and dashed lines) to the results of the numerical “collocation point” method (symbols) along y -direction for non-zero b_x

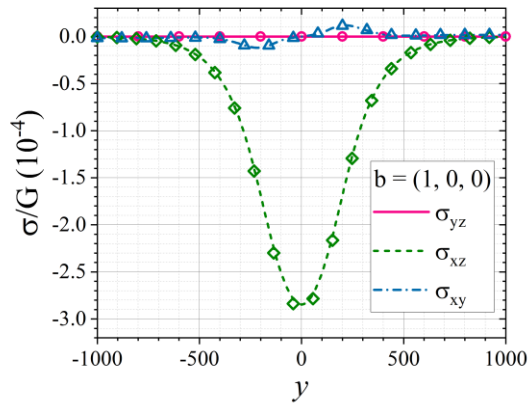


Fig.9.

Fig.9. Comparison of analytical solutions (solid and dashed lines) to the results of the numerical “collocation point” method (symbols) along y -direction for non-zero b_x

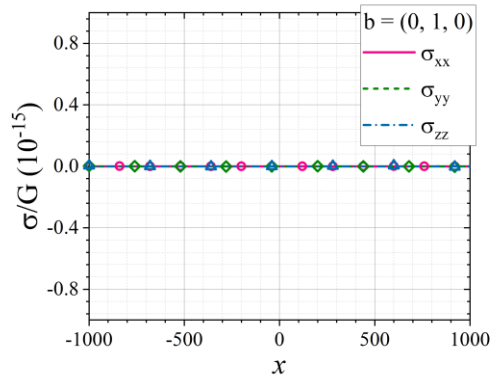


Fig.10.

Fig.10. Comparison of analytical solutions (solid and dashed lines) to the results of the numerical “collocation point” method (symbols) along x -direction for non-zero b_y

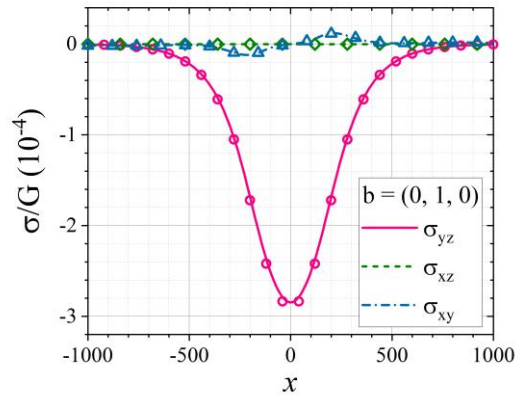


Fig.11.

Fig.11. Comparison of analytical solutions (solid and dashed lines) to the results of the numerical “collocation point” method (symbols) along x -direction for non-zero b_y

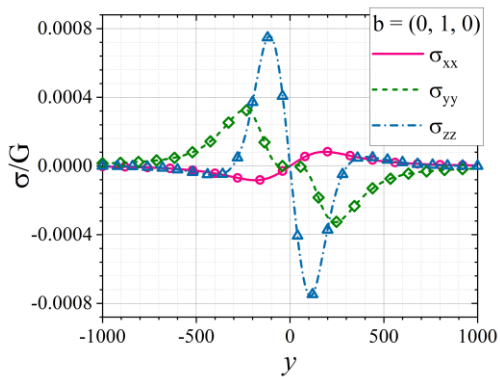


Fig.12.

Fig.12. Comparison of analytical solutions (solid and dashed lines) to the results of the numerical “collocation point” method (symbols) along y -direction for non-zero b_y

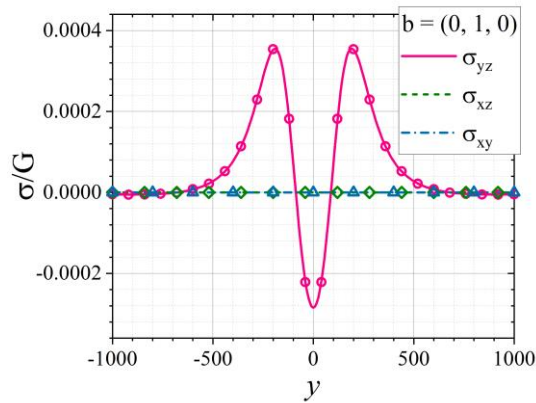


Fig.13.

Fig.13. Comparison of analytical solutions (solid and dashed lines) to the results of the numerical “collocation point” method (symbols) along y -direction for non-zero b_y

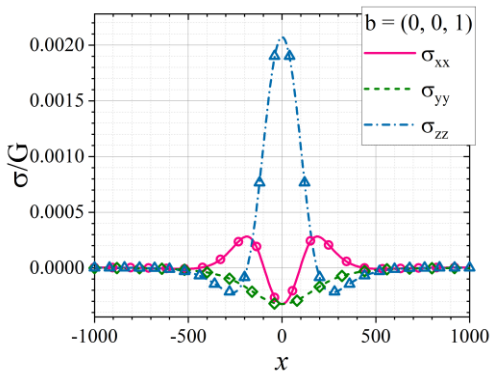


Fig.14.

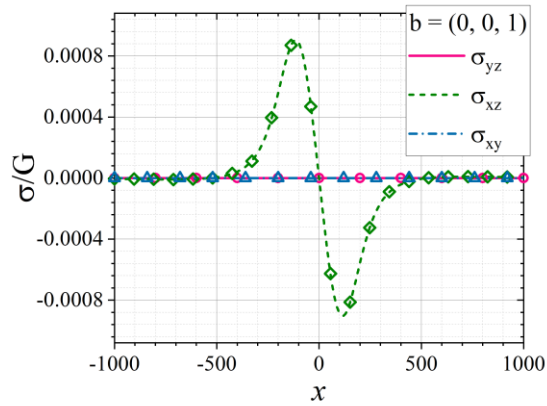


Fig.15.

Fig.14. Comparison of analytical solutions (solid and dashed lines) to the results of the numerical “collocation point” method (symbols) along x -direction for non-zero b_z

Fig.15. Comparison of analytical solutions (solid and dashed lines) to the results of the numerical “collocation point” method (symbols) along x -direction for non-zero b_z

CONCLUSIONS

In conclusion, the strain and stress fields associated with a sub-surface rectangular dislocation loop that is parallel to the free surface of a semi-infinite solid have been developed. These are obtained from three different contributions or terms: a term associated with the loop being in an infinite medium, another term associated with an opposite Burgers vector image loop, and the third from surface correction terms. The infinite terms and the surface correction terms were developed here.

The developed field solutions were verified using analytical equations and numerical comparisons. The verifications were to ensure satisfaction of the zero-traction boundary condition on the free surface, the satisfaction of the equilibrium equations, the satisfaction of the strain compatibility equations, and comparisons against numerical results from the proven “collocation point” numerical method.

APPENDICES

APPENDIX A

The surface correction terms for stress considering only b_x (the x -component of the Burgers vector):

$$\begin{aligned}
 \frac{\sigma_{xx}}{\mu} = & \frac{1}{2K\pi} b_x c \left(K2 \left(\frac{Q3}{\sqrt{A2B1}} - \frac{Q3}{\sqrt{A4B2}} - \frac{2Q1^2Q3}{\sqrt{A2B1^2}} - \frac{Q1^2Q3}{A2^{3/2}B1} + \frac{2Q2^2Q3}{\sqrt{A4B2^2}} + \frac{Q2^2Q3}{A4^{3/2}B2} - \frac{Q4}{\sqrt{A1B1}} + \frac{Q4}{\sqrt{A3B2}} + \frac{2Q1^2Q4}{\sqrt{A1B1^2}} + \frac{Q1^2Q4}{A1^{3/2}B1} - \right. \right. \\
 & \left. \frac{2Q2^2Q4}{\sqrt{A3B2^2}} - \frac{Q2^2Q4}{A3^{3/2}B2} \right) + \frac{6pQ1^2Q3z}{A2^{3/2}B1^2} - \frac{6pQ2^2Q3z}{A4^{3/2}B2^2} - \frac{6pQ1^2Q4z}{A1^{3/2}B1^2} + \frac{6pQ2^2Q4z}{A3^{3/2}B2^2} - \frac{pQ4(3A1-Q4^2)z}{A1^{3/2}B1^2} + \frac{4pQ1^2Q4(3A1-Q4^2)z}{A1^{3/2}B1^3} + \\
 & \frac{3pQ1^2Q4(3A1-Q4^2)z}{A1^{5/2}B1^2} + \frac{pQ4(3A3-Q4^2)z}{A3^{3/2}B2^2} - \frac{4pQ2^2Q4(3A3-Q4^2)z}{A3^{3/2}B2^3} - \frac{3pQ2^2Q4(3A3-Q4^2)z}{A3^{5/2}B2^2} + \frac{pQ3S1z}{A2^{3/2}B1^2} - \frac{4pQ1^2Q3S1z}{A2^{3/2}B1^3} - \\
 & \frac{3pQ1^2Q3S1z}{A2^{5/2}B1^2} - \frac{pQ3S2z}{A4^{3/2}B2^2} + \frac{4pQ2^2Q3S2z}{A4^{3/2}B2^3} + \frac{3pQ2^2Q3S2z}{A4^{5/2}B2^2} \Big) - \frac{1}{K2} 2\nu \left(-\frac{1}{4K\pi} b_x c \left(-\frac{K2Q3}{\sqrt{A2B1}} + \frac{K2Q3}{\sqrt{A4B2}} - \frac{2K4pQ3}{\sqrt{A2B1^2}} - \frac{K4pQ3}{A2^{3/2}B1} + \right. \right. \\
 & \left. \frac{2K4pQ3}{\sqrt{A4B2^2}} + \frac{K4pQ3}{A4^{3/2}B2} + \frac{K2Q4}{\sqrt{A1B1}} - \frac{K2Q4}{\sqrt{A3B2}} + \frac{2K4pQ4}{\sqrt{A1B1^2}} + \frac{K4pQ4}{A1^{3/2}B1} - \frac{2K4pQ4}{\sqrt{A3B2^2}} - \frac{K4pQ4}{A3^{3/2}B2} - \frac{p^2Q4(3A1-Q4^2)}{A1^{3/2}B1^2} + \frac{p^2Q4(3A3-Q4^2)}{A3^{3/2}B2^2} + \right. \\
 & \left. \frac{p^2Q3S1}{A2^{3/2}B1^2} - \frac{p^2Q3S2}{A4^{3/2}B2^2} + \frac{6p^3Q3z}{A2^{3/2}B1^2} - \frac{6p^3Q3z}{A4^{3/2}B2^2} - \frac{6p^3Q4z}{A1^{3/2}B1^2} + \frac{6p^3Q4z}{A3^{3/2}B2^2} - \frac{2pQ4(3A1-Q4^2)z}{A1^{3/2}B1^2} + \frac{4p^3Q4(3A1-Q4^2)z}{A1^{3/2}B1^3} + \right. \\
 & \left. \frac{3p^3Q4(3A1-Q4^2)z}{A1^{5/2}B1^2} + \frac{2pQ4(3A3-Q4^2)z}{A3^{3/2}B2^2} - \frac{4p^3Q4(3A3-Q4^2)z}{A3^{3/2}B2^3} - \frac{3p^3Q4(3A3-Q4^2)z}{A3^{5/2}B2^2} + \frac{2pQ3S1z}{A2^{3/2}B1^2} - \frac{4p^3Q3S1z}{A2^{3/2}B1^3} - \frac{3p^3Q3S1z}{A2^{5/2}B1^2} - \right. \\
 & \left. \frac{2pQ3S2z}{A4^{3/2}B2^2} + \frac{4p^3Q3S2z}{A4^{3/2}B2^3} + \frac{3p^3Q3S2z}{A4^{5/2}B2^2} \right) - \frac{1}{4K\pi} b_x c \left(K2 \left(\frac{Q3}{\sqrt{A2B1}} - \frac{Q3}{\sqrt{A4B2}} - \frac{2Q1^2Q3}{\sqrt{A2B1^2}} - \frac{Q1^2Q3}{A2^{3/2}B1} + \frac{2Q2^2Q3}{\sqrt{A4B2^2}} + \frac{Q2^2Q3}{A4^{3/2}B2} - \frac{Q4}{\sqrt{A1B1}} + \right. \right. \\
 & \left. \frac{Q4}{\sqrt{A3B2}} + \frac{2Q1^2Q4}{\sqrt{A1B1^2}} + \frac{Q1^2Q4}{A1^{3/2}B1} - \frac{2Q2^2Q4}{\sqrt{A3B2^2}} - \frac{Q2^2Q4}{A3^{3/2}B2} \right) + \frac{6pQ1^2Q3z}{A2^{3/2}B1^2} - \frac{6pQ2^2Q3z}{A4^{3/2}B2^2} - \frac{6pQ1^2Q4z}{A1^{3/2}B1^2} + \frac{6pQ2^2Q4z}{A3^{3/2}B2^2} - \frac{pQ4(3A1-Q4^2)z}{A1^{3/2}B1^2} + \\
 & \frac{4pQ1^2Q4(3A1-Q4^2)z}{A1^{3/2}B1^3} + \frac{3pQ1^2Q4(3A1-Q4^2)z}{A1^{5/2}B1^2} + \frac{pQ4(3A3-Q4^2)z}{A3^{3/2}B2^2} - \frac{4pQ2^2Q4(3A3-Q4^2)z}{A3^{3/2}B2^3} - \frac{3pQ2^2Q4(3A3-Q4^2)z}{A3^{5/2}B2^2} + \frac{pQ3S1z}{A2^{3/2}B1^2} - \\
 & \frac{4pQ1^2Q3S1z}{A2^{3/2}B1^3} - \frac{3pQ1^2Q3S1z}{A2^{5/2}B1^2} - \frac{pQ3S2z}{A4^{3/2}B2^2} + \frac{4pQ2^2Q3S2z}{A4^{3/2}B2^3} + \frac{3pQ2^2Q3S2z}{A4^{5/2}B2^2} \Big) + \frac{b_x c}{-4\pi K} \left(K2 \left(\frac{Q3}{A2^{3/2}} - \frac{Q3}{A4^{3/2}} - \frac{Q4}{A1^{3/2}} + \frac{Q4}{A3^{3/2}} \right) + \right. \\
 & \left. \frac{3pQ3z}{A2^{5/2}} - \frac{3pQ3z}{A4^{5/2}} - \frac{3pQ4z}{A1^{5/2}} + \frac{3pQ4z}{A3^{5/2}} \right); \\
 \frac{\sigma_{yy}}{\mu} = & \frac{b_x}{2K\pi} c \left(K2 \left(\frac{Q3}{A2^{3/2}} - \frac{Q3}{A4^{3/2}} - \frac{Q4}{A1^{3/2}} + \frac{Q4}{A3^{3/2}} \right) + \frac{3pQ3z}{A2^{5/2}} - \frac{3pQ3z}{A4^{5/2}} - \frac{3pQ4z}{A1^{5/2}} + \frac{3pQ4z}{A3^{5/2}} \right) - \frac{1}{K2} 2\nu \left(-\frac{1}{4K\pi} b_x c \left(-\frac{K2Q3}{\sqrt{A2B1}} + \right. \right. \\
 & \left. \frac{K2Q3}{\sqrt{A4B2}} - \frac{2K4pQ3}{\sqrt{A2B1^2}} - \frac{K4pQ3}{A2^{3/2}B1} + \frac{2K4pQ3}{\sqrt{A4B2^2}} + \frac{K4pQ3}{A4^{3/2}B2} + \frac{K2Q4}{\sqrt{A1B1}} - \frac{K2Q4}{\sqrt{A3B2}} + \frac{2K4pQ4}{\sqrt{A1B1^2}} + \frac{K4pQ4}{A1^{3/2}B1} - \frac{2K4pQ4}{\sqrt{A3B2^2}} - \frac{K4pQ4}{A3^{3/2}B2} - \right. \\
 & \left. \frac{p^2Q4(3A1-Q4^2)}{A1^{3/2}B1^2} + \frac{p^2Q4(3A3-Q4^2)}{A3^{3/2}B2^2} + \frac{p^2Q3S1}{A2^{3/2}B1^2} - \frac{p^2Q3S2}{A4^{3/2}B2^2} + \frac{6p^3Q3z}{A2^{3/2}B1^2} - \frac{6p^3Q3z}{A4^{3/2}B2^2} - \frac{6p^3Q4z}{A1^{3/2}B1^2} + \frac{6p^3Q4z}{A3^{3/2}B2^2} - \right. \\
 & \left. \frac{2pQ4(3A1-Q4^2)z}{A1^{3/2}B1^2} + \frac{4p^3Q4(3A1-Q4^2)z}{A1^{3/2}B1^3} + \frac{3p^3Q4(3A1-Q4^2)z}{A1^{5/2}B1^2} + \frac{2pQ4(3A3-Q4^2)z}{A3^{3/2}B2^2} - \frac{4p^3Q4(3A3-Q4^2)z}{A3^{3/2}B2^3} - \frac{3p^3Q4(3A3-Q4^2)z}{A3^{5/2}B2^2} + \right. \\
 & \left. \frac{2pQ3S1z}{A2^{3/2}B1^2} - \frac{4p^3Q3S1z}{A2^{3/2}B1^3} - \frac{3p^3Q3S1z}{A2^{5/2}B1^2} - \frac{2pQ3S2z}{A4^{3/2}B2^2} + \frac{4p^3Q3S2z}{A4^{3/2}B2^3} + \frac{3p^3Q3S2z}{A4^{5/2}B2^2} \right) - \frac{1}{4K\pi} b_x c \left(K2 \left(\frac{Q3}{\sqrt{A2B1}} - \frac{Q3}{\sqrt{A4B2}} - \frac{2Q1^2Q3}{\sqrt{A2B1^2}} - \right. \right. \\
 & \left. \frac{Q1^2Q3}{A2^{3/2}B1} + \frac{2Q2^2Q3}{\sqrt{A4B2^2}} + \frac{Q2^2Q3}{A4^{3/2}B2} - \frac{Q4}{\sqrt{A1B1}} + \frac{Q4}{\sqrt{A3B2}} + \frac{2Q1^2Q4}{\sqrt{A1B1^2}} + \frac{Q1^2Q4}{A1^{3/2}B1} - \frac{2Q2^2Q4}{\sqrt{A3B2^2}} - \frac{Q2^2Q4}{A3^{3/2}B2} \right) + \frac{6pQ1^2Q3z}{A2^{3/2}B1^2} - \frac{6pQ2^2Q3z}{A4^{3/2}B2^2} - \\
 & \frac{6pQ1^2Q4z}{A1^{3/2}B1^2} + \frac{6pQ2^2Q4z}{A3^{3/2}B2^2} - \frac{pQ4(3A1-Q4^2)z}{A1^{3/2}B1^2} + \frac{4pQ1^2Q4(3A1-Q4^2)z}{A1^{3/2}B1^3} + \frac{3pQ1^2Q4(3A1-Q4^2)z}{A1^{5/2}B1^2} + \frac{pQ4(3A3-Q4^2)z}{A3^{3/2}B2^2} - \\
 & \frac{4pQ2^2Q4(3A3-Q4^2)z}{A3^{3/2}B2^3} - \frac{3pQ2^2Q4(3A3-Q4^2)z}{A3^{5/2}B2^2} + \frac{pQ3S1z}{A2^{3/2}B1^2} - \frac{4pQ1^2Q3S1z}{A2^{3/2}B1^3} - \frac{3pQ1^2Q3S1z}{A2^{5/2}B1^2} - \frac{pQ3S2z}{A4^{3/2}B2^2} + \frac{4pQ2^2Q3S2z}{A4^{3/2}B2^3} + \\
 & \left. \frac{3pQ2^2Q3S2z}{A4^{5/2}B2^2} \right) - \frac{b_x c}{4\pi K} \left(K2 \left(\frac{Q3}{A2^{3/2}} - \frac{Q3}{A4^{3/2}} - \frac{Q4}{A1^{3/2}} + \frac{Q4}{A3^{3/2}} \right) + \frac{3pQ3z}{A2^{5/2}} - \frac{3pQ3z}{A4^{5/2}} - \frac{3pQ4z}{A1^{5/2}} + \frac{3pQ4z}{A3^{5/2}} \right);
 \end{aligned}$$

$$\begin{aligned}
\frac{\sigma_{zz}}{\mu} = & \frac{1}{2K\pi} b_x c \left(-\frac{K2Q3}{\sqrt{A2B1}} + \frac{K2Q3}{\sqrt{A4B2}} - \frac{2G1pQ3}{\sqrt{A2B1^2}} - \frac{G1pQ3}{A2^{3/2}B1} + \frac{2G1pQ3}{\sqrt{A4B2^2}} + \frac{G1pQ3}{A4^{3/2}B2} + \frac{K2Q4}{\sqrt{A1B1}} - \frac{K2Q4}{\sqrt{A3B2}} + \frac{2G1pQ4}{\sqrt{A1B1^2}} + \frac{G1pQ4}{A1^{3/2}B1} - \right. \\
& \frac{2G1pQ4}{\sqrt{A3B2^2}} - \frac{G1pQ4}{A3^{3/2}B2} - \frac{p^2Q4(3A1-Q4^2)}{A1^{3/2}B1^2} + \frac{p^2Q4(3A3-Q4^2)}{A3^{3/2}B2^2} + \frac{p^2Q3S1}{A2^{3/2}B1^2} - \frac{p^2Q3S2}{A4^{3/2}B2^2} + \frac{6p^3Q3z}{A2^{3/2}B1^2} - \frac{6p^3Q3z}{A4^{3/2}B2^2} - \frac{6p^3Q4z}{A1^{3/2}B1^2} + \\
& \frac{6p^3Q4z}{A3^{3/2}B2^2} - \frac{2pQ4(3A1-Q4^2)z}{A1^{3/2}B1^2} + \frac{4p^3Q4(3A1-Q4^2)z}{A1^{3/2}B1^3} + \frac{3p^3Q4(3A1-Q4^2)z}{A1^{5/2}B1^2} + \frac{2pQ4(3A3-Q4^2)z}{A3^{3/2}B2^2} - \frac{4p^3Q4(3A3-Q4^2)z}{A3^{3/2}B2^3} - \\
& \left. \frac{3p^3Q4(3A3-Q4^2)z}{A3^{5/2}B2^2} + \frac{2pQ3S1z}{A2^{3/2}B1^2} - \frac{4p^3Q3S1z}{A2^{3/2}B1^3} - \frac{3p^3Q3S1z}{A2^{5/2}B1^2} - \frac{2pQ3S2z}{A4^{3/2}B2^2} + \frac{4p^3Q3S2z}{A4^{3/2}B2^3} + \frac{3p^3Q3S2z}{A4^{5/2}B2^2} \right) - \\
\frac{1}{K2} 2\nu \left(-\frac{1}{4K\pi} b_x c \left(-\frac{K2Q3}{\sqrt{A2B1}} + \frac{K2Q3}{\sqrt{A4B2}} - \frac{2K4pQ3}{\sqrt{A2B1^2}} - \frac{K4pQ3}{A2^{3/2}B1} + \frac{2K4pQ3}{\sqrt{A4B2^2}} + \frac{K4pQ3}{A4^{3/2}B2} + \frac{K2Q4}{\sqrt{A1B1}} - \frac{K2Q4}{\sqrt{A3B2}} + \frac{2K4pQ4}{\sqrt{A1B1^2}} + \frac{K4pQ4}{A1^{3/2}B1} - \right. \right. \\
& \frac{2K4pQ4}{\sqrt{A3B2^2}} - \frac{K4pQ4}{A3^{3/2}B2} - \frac{p^2Q4(3A1-Q4^2)}{A1^{3/2}B1^2} + \frac{p^2Q4(3A3-Q4^2)}{A3^{3/2}B2^2} + \frac{p^2Q3S1}{A2^{3/2}B1^2} - \frac{p^2Q3S2}{A4^{3/2}B2^2} + \frac{6p^3Q3z}{A2^{3/2}B1^2} - \frac{6p^3Q3z}{A4^{3/2}B2^2} - \frac{6p^3Q4z}{A1^{3/2}B1^2} + \\
& \frac{6p^3Q4z}{A3^{3/2}B2^2} - \frac{2pQ4(3A1-Q4^2)z}{A1^{3/2}B1^2} + \frac{4p^3Q4(3A1-Q4^2)z}{A1^{3/2}B1^3} + \frac{3p^3Q4(3A1-Q4^2)z}{A1^{5/2}B1^2} + \frac{2pQ4(3A3-Q4^2)z}{A3^{3/2}B2^2} - \frac{4p^3Q4(3A3-Q4^2)z}{A3^{3/2}B2^3} - \\
& \left. \frac{3p^3Q4(3A3-Q4^2)z}{A3^{5/2}B2^2} + \frac{2pQ3S1z}{A2^{3/2}B1^2} - \frac{4p^3Q3S1z}{A2^{3/2}B1^3} - \frac{3p^3Q3S1z}{A2^{5/2}B1^2} - \frac{2pQ3S2z}{A4^{3/2}B2^2} + \frac{4p^3Q3S2z}{A4^{3/2}B2^3} + \frac{3p^3Q3S2z}{A4^{5/2}B2^2} \right) - \frac{1}{4K\pi} b_x c \left(K2 \left(\frac{Q3}{\sqrt{A2B1}} - \right. \right. \\
& \frac{Q3}{\sqrt{A4B2}} - \frac{2Q1^2Q3}{\sqrt{A2B1^2}} - \frac{Q1^2Q3}{A2^{3/2}B1} + \frac{2Q2^2Q3}{\sqrt{A4B2^2}} + \frac{Q2^2Q3}{A4^{3/2}B2} - \frac{Q4}{\sqrt{A1B1}} + \frac{Q4}{\sqrt{A3B2}} + \frac{2Q1^2Q4}{\sqrt{A1B1^2}} + \frac{Q1^2Q4}{A1^{3/2}B1} - \frac{2Q2^2Q4}{\sqrt{A3B2^2}} - \frac{Q2^2Q4}{A3^{3/2}B2} \Big) + \\
& \frac{6pQ1^2Q3z}{A2^{3/2}B1^2} - \frac{6pQ2^2Q3z}{A4^{3/2}B2^2} - \frac{6pQ1^2Q4z}{A1^{3/2}B1^2} + \frac{6pQ2^2Q4z}{A3^{3/2}B2^2} - \frac{pQ4(3A1-Q4^2)z}{A1^{3/2}B1^2} + \frac{4pQ1^2Q4(3A1-Q4^2)z}{A1^{3/2}B1^3} + \frac{3pQ1^2Q4(3A1-Q4^2)z}{A1^{5/2}B1^2} + \\
& \frac{pQ4(3A3-Q4^2)z}{A3^{3/2}B2^2} - \frac{4pQ2^2Q4(3A3-Q4^2)z}{A3^{3/2}B2^3} - \frac{3pQ2^2Q4(3A3-Q4^2)z}{A3^{5/2}B2^2} + \frac{pQ3S1z}{A2^{3/2}B1^2} - \frac{4pQ1^2Q3S1z}{A2^{3/2}B1^3} - \frac{3pQ1^2Q3S1z}{A2^{5/2}B1^2} - \frac{pQ3S2z}{A4^{3/2}B2^2} + \\
& \left. \frac{4pQ2^2Q3S2z}{A4^{3/2}B2^3} + \frac{3pQ2^2Q3S2z}{A4^{5/2}B2^2} \right) + \frac{b_x c}{-4\pi K} \left(K2 \left(\frac{Q3}{A2^{3/2}} - \frac{Q3}{A4^{3/2}} - \frac{Q4}{A1^{3/2}} + \frac{Q4}{A3^{3/2}} \right) + \frac{3pQ3z}{A2^{5/2}} - \frac{3pQ3z}{A4^{5/2}} - \frac{3pQ4z}{A1^{5/2}} + \frac{3pQ4z}{A3^{5/2}} \right); \\
\frac{\sigma_{xy}}{\mu} = & \frac{b_x c}{4K\pi} \left(K2 \left(\frac{Q1}{A1^{3/2}} - \frac{Q1}{A2^{3/2}} + \frac{Q2}{A3^{3/2}} - \frac{Q2}{A4^{3/2}} \right) + \frac{3pQ1z}{A1^{5/2}} - \frac{3pQ1z}{A2^{5/2}} + \frac{3pQ2z}{A3^{5/2}} - \frac{3pQ2z}{A4^{5/2}} \right) + \frac{1}{4K\pi} b_x c \left(K2 \left(\frac{Q1}{\sqrt{A1B1}} - \frac{Q1}{\sqrt{A2B1}} + \right. \right. \\
& \frac{Q2}{\sqrt{A3B2}} - \frac{Q2}{\sqrt{A4B2}} + \frac{Q1Q3^2}{A2^{3/2}B1} + \frac{Q2Q3^2}{A4^{3/2}B2} - \frac{Q1Q4^2}{A1^{3/2}B1} - \frac{Q2Q4^2}{A3^{3/2}B2} \Big) - \frac{4pQ1Q3^2z}{A2^{3/2}B1^2} - \frac{4pQ2Q3^2z}{A4^{3/2}B2^2} + \frac{4pQ1Q4^2z}{A1^{3/2}B1^2} + \frac{4pQ2Q4^2z}{A3^{3/2}B2^2} + \\
& \frac{pQ1(3A1-Q4^2)z}{A1^{3/2}B1^2} - \frac{3pQ1Q4^2(3A1-Q4^2)z}{A1^{5/2}B1^2} + \frac{pQ2(3A3-Q4^2)z}{A3^{3/2}B2^2} - \frac{3pQ2Q4^2(3A3-Q4^2)z}{A3^{5/2}B2^2} - \frac{pQ1S1z}{A2^{3/2}B1^2} + \frac{3pQ1Q3^2S1z}{A2^{5/2}B1^2} - \frac{pQ2S2z}{A4^{3/2}B2^2} + \\
& \left. \frac{3pQ2Q3^2S2z}{A4^{5/2}B2^2} \right); \\
\frac{\sigma_{xz}}{\mu} = & \frac{1}{4K\pi} b_x c \left(\frac{2G1Q1Q3}{\sqrt{A2B1^2}} + \frac{G1Q1Q3}{A2^{3/2}B1} + \frac{2G1Q2Q3}{\sqrt{A4B2^2}} + \frac{G1Q2Q3}{A4^{3/2}B2} - \frac{2G1Q1Q4}{\sqrt{A1B1^2}} - \frac{G1Q1Q4}{A1^{3/2}B1} - \frac{2G1Q2Q4}{\sqrt{A3B2^2}} - \frac{G1Q2Q4}{A3^{3/2}B2} - \frac{6p^2Q1Q3z}{A2^{3/2}B1^2} - \right. \\
& \frac{6p^2Q2Q3z}{A4^{3/2}B2^2} + \frac{6p^2Q1Q4z}{A1^{3/2}B1^2} + \frac{6p^2Q2Q4z}{A3^{3/2}B2^2} - \frac{4p^2Q1Q4(3A1-Q4^2)z}{A1^{3/2}B1^3} - \frac{3p^2Q1Q4(3A1-Q4^2)z}{A1^{5/2}B1^2} - \frac{4p^2Q2Q4(3A3-Q4^2)z}{A3^{3/2}B2^3} - \\
& \frac{3p^2Q2Q4(3A3-Q4^2)z}{A3^{5/2}B2^2} + \frac{4p^2Q1Q3S1z}{A2^{3/2}B1^3} + \frac{3p^2Q1Q3S1z}{A2^{5/2}B1^2} + \frac{4p^2Q2Q3S2z}{A4^{3/2}B2^3} + \frac{3p^2Q2Q3S2z}{A4^{5/2}B2^2} \Big) + \frac{1}{4K\pi} b_x c \left(K2 \left(\frac{2pQ1Q3}{\sqrt{A2B1^2}} + \frac{pQ1Q3}{A2^{3/2}B1} + \right. \right. \\
& \frac{2pQ2Q3}{\sqrt{A4B2^2}} + \frac{pQ2Q3}{A4^{3/2}B2} - \frac{2pQ1Q4}{\sqrt{A1B1^2}} - \frac{pQ1Q4}{A1^{3/2}B1} - \frac{2pQ2Q4}{\sqrt{A3B2^2}} - \frac{pQ2Q4}{A3^{3/2}B2} \Big) + \frac{pQ1Q4(3A1-Q4^2)}{A1^{3/2}B1^2} + \frac{pQ2Q4(3A3-Q4^2)}{A3^{3/2}B2^2} - \frac{pQ1Q3S1}{A2^{3/2}B1^2} - \\
& \frac{pQ2Q3S2}{A4^{3/2}B2^2} - \frac{6p^2Q1Q3z}{A2^{3/2}B1^2} - \frac{6p^2Q2Q3z}{A4^{3/2}B2^2} + \frac{6p^2Q1Q4z}{A1^{3/2}B1^2} + \frac{6p^2Q2Q4z}{A3^{3/2}B2^2} + \frac{Q1Q4(3A1-Q4^2)z}{A1^{3/2}B1^2} - \frac{4p^2Q1Q4(3A1-Q4^2)z}{A1^{3/2}B1^3} - \\
& \frac{3p^2Q1Q4(3A1-Q4^2)z}{A1^{5/2}B1^2} + \frac{Q2Q4(3A3-Q4^2)z}{A3^{3/2}B2^2} - \frac{4p^2Q2Q4(3A3-Q4^2)z}{A3^{3/2}B2^3} - \frac{3p^2Q2Q4(3A3-Q4^2)z}{A3^{5/2}B2^2} - \frac{Q1Q3S1z}{A2^{3/2}B1^2} + \frac{4p^2Q1Q3S1z}{A2^{3/2}B1^3} + \\
& \left. \frac{3p^2Q1Q3S1z}{A2^{5/2}B1^2} - \frac{Q2Q3S2z}{A4^{3/2}B2^2} + \frac{4p^2Q2Q3S2z}{A4^{3/2}B2^3} + \frac{3p^2Q2Q3S2z}{A4^{5/2}B2^2} \right); \\
\frac{\sigma_{yz}}{\mu} = & \frac{b_x c}{4K\pi} \left(\frac{p}{A1^{3/2}} - \frac{p}{A2^{3/2}} - \frac{p}{A3^{3/2}} + \frac{p}{A4^{3/2}} + K2 \left(-\frac{p}{A1^{3/2}} + \frac{p}{A2^{3/2}} + \frac{p}{A3^{3/2}} - \frac{p}{A4^{3/2}} \right) + \frac{z}{A1^{3/2}} - \frac{z}{A2^{3/2}} - \frac{z}{A3^{3/2}} + \right. \\
& \frac{z}{A4^{3/2}} - \frac{3p^2z}{A1^{5/2}} + \frac{3p^2z}{A2^{5/2}} + \frac{3p^2z}{A3^{5/2}} - \frac{3p^2z}{A4^{5/2}} \Big) + \frac{1}{4K\pi} b_x c \left(-\frac{G1}{\sqrt{A1B1}} + \frac{G1}{\sqrt{A2B1}} + \frac{G1}{\sqrt{A3B2}} - \frac{G1}{\sqrt{A4B2}} - \frac{G1Q3^2}{A2^{3/2}B1} + \frac{G1Q3^2}{A4^{3/2}B2} + \right. \\
& \frac{G1Q4^2}{A1^{3/2}B1} - \frac{G1Q4^2}{A3^{3/2}B2} + \frac{4p^2Q3^2z}{A2^{3/2}B1^2} - \frac{4p^2Q3^2z}{A4^{3/2}B2^2} - \frac{4p^2Q4^2z}{A1^{3/2}B1^2} + \frac{4p^2Q4^2z}{A3^{3/2}B2^2} - \frac{p^2(3A1-Q4^2)z}{A1^{3/2}B1^2} + \frac{3p^2Q4^2(3A1-Q4^2)z}{A1^{5/2}B1^2} + \\
& \left. \frac{p^2(3A3-Q4^2)z}{A3^{3/2}B2^2} - \frac{3p^2Q4^2(3A3-Q4^2)z}{A3^{5/2}B2^2} + \frac{p^2S1z}{A2^{3/2}B1^2} - \frac{3p^2Q3^2S1z}{A2^{5/2}B1^2} - \frac{p^2S2z}{A4^{3/2}B2^2} + \frac{3p^2Q3^2S2z}{A4^{5/2}B2^2} \right);
\end{aligned}$$

APPENDIX B

The surface correction terms for stress considering only b_y (the y -component of the Burgers vector):

$$\begin{aligned}
\frac{\sigma_{xx}}{\mu} = & \frac{b_y c}{2K\pi} \left(K2 \left(\frac{Q1}{A1^{3/2}} - \frac{Q1}{A2^{3/2}} + \frac{Q2}{A3^{3/2}} - \frac{Q2}{A4^{3/2}} \right) + \frac{3pQ1z}{A1^{5/2}} - \frac{3pQ1z}{A2^{5/2}} + \frac{3pQ2z}{A3^{5/2}} - \frac{3pQ2z}{A4^{5/2}} \right) - \frac{1}{K2} 2\nu \left(-\frac{1}{4K\pi} b_y c \left(\frac{K2Q1}{\sqrt{A2}C1} - \right. \right. \\
& \frac{K2Q1}{\sqrt{A1}C2} + \frac{2K4pQ1}{\sqrt{A2}C1^2} + \frac{K4pQ1}{A2^{3/2}C1} - \frac{2K4pQ1}{\sqrt{A1}C2^2} - \frac{K4pQ1}{A1^{3/2}C2} - \frac{H1p^2Q1}{A2^{3/2}C1^2} + \frac{H3p^2Q1}{A1^{3/2}C2^2} + \frac{K2Q2}{\sqrt{A4}C1} - \frac{K2Q2}{\sqrt{A3}C2} + \frac{2K4pQ2}{\sqrt{A4}C1^2} + \frac{K4pQ2}{A4^{3/2}C1} - \\
& \frac{2K4pQ2}{\sqrt{A3}C2^2} - \frac{K4pQ2}{A3^{3/2}C2} - \frac{H2p^2Q2}{A4^{3/2}C1^2} + \frac{H4p^2Q2}{A3^{3/2}C2^2} - \frac{2H1pQ1z}{A2^{3/2}C1^2} + \frac{2H3pQ1z}{A1^{3/2}C2^2} - \frac{6p^3Q1z}{A2^{3/2}C1^2} + \frac{6p^3Q1z}{A1^{3/2}C2^2} + \frac{4H1p^3Q1z}{A2^{3/2}C1^3} + \frac{3H1p^3Q1z}{A2^{5/2}C1^2} - \\
& \frac{4H3p^3Q1z}{A1^{3/2}C2^3} - \frac{3H3p^3Q1z}{A1^{5/2}C2^2} - \frac{2H2pQ2z}{A4^{3/2}C1^2} + \frac{2H4pQ2z}{A3^{3/2}C2^2} - \frac{6p^3Q2z}{A4^{3/2}C1^2} + \frac{6p^3Q2z}{A3^{3/2}C2^2} + \frac{4H2p^3Q2z}{A4^{3/2}C1^3} + \frac{3H2p^3Q2z}{A4^{5/2}C1^2} - \frac{4H4p^3Q2z}{A3^{3/2}C2^3} - \\
& \left. \frac{3H4p^3Q2z}{A3^{5/2}C2^2} \right) - \frac{1}{4K\pi} b_y c \left(K2 \left(-\frac{Q1}{\sqrt{A2}C1} + \frac{Q1}{\sqrt{A1}C2} - \frac{Q2}{\sqrt{A4}C1} + \frac{Q2}{\sqrt{A3}C2} + \frac{2Q1Q3^2}{\sqrt{A2}C1^2} + \frac{Q1Q3^2}{A2^{3/2}C1} + \frac{2Q2Q3^2}{\sqrt{A4}C1^2} + \frac{Q2Q3^2}{A4^{3/2}C1} - \frac{2Q1Q4^2}{\sqrt{A1}C2^2} - \right. \right. \\
& \frac{Q1Q4^2}{A1^{3/2}C2} - \frac{2Q2Q4^2}{\sqrt{A3}C2^2} - \frac{Q2Q4^2}{A3^{3/2}C2} \left. \right) - \frac{H1pQ1z}{A2^{3/2}C1^2} + \frac{H3pQ1z}{A1^{3/2}C2^2} - \frac{H2pQ2z}{A4^{3/2}C1^2} + \frac{H4pQ2z}{A3^{3/2}C2^2} - \frac{6pQ1Q3^2z}{A2^{3/2}C1^2} + \frac{4H1pQ1Q3^2z}{A2^{3/2}C1^3} + \\
& \frac{3H1pQ1Q3^2z}{A2^{5/2}C1^2} - \frac{6pQ2Q3^2z}{A4^{3/2}C1^2} + \frac{4H2pQ2Q3^2z}{A4^{3/2}C1^3} + \frac{3H2pQ2Q3^2z}{A4^{5/2}C1^2} + \frac{6pQ1Q4^2z}{A1^{3/2}C2^2} - \frac{4H3pQ1Q4^2z}{A1^{3/2}C2^3} - \frac{3H3pQ1Q4^2z}{A1^{5/2}C2^2} + \frac{6pQ2Q4^2z}{A3^{3/2}C2^2} - \\
& \frac{4H4pQ2Q4^2z}{A3^{3/2}C2^3} - \frac{3H4pQ2Q4^2z}{A3^{5/2}C2^2} \left. \right) + \frac{b_y c}{-4\pi K} \left(K2 \left(\frac{Q1}{A1^{3/2}} - \frac{Q1}{A2^{3/2}} + \frac{Q2}{A3^{3/2}} - \frac{Q2}{A4^{3/2}} \right) + \frac{3pQ1z}{A1^{5/2}} - \frac{3pQ1z}{A2^{5/2}} + \frac{3pQ2z}{A3^{5/2}} - \frac{3pQ2z}{A4^{5/2}} \right); \\
\frac{\sigma_{yy}}{\mu} = & \frac{1}{2K\pi} b_y c \left(K2 \left(-\frac{Q1}{\sqrt{A2}C1} + \frac{Q1}{\sqrt{A1}C2} - \frac{Q2}{\sqrt{A4}C1} + \frac{Q2}{\sqrt{A3}C2} + \frac{2Q1Q3^2}{\sqrt{A2}C1^2} + \frac{Q1Q3^2}{A2^{3/2}C1} + \frac{2Q2Q3^2}{\sqrt{A4}C1^2} + \frac{Q2Q3^2}{A4^{3/2}C1} - \frac{2Q1Q4^2}{\sqrt{A1}C2^2} - \right. \right. \\
& \frac{Q1Q4^2}{A1^{3/2}C2} - \frac{2Q2Q4^2}{\sqrt{A3}C2^2} - \frac{Q2Q4^2}{A3^{3/2}C2} \left. \right) - \frac{6pQ1Q3^2z}{A2^{3/2}C1^2} - \frac{6pQ2Q3^2z}{A4^{3/2}C1^2} + \frac{6pQ1Q4^2z}{A1^{3/2}C2^2} + \frac{6pQ2Q4^2z}{A3^{3/2}C2^2} + \frac{pQ1S5z}{A1^{3/2}C2^2} - \frac{4pQ1Q4^2S5z}{A1^{3/2}C2^3} - \\
& \frac{3pQ1Q4^2S5z}{A1^{5/2}C2^2} - \frac{pQ1S6z}{A2^{3/2}C1^2} + \frac{4pQ1Q3^2S6z}{A2^{3/2}C1^3} + \frac{3pQ1Q3^2S6z}{A2^{5/2}C1^2} + \frac{pQ2S7z}{A3^{3/2}C2^2} - \frac{4pQ2Q4^2S7z}{A3^{3/2}C2^3} - \frac{3pQ2Q4^2S7z}{A3^{5/2}C2^2} - \frac{pQ2S8z}{A4^{3/2}C1^2} + \\
& \frac{4pQ2Q3^2S8z}{A4^{3/2}C1^3} + \frac{3pQ2Q3^2S8z}{A4^{5/2}C1^2} \left. \right) - \frac{1}{K2} 2\nu \left(-\frac{1}{4K\pi} b_y c \left(\frac{K2Q1}{\sqrt{A2}C1} - \frac{K2Q1}{\sqrt{A1}C2} + \frac{2K4pQ1}{\sqrt{A2}C1^2} + \frac{K4pQ1}{A2^{3/2}C1} - \frac{2K4pQ1}{\sqrt{A1}C2^2} - \frac{K4pQ1}{A1^{3/2}C2} - \frac{H1p^2Q1}{A2^{3/2}C1^2} + \right. \right. \\
& \frac{H3p^2Q1}{A1^{3/2}C2^2} + \frac{K2Q2}{\sqrt{A4}C1} - \frac{K2Q2}{\sqrt{A3}C2} + \frac{2K4pQ2}{\sqrt{A4}C1^2} + \frac{K4pQ2}{A4^{3/2}C1} - \frac{2K4pQ2}{\sqrt{A3}C2^2} - \frac{K4pQ2}{A3^{3/2}C2} - \frac{H2p^2Q2}{A4^{3/2}C1^2} + \frac{H4p^2Q2}{A3^{3/2}C2^2} - \frac{2H1pQ1z}{A2^{3/2}C1^2} + \frac{2H3pQ1z}{A1^{3/2}C2^2} - \\
& \frac{6p^3Q1z}{A2^{3/2}C1^2} + \frac{6p^3Q1z}{A1^{3/2}C2^2} + \frac{4H1p^3Q1z}{A2^{3/2}C1^3} + \frac{3H1p^3Q1z}{A2^{5/2}C1^2} - \frac{4H3p^3Q1z}{A1^{3/2}C2^3} - \frac{3H3p^3Q1z}{A1^{5/2}C2^2} - \frac{2H2pQ2z}{A4^{3/2}C1^2} + \frac{2H4pQ2z}{A3^{3/2}C2^2} - \frac{6p^3Q2z}{A4^{3/2}C1^2} + \frac{6p^3Q2z}{A3^{3/2}C2^2} + \\
& \frac{4H2p^3Q2z}{A4^{3/2}C1^3} + \frac{3H2p^3Q2z}{A4^{5/2}C1^2} - \frac{4H4p^3Q2z}{A3^{3/2}C2^3} - \frac{3H4p^3Q2z}{A3^{5/2}C2^2} \left. \right) - \frac{1}{4K\pi} b_y c \left(K2 \left(-\frac{Q1}{\sqrt{A2}C1} + \frac{Q1}{\sqrt{A1}C2} - \frac{Q2}{\sqrt{A4}C1} + \frac{Q2}{\sqrt{A3}C2} + \frac{2Q1Q3^2}{\sqrt{A2}C1^2} + \right. \right. \\
& \frac{Q1Q3^2}{A2^{3/2}C1} + \frac{2Q2Q3^2}{\sqrt{A4}C1^2} + \frac{Q2Q3^2}{A4^{3/2}C1} - \frac{2Q1Q4^2}{\sqrt{A1}C2^2} - \frac{Q1Q4^2}{A1^{3/2}C2} - \frac{2Q2Q4^2}{\sqrt{A3}C2^2} - \frac{Q2Q4^2}{A3^{3/2}C2} \left. \right) - \frac{H1pQ1z}{A2^{3/2}C1^2} + \frac{H3pQ1z}{A1^{3/2}C2^2} - \frac{H2pQ2z}{A4^{3/2}C1^2} + \frac{H4pQ2z}{A3^{3/2}C2^2} - \\
& \frac{6pQ1Q3^2z}{A2^{3/2}C1^2} + \frac{4H1pQ1Q3^2z}{A2^{3/2}C1^3} + \frac{3H1pQ1Q3^2z}{A2^{5/2}C1^2} - \frac{6pQ2Q3^2z}{A4^{3/2}C1^2} + \frac{4H2pQ2Q3^2z}{A4^{3/2}C1^3} + \frac{3H2pQ2Q3^2z}{A4^{5/2}C1^2} + \frac{6pQ1Q4^2z}{A1^{3/2}C2^2} - \frac{4H3pQ1Q4^2z}{A1^{3/2}C2^3} - \\
& \frac{3H3pQ1Q4^2z}{A1^{5/2}C2^2} + \frac{6pQ2Q4^2z}{A3^{3/2}C2^2} - \frac{4H4pQ2Q4^2z}{A3^{3/2}C2^3} - \frac{3H4pQ2Q4^2z}{A3^{5/2}C2^2} \left. \right) + \frac{b_y c}{-4\pi K} \left(K2 \left(\frac{Q1}{A1^{3/2}} - \frac{Q1}{A2^{3/2}} + \frac{Q2}{A3^{3/2}} - \frac{Q2}{A4^{3/2}} \right) + \frac{3pQ1z}{A1^{5/2}} - \right. \\
& \left. \frac{3pQ1z}{A2^{5/2}} + \frac{3pQ2z}{A3^{5/2}} - \frac{3pQ2z}{A4^{5/2}} \right);
\end{aligned}$$

$$\begin{aligned}
\frac{\sigma_{zz}}{\mu} = & \frac{1}{2K\pi} b_y c \left(\frac{K2Q1}{\sqrt{A2C1}} - \frac{K2Q1}{\sqrt{A1C2}} + \frac{2G1pQ1}{\sqrt{A2C1^2}} + \frac{G1pQ1}{A2^{3/2}C1} - \frac{2G1pQ1}{\sqrt{A1C2^2}} - \frac{G1pQ1}{A1^{3/2}C2} + \frac{K2Q2}{\sqrt{A4C1}} - \frac{K2Q2}{\sqrt{A3C2}} + \frac{2G1pQ2}{\sqrt{A4C1^2}} + \frac{G1pQ2}{A4^{3/2}C1} - \right. \\
& \frac{2G1pQ2}{\sqrt{A3C2^2}} - \frac{G1pQ2}{A3^{3/2}C2} + \frac{p^2Q1S5}{A1^{3/2}C2^2} - \frac{p^2Q1S6}{A2^{3/2}C1^2} + \frac{p^2Q2S7}{A3^{3/2}C2^2} - \frac{p^2Q2S8}{A4^{3/2}C1^2} - \frac{6p^3Q1z}{A2^{3/2}C1^2} + \frac{6p^3Q1z}{A1^{3/2}C2^2} - \frac{6p^3Q2z}{A4^{3/2}C1^2} + \frac{6p^3Q2z}{A3^{3/2}C2^2} + \\
& \frac{2pQ1S5z}{A1^{3/2}C2^2} - \frac{4p^3Q1S5z}{A1^{3/2}C2^3} - \frac{3p^3Q1S5z}{A1^{5/2}C2^2} - \frac{2pQ1S6z}{A2^{3/2}C1^2} + \frac{4p^3Q1S6z}{A2^{3/2}C1^3} + \frac{3p^3Q1S6z}{A2^{5/2}C1^2} + \frac{2pQ2S7z}{A3^{3/2}C2^2} - \frac{4p^3Q2S7z}{A3^{3/2}C2^3} - \frac{3p^3Q2S7z}{A3^{5/2}C2^2} - \frac{2pQ2S8z}{A4^{3/2}C1^2} + \\
& \left. \frac{4p^3Q2S8z}{A4^{3/2}C1^3} + \frac{3p^3Q2S8z}{A4^{5/2}C1^2} \right) - \frac{1}{K2} 2\nu \left(-\frac{1}{4K\pi} b_y c \left(\frac{K2Q1}{\sqrt{A2C1}} - \frac{K2Q1}{\sqrt{A1C2}} + \frac{2K4pQ1}{\sqrt{A2C1^2}} + \frac{K4pQ1}{A2^{3/2}C1} - \frac{2K4pQ1}{\sqrt{A1C2^2}} - \frac{K4pQ1}{A1^{3/2}C2} - \frac{H1p^2Q1}{A2^{3/2}C1^2} + \right. \right. \\
& \frac{H3p^2Q1}{A1^{3/2}C2^2} + \frac{K2Q2}{\sqrt{A4C1}} - \frac{K2Q2}{\sqrt{A3C2}} + \frac{2K4pQ2}{\sqrt{A4C1^2}} + \frac{K4pQ2}{A4^{3/2}C1} - \frac{2K4pQ2}{\sqrt{A3C2^2}} - \frac{K4pQ2}{A3^{3/2}C2} - \frac{H2p^2Q2}{A4^{3/2}C1^2} + \frac{H4p^2Q2}{A3^{3/2}C2^2} - \frac{2H1pQ1z}{A2^{3/2}C1^2} + \frac{2H3pQ1z}{A1^{3/2}C2^2} - \\
& \frac{6p^3Q1z}{A2^{3/2}C1^2} + \frac{6p^3Q1z}{A1^{3/2}C2^2} + \frac{4H1p^3Q1z}{A2^{3/2}C1^3} + \frac{3H1p^3Q1z}{A2^{5/2}C1^2} - \frac{4H3p^3Q1z}{A1^{3/2}C2^3} - \frac{3H3p^3Q1z}{A1^{5/2}C2^2} - \frac{2H2pQ2z}{A4^{3/2}C1^2} + \frac{2H4pQ2z}{A3^{3/2}C2^2} - \frac{6p^3Q2z}{A4^{3/2}C1^2} + \frac{6p^3Q2z}{A3^{3/2}C2^2} + \\
& \frac{4H2p^3Q2z}{A4^{3/2}C1^3} + \frac{3H2p^3Q2z}{A4^{5/2}C1^2} - \frac{4H4p^3Q2z}{A3^{3/2}C2^3} - \frac{3H4p^3Q2z}{A3^{5/2}C2^2} \left. \right) - \frac{1}{4K\pi} b_y c \left(K2 \left(-\frac{Q1}{\sqrt{A2C1}} + \frac{Q1}{\sqrt{A1C2}} - \frac{Q2}{\sqrt{A4C1}} + \frac{Q2}{\sqrt{A3C2}} + \frac{2Q1Q3^2}{\sqrt{A2C1^2}} + \right. \right. \\
& \frac{Q1Q3^2}{A2^{3/2}C1} + \frac{2Q2Q3^2}{\sqrt{A4C1^2}} + \frac{Q2Q3^2}{A4^{3/2}C1} - \frac{2Q1Q4^2}{\sqrt{A1C2^2}} - \frac{Q1Q4^2}{A1^{3/2}C2} - \frac{2Q2Q4^2}{\sqrt{A3C2^2}} - \frac{Q2Q4^2}{A3^{3/2}C2} \left. \right) - \frac{H1pQ1z}{A2^{3/2}C1^2} + \frac{H3pQ1z}{A1^{3/2}C2^2} - \frac{H2pQ2z}{A4^{3/2}C1^2} + \frac{H4pQ2z}{A3^{3/2}C2^2} - \\
& \frac{6pQ1Q3^2z}{A2^{3/2}C1^2} + \frac{4H1pQ1Q3^2z}{A2^{3/2}C1^3} + \frac{3H1pQ1Q3^2z}{A2^{5/2}C1^2} - \frac{6pQ2Q3^2z}{A4^{3/2}C1^2} + \frac{4H2pQ2Q3^2z}{A4^{3/2}C1^3} + \frac{3H2pQ2Q3^2z}{A4^{5/2}C1^2} + \frac{6pQ1Q4^2z}{A1^{3/2}C2^2} - \frac{4H3pQ1Q4^2z}{A1^{3/2}C2^3} - \\
& \frac{3H3pQ1Q4^2z}{A1^{5/2}C2^2} + \frac{6pQ2Q4^2z}{A3^{3/2}C2^2} - \frac{4H4pQ2Q4^2z}{A3^{3/2}C2^3} - \frac{3H4pQ2Q4^2z}{A3^{5/2}C2^2} \left. \right) + \frac{b_y c}{-4\pi K} \left(K2 \left(\frac{Q1}{A1^{3/2}} - \frac{Q1}{A2^{3/2}} + \frac{Q2}{A3^{3/2}} - \frac{Q2}{A4^{3/2}} \right) + \frac{3pQ1z}{A1^{5/2}} - \right. \\
& \left. \frac{3pQ1z}{A2^{5/2}} + \frac{3pQ2z}{A3^{5/2}} - \frac{3pQ2z}{A4^{5/2}} \right); \\
\frac{\sigma_{xy}}{\mu} = & \frac{b_y c}{4K\pi} \left(K2 \left(\frac{Q3}{A2^{3/2}} - \frac{Q3}{A4^{3/2}} - \frac{Q4}{A1^{3/2}} + \frac{Q4}{A3^{3/2}} \right) + \frac{3pQ3z}{A2^{5/2}} - \frac{3pQ3z}{A4^{5/2}} - \frac{3pQ4z}{A1^{5/2}} + \frac{3pQ4z}{A3^{5/2}} \right) + \frac{1}{4K\pi} b_y c \left(K2 \left(\frac{Q3}{\sqrt{A2C1}} - \frac{Q3}{\sqrt{A4C1}} - \right. \right. \\
& \frac{Q1^2Q3}{A2^{3/2}C1} + \frac{Q2^2Q3}{A4^{3/2}C1} - \frac{Q4}{\sqrt{A1C2}} + \frac{Q4}{\sqrt{A3C2}} + \frac{Q1^2Q4}{A1^{3/2}C2} - \frac{Q2^2Q4}{A3^{3/2}C2} \left. \right) + \frac{4pQ1^2Q3z}{A2^{3/2}C1^2} - \frac{4pQ2^2Q3z}{A4^{3/2}C1^2} - \frac{4pQ1^2Q4z}{A1^{3/2}C2^2} + \frac{4pQ2^2Q4z}{A3^{3/2}C2^2} - \\
& \left. \frac{pQ4S5z}{A1^{3/2}C2^2} + \frac{3pQ1^2Q4S5z}{A1^{5/2}C2^2} + \frac{pQ3S6z}{A2^{3/2}C1^2} - \frac{3pQ1^2Q3S6z}{A2^{5/2}C1^2} + \frac{pQ4S7z}{A3^{3/2}C2^2} - \frac{3pQ2^2Q4S7z}{A3^{5/2}C2^2} - \frac{pQ3S8z}{A4^{3/2}C1^2} + \frac{3pQ2^2Q3S8z}{A4^{5/2}C1^2} \right); \\
\frac{\sigma_{xz}}{\mu} = & \frac{b_y c}{4K\pi} \left(\frac{p}{A1^{3/2}} - \frac{p}{A2^{3/2}} - \frac{p}{A3^{3/2}} + \frac{p}{A4^{3/2}} + K2 \left(-\frac{p}{A1^{3/2}} + \frac{p}{A2^{3/2}} + \frac{p}{A3^{3/2}} - \frac{p}{A4^{3/2}} \right) + \frac{z}{A1^{3/2}} - \frac{z}{A2^{3/2}} - \frac{z}{A3^{3/2}} + \right. \\
& \frac{z}{A4^{3/2}} - \frac{3p^2z}{A1^{5/2}} + \frac{3p^2z}{A2^{5/2}} + \frac{3p^2z}{A3^{5/2}} - \frac{3p^2z}{A4^{5/2}} \left. \right) + \frac{1}{4K\pi} b_y c \left(\frac{G1}{\sqrt{A2C1}} - \frac{G1}{\sqrt{A4C1}} - \frac{G1}{\sqrt{A1C2}} + \frac{G1}{\sqrt{A3C2}} - \frac{G1Q1^2}{A2^{3/2}C1} + \frac{G1Q1^2}{A1^{3/2}C2} + \right. \\
& \frac{G1Q2^2}{A4^{3/2}C1} - \frac{G1Q2^2}{A3^{3/2}C2} + \frac{4p^2Q1^2z}{A2^{3/2}C1^2} - \frac{4p^2Q1^2z}{A1^{3/2}C2^2} - \frac{4p^2Q2^2z}{A4^{3/2}C1^2} + \frac{4p^2Q2^2z}{A3^{3/2}C2^2} - \frac{p^2S5z}{A1^{3/2}C2^2} + \frac{3p^2Q1^2S5z}{A1^{5/2}C2^2} + \frac{p^2S6z}{A2^{3/2}C1^2} - \frac{3p^2Q1^2S6z}{A2^{5/2}C1^2} + \\
& \left. \frac{p^2S7z}{A3^{3/2}C2^2} - \frac{3p^2Q2^2S7z}{A3^{5/2}C2^2} - \frac{p^2S8z}{A4^{3/2}C1^2} + \frac{3p^2Q2^2S8z}{A4^{5/2}C1^2} \right); \\
\frac{\sigma_{yz}}{\mu} = & \frac{1}{4K\pi} b_y c \left(\frac{2G1Q1Q3}{\sqrt{A2C1^2}} + \frac{G1Q1Q3}{A2^{3/2}C1} + \frac{2G1Q2Q3}{\sqrt{A4C1^2}} + \frac{G1Q2Q3}{A4^{3/2}C1} - \frac{2G1Q1Q4}{\sqrt{A1C2^2}} - \frac{G1Q1Q4}{A1^{3/2}C2} - \frac{2G1Q2Q4}{\sqrt{A3C2^2}} - \frac{G1Q2Q4}{A3^{3/2}C2} - \frac{6p^2Q1Q3z}{A2^{3/2}C1^2} - \right. \\
& \frac{6p^2Q2Q3z}{A4^{3/2}C1^2} + \frac{6p^2Q1Q4z}{A1^{3/2}C2^2} + \frac{6p^2Q2Q4z}{A3^{3/2}C2^2} - \frac{4p^2Q1Q4S5z}{A1^{3/2}C2^3} - \frac{3p^2Q1Q4S5z}{A1^{5/2}C2^2} + \frac{4p^2Q1Q3S6z}{A2^{3/2}C1^3} + \frac{3p^2Q1Q3S6z}{A2^{5/2}C1^2} - \frac{4p^2Q2Q4S7z}{A3^{3/2}C2^3} - \\
& \frac{3p^2Q2Q4S7z}{A3^{5/2}C2^2} + \frac{4p^2Q2Q3S8z}{A4^{3/2}C1^3} + \frac{3p^2Q2Q3S8z}{A4^{5/2}C1^2} \left. \right) + \frac{1}{4K\pi} b_y c \left(K2 \left(\frac{2pQ1Q3}{\sqrt{A2C1^2}} + \frac{pQ1Q3}{A2^{3/2}C1} + \frac{2pQ2Q3}{\sqrt{A4C1^2}} + \frac{pQ2Q3}{A4^{3/2}C1} - \frac{2pQ1Q4}{\sqrt{A1C2^2}} - \right. \right. \\
& \frac{pQ1Q4}{A1^{3/2}C2} - \frac{2pQ2Q4}{\sqrt{A3C2^2}} - \frac{pQ2Q4}{A3^{3/2}C2} \left. \right) + \frac{pQ1Q4S5}{A1^{3/2}C2^2} - \frac{pQ1Q3S6}{A2^{3/2}C1^2} + \frac{pQ2Q4S7}{A3^{3/2}C2^2} - \frac{pQ2Q3S8}{A4^{3/2}C1^2} - \frac{6p^2Q1Q3z}{A2^{3/2}C1^2} - \frac{6p^2Q2Q3z}{A4^{3/2}C1^2} + \frac{6p^2Q1Q4z}{A1^{3/2}C2^2} + \\
& \frac{6p^2Q2Q4z}{A3^{3/2}C2^2} + \frac{Q1Q4S5z}{A1^{3/2}C2^2} - \frac{4p^2Q1Q4S5z}{A1^{3/2}C2^3} - \frac{3p^2Q1Q4S5z}{A1^{5/2}C2^2} - \frac{Q1Q3S6z}{A2^{3/2}C1^2} + \frac{4p^2Q1Q3S6z}{A2^{3/2}C1^3} + \frac{3p^2Q1Q3S6z}{A2^{5/2}C1^2} + \frac{Q2Q4S7z}{A3^{3/2}C2^2} - \frac{4p^2Q2Q4S7z}{A3^{3/2}C2^3} - \\
& \left. \frac{3p^2Q2Q4S7z}{A3^{5/2}C2^2} - \frac{Q2Q3S8z}{A4^{3/2}C1^2} + \frac{4p^2Q2Q3S8z}{A4^{3/2}C1^3} + \frac{3p^2Q2Q3S8z}{A4^{5/2}C1^2} \right);
\end{aligned}$$

APPENDIX C

The surface correction terms for stress considering only b_z (the z -component of the Burgers vector):

$$\begin{aligned}
\frac{\sigma_{xx}}{\mu} = & \frac{1}{2K\pi} b_z c \left(G_2 \left(\frac{2Q_1Q_3}{\sqrt{A_2}B_1^2} + \frac{Q_1Q_3}{A_2^{3/2}B_1} + \frac{2Q_2Q_3}{\sqrt{A_4}B_2^2} + \frac{Q_2Q_3}{A_4^{3/2}B_2} - \frac{2Q_1Q_4}{\sqrt{A_1}B_1^2} - \frac{Q_1Q_4}{A_1^{3/2}B_1} - \frac{2Q_2Q_4}{\sqrt{A_3}B_2^2} - \frac{Q_2Q_4}{A_3^{3/2}B_2} \right) + \frac{6p^2Q_1Q_3z}{A_2^{3/2}B_1^2} + \right. \\
& \frac{6p^2Q_2Q_3z}{A_4^{3/2}B_2^2} - \frac{6p^2Q_1Q_4z}{A_1^{3/2}B_1^2} - \frac{6p^2Q_2Q_4z}{A_3^{3/2}B_2^2} - \frac{4p^2Q_1Q_3S_1z}{A_2^{3/2}B_1^3} - \frac{3p^2Q_1Q_3S_1z}{A_2^{5/2}B_1^2} + \frac{4p^2Q_2Q_4S_10z}{A_3^{3/2}B_2^3} + \frac{3p^2Q_2Q_4S_10z}{A_3^{5/2}B_2^2} - \frac{4p^2Q_2Q_3S_2z}{A_4^{3/2}B_2^3} - \\
& \left. \frac{3p^2Q_2Q_3S_2z}{A_4^{5/2}B_2^2} + \frac{4p^2Q_1Q_4S_9z}{A_1^{3/2}B_1^3} + \frac{3p^2Q_1Q_4S_9z}{A_1^{5/2}B_1^2} \right) - \frac{1}{K_2} 2 \left(\frac{1}{4K\pi} b_z c \left(-\frac{M_2pQ_1Q_3}{A_2^{3/2}} - \frac{M_3pQ_2Q_3}{A_4^{3/2}} + \frac{M_4pQ_1Q_4}{A_1^{3/2}} + \frac{M_1pQ_2Q_4}{A_3^{3/2}} + \right. \right. \\
& K_2 \left(\frac{4pQ_1Q_3}{\sqrt{A_2}B_1C_1} - \frac{2H_5pQ_1Q_3}{\sqrt{A_2}B_1C_1^2} - \frac{2H_5pQ_1Q_3}{\sqrt{A_2}B_1^2C_1} - \frac{H_5pQ_1Q_3}{A_2^{3/2}B_1C_1} + \frac{4pQ_2Q_3}{\sqrt{A_4}B_2C_1} - \frac{2H_6pQ_2Q_3}{\sqrt{A_4}B_2C_1^2} - \frac{2H_6pQ_2Q_3}{\sqrt{A_4}B_2^2C_1} - \frac{H_6pQ_2Q_3}{A_4^{3/2}B_2C_1} + \frac{2H_7pQ_1Q_4}{\sqrt{A_1}B_1S_1^2} + \right. \\
& \left. \frac{2H_8pQ_2Q_4}{\sqrt{A_3}B_2S_1^2} - \frac{4pQ_1Q_4}{\sqrt{A_1}B_1S_1} + \frac{2H_7pQ_1Q_4}{\sqrt{A_1}B_1^2S_1} + \frac{H_7pQ_1Q_4}{A_1^{3/2}B_1S_1} - \frac{4pQ_2Q_4}{\sqrt{A_3}B_2S_1} + \frac{2H_8pQ_2Q_4}{\sqrt{A_3}B_2^2S_1} + \frac{H_8pQ_2Q_4}{A_3^{3/2}B_2S_1} \right) - \frac{M_2Q_1Q_3z}{A_2^{3/2}} - \frac{M_6pQ_1Q_3z}{A_2^{3/2}} + \\
& \frac{3M_2p^2Q_1Q_3z}{A_2^{5/2}} - \frac{M_3Q_2Q_3z}{A_4^{3/2}} - \frac{M_7pQ_2Q_3z}{A_4^{3/2}} + \frac{3M_3p^2Q_2Q_3z}{A_4^{5/2}} + \frac{M_4Q_1Q_4z}{A_1^{3/2}} + \frac{M_8pQ_1Q_4z}{A_1^{3/2}} - \frac{3M_4p^2Q_1Q_4z}{A_1^{5/2}} + \frac{M_1Q_2Q_4z}{A_3^{3/2}} + \frac{M_5pQ_2Q_4z}{A_3^{3/2}} - \\
& \left. \frac{3M_1p^2Q_2Q_4z}{A_3^{5/2}} \right) + \frac{1}{4K\pi} b_z c \left(-\frac{G_2M_{10}}{C_1} + \frac{G_2M_{12}}{C_2} + \frac{2G_2M_9Q_3}{C_1^2} - \frac{2G_2M_{11}Q_4}{C_2^2} + \frac{6p^2Q_1Q_3z}{A_2^{3/2}C_1^2} + \frac{6p^2Q_2Q_3z}{A_4^{3/2}C_1^2} - \frac{6p^2Q_1Q_4z}{A_1^{3/2}C_2^2} - \frac{6p^2Q_2Q_4z}{A_3^{3/2}C_2^2} + \right. \\
& \left. \frac{4p^2Q_1Q_4S_5z}{A_1^{3/2}C_2^3} + \frac{3p^2Q_1Q_4S_5z}{A_1^{5/2}C_2^2} - \frac{4p^2Q_1Q_3S_6z}{A_2^{3/2}C_1^3} - \frac{3p^2Q_1Q_3S_6z}{A_2^{5/2}C_1^2} + \frac{4p^2Q_2Q_4S_7z}{A_3^{3/2}C_2^3} + \frac{3p^2Q_2Q_4S_7z}{A_3^{5/2}C_2^2} - \frac{4p^2Q_2Q_3S_8z}{A_4^{3/2}C_1^3} - \frac{3p^2Q_2Q_3S_8z}{A_4^{5/2}C_1^2} \right) + \\
& \frac{1}{4K\pi} b_z c \left(G_2 \left(\frac{2Q_1Q_3}{\sqrt{A_2}B_1^2} + \frac{Q_1Q_3}{A_2^{3/2}B_1} + \frac{2Q_2Q_3}{\sqrt{A_4}B_2^2} + \frac{Q_2Q_3}{A_4^{3/2}B_2} - \frac{2Q_1Q_4}{\sqrt{A_1}B_1^2} - \frac{Q_1Q_4}{A_1^{3/2}B_1} - \frac{2Q_2Q_4}{\sqrt{A_3}B_2^2} - \frac{Q_2Q_4}{A_3^{3/2}B_2} \right) + \frac{6p^2Q_1Q_3z}{A_2^{3/2}B_1^2} + \right. \\
& \frac{6p^2Q_2Q_3z}{A_4^{3/2}B_2^2} - \frac{6p^2Q_1Q_4z}{A_1^{3/2}B_1^2} - \frac{6p^2Q_2Q_4z}{A_3^{3/2}B_2^2} - \frac{4p^2Q_1Q_3S_1z}{A_2^{3/2}B_1^3} - \frac{3p^2Q_1Q_3S_1z}{A_2^{5/2}B_1^2} + \frac{4p^2Q_2Q_4S_10z}{A_3^{3/2}B_2^3} + \frac{3p^2Q_2Q_4S_10z}{A_3^{5/2}B_2^2} - \frac{4p^2Q_2Q_3S_2z}{A_4^{3/2}B_2^3} - \\
& \left. \frac{3p^2Q_2Q_3S_2z}{A_4^{5/2}B_2^2} + \frac{4p^2Q_1Q_4S_9z}{A_1^{3/2}B_1^3} + \frac{3p^2Q_1Q_4S_9z}{A_1^{5/2}B_1^2} \right) \Big) v; \\
\frac{\sigma_{yy}}{\mu} = & \frac{1}{2K\pi} b_z c \left(-\frac{G_2M_{10}}{C_1} + \frac{G_2M_{12}}{C_2} + \frac{2G_2M_9Q_3}{C_1^2} - \frac{2G_2M_{11}Q_4}{C_2^2} + \frac{6p^2Q_1Q_3z}{A_2^{3/2}C_1^2} + \frac{6p^2Q_2Q_3z}{A_4^{3/2}C_1^2} - \frac{6p^2Q_1Q_4z}{A_1^{3/2}C_2^2} - \frac{6p^2Q_2Q_4z}{A_3^{3/2}C_2^2} + \right. \\
& \left. \frac{4p^2Q_1Q_4S_5z}{A_1^{3/2}C_2^3} + \frac{3p^2Q_1Q_4S_5z}{A_1^{5/2}C_2^2} - \frac{4p^2Q_1Q_3S_6z}{A_2^{3/2}C_1^3} - \frac{3p^2Q_1Q_3S_6z}{A_2^{5/2}C_1^2} + \frac{4p^2Q_2Q_4S_7z}{A_3^{3/2}C_2^3} + \frac{3p^2Q_2Q_4S_7z}{A_3^{5/2}C_2^2} - \frac{4p^2Q_2Q_3S_8z}{A_4^{3/2}C_1^3} - \frac{3p^2Q_2Q_3S_8z}{A_4^{5/2}C_1^2} \right) - \\
& \frac{1}{K_2} 2 \left(\frac{1}{4K\pi} b_z c \left(-\frac{M_2pQ_1Q_3}{A_2^{3/2}} - \frac{M_3pQ_2Q_3}{A_4^{3/2}} + \frac{M_4pQ_1Q_4}{A_1^{3/2}} + \frac{M_1pQ_2Q_4}{A_3^{3/2}} + K_2 \left(\frac{4pQ_1Q_3}{\sqrt{A_2}B_1C_1} - \frac{2H_5pQ_1Q_3}{\sqrt{A_2}B_1C_1^2} - \frac{2H_5pQ_1Q_3}{\sqrt{A_2}B_1^2C_1} - \frac{H_5pQ_1Q_3}{A_2^{3/2}B_1C_1} + \right. \right. \right. \\
& \frac{4pQ_2Q_3}{\sqrt{A_4}B_2C_1} - \frac{2H_6pQ_2Q_3}{\sqrt{A_4}B_2C_1^2} - \frac{2H_6pQ_2Q_3}{\sqrt{A_4}B_2^2C_1} - \frac{H_6pQ_2Q_3}{A_4^{3/2}B_2C_1} + \frac{2H_7pQ_1Q_4}{\sqrt{A_1}B_1S_1^2} + \frac{2H_8pQ_2Q_4}{\sqrt{A_3}B_2S_1^2} - \frac{4pQ_1Q_4}{\sqrt{A_1}B_1S_1} + \frac{2H_7pQ_1Q_4}{\sqrt{A_1}B_1^2S_1} + \frac{H_7pQ_1Q_4}{A_1^{3/2}B_1S_1} - \\
& \left. \frac{4pQ_2Q_4}{\sqrt{A_3}B_2S_1} + \frac{2H_8pQ_2Q_4}{\sqrt{A_3}B_2^2S_1} + \frac{H_8pQ_2Q_4}{A_3^{3/2}B_2S_1} \right) - \frac{M_2Q_1Q_3z}{A_2^{3/2}} - \frac{M_6pQ_1Q_3z}{A_2^{3/2}} + \frac{3M_2p^2Q_1Q_3z}{A_2^{5/2}} - \frac{M_3Q_2Q_3z}{A_4^{3/2}} - \frac{M_7pQ_2Q_3z}{A_4^{3/2}} + \frac{3M_3p^2Q_2Q_3z}{A_4^{5/2}} + \\
& \frac{M_4Q_1Q_4z}{A_1^{3/2}} + \frac{M_8pQ_1Q_4z}{A_1^{3/2}} - \frac{3M_4p^2Q_1Q_4z}{A_1^{5/2}} + \frac{M_1Q_2Q_4z}{A_3^{3/2}} + \frac{M_5pQ_2Q_4z}{A_3^{3/2}} - \frac{3M_1p^2Q_2Q_4z}{A_3^{5/2}} \right) + \frac{1}{4K\pi} b_z c \left(-\frac{G_2M_{10}}{C_1} + \frac{G_2M_{12}}{C_2} + \right. \\
& \frac{2G_2M_9Q_3}{C_1^2} - \frac{2G_2M_{11}Q_4}{C_2^2} + \frac{6p^2Q_1Q_3z}{A_2^{3/2}C_1^2} + \frac{6p^2Q_2Q_3z}{A_4^{3/2}C_1^2} - \frac{6p^2Q_1Q_4z}{A_1^{3/2}C_2^2} - \frac{6p^2Q_2Q_4z}{A_3^{3/2}C_2^2} + \frac{4p^2Q_1Q_4S_5z}{A_1^{3/2}C_2^3} + \frac{3p^2Q_1Q_4S_5z}{A_1^{5/2}C_2^2} - \frac{4p^2Q_1Q_3S_6z}{A_2^{3/2}C_1^3} - \\
& \left. \frac{3p^2Q_1Q_3S_6z}{A_2^{5/2}C_1^2} + \frac{4p^2Q_2Q_4S_7z}{A_3^{3/2}C_2^3} + \frac{3p^2Q_2Q_4S_7z}{A_3^{5/2}C_2^2} - \frac{4p^2Q_2Q_3S_8z}{A_4^{3/2}C_1^3} - \frac{3p^2Q_2Q_3S_8z}{A_4^{5/2}C_1^2} \right) + \frac{1}{4K\pi} b_z c \left(G_2 \left(\frac{2Q_1Q_3}{\sqrt{A_2}B_1^2} + \frac{Q_1Q_3}{A_2^{3/2}B_1} + \frac{2Q_2Q_3}{\sqrt{A_4}B_2^2} + \right. \right. \\
& \left. \frac{Q_2Q_3}{A_4^{3/2}B_2} - \frac{2Q_1Q_4}{\sqrt{A_1}B_1^2} - \frac{Q_1Q_4}{A_1^{3/2}B_1} - \frac{2Q_2Q_4}{\sqrt{A_3}B_2^2} - \frac{Q_2Q_4}{A_3^{3/2}B_2} \right) + \frac{6p^2Q_1Q_3z}{A_2^{3/2}B_1^2} + \frac{6p^2Q_2Q_3z}{A_4^{3/2}B_2^2} - \frac{6p^2Q_1Q_4z}{A_1^{3/2}B_1^2} - \frac{6p^2Q_2Q_4z}{A_3^{3/2}B_2^2} - \frac{4p^2Q_1Q_3S_1z}{A_2^{3/2}B_1^3} - \\
& \left. \frac{3p^2Q_1Q_3S_1z}{A_2^{5/2}B_1^2} + \frac{4p^2Q_2Q_4S_10z}{A_3^{3/2}B_2^3} + \frac{3p^2Q_2Q_4S_10z}{A_3^{5/2}B_2^2} - \frac{4p^2Q_2Q_3S_2z}{A_4^{3/2}B_2^3} - \frac{3p^2Q_2Q_3S_2z}{A_4^{5/2}B_2^2} + \frac{4p^2Q_1Q_4S_9z}{A_1^{3/2}B_1^3} + \frac{3p^2Q_1Q_4S_9z}{A_1^{5/2}B_1^2} \right) \Big) v;
\end{aligned}$$

$$\begin{aligned}
\frac{\sigma_{zz}}{\mu} = & \frac{1}{2K\pi} b_z c \left(-\frac{M2pQ1Q3}{A2^{3/2}} - \frac{M3pQ2Q3}{A4^{3/2}} + \frac{M4pQ1Q4}{A1^{3/2}} + \frac{M1pQ2Q4}{A3^{3/2}} + K2 \left(\frac{4pQ1Q3}{\sqrt{A2B1C1}} - \frac{2H5pQ1Q3}{\sqrt{A2B1C1^2}} - \frac{2H5pQ1Q3}{\sqrt{A2B1^2C1}} - \frac{H5pQ1Q3}{A2^{3/2}B1C1} + \right. \right. \\
& \frac{4pQ2Q3}{\sqrt{A4B2C1}} - \frac{2H6pQ2Q3}{\sqrt{A4B2C1^2}} - \frac{2H6pQ2Q3}{\sqrt{A4B2^2C1}} - \frac{H6pQ2Q3}{A4^{3/2}B2C1} + \frac{2H7pQ1Q4}{\sqrt{A1B1S11^2}} + \frac{2H8pQ2Q4}{\sqrt{A3B2S11^2}} - \frac{4pQ1Q4}{\sqrt{A1B1S11}} + \frac{2H7pQ1Q4}{\sqrt{A1B1^2S11}} + \frac{H7pQ1Q4}{A1^{3/2}B1S11} - \\
& \left. \frac{4pQ2Q4}{\sqrt{A3B2S11}} + \frac{2H8pQ2Q4}{\sqrt{A3B2^2S11}} + \frac{H8pQ2Q4}{A3^{3/2}B2S11} \right) - \frac{M2Q1Q3z}{A2^{3/2}} - \frac{M6pQ1Q3z}{A2^{3/2}} + \frac{3M2p^2Q1Q3z}{A2^{5/2}} - \frac{M3Q2Q3z}{A4^{3/2}} - \frac{M7pQ2Q3z}{A4^{3/2}} + \frac{3M3p^2Q2Q3z}{A4^{5/2}} + \\
& \frac{M4Q1Q4z}{A1^{3/2}} + \frac{M8pQ1Q4z}{A1^{3/2}} - \frac{3M4p^2Q1Q4z}{A1^{5/2}} + \frac{M1Q2Q4z}{A3^{3/2}} + \frac{M5pQ2Q4z}{A3^{3/2}} - \frac{3M1p^2Q2Q4z}{A3^{5/2}} \left) - \frac{1}{K2} 2 \left(\frac{1}{4K\pi} b_z c \left(-\frac{M2pQ1Q3}{A2^{3/2}} - \right. \right. \right. \\
& \left. \left. \frac{M3pQ2Q3}{A4^{3/2}} + \frac{M4pQ1Q4}{A1^{3/2}} + \frac{M1pQ2Q4}{A3^{3/2}} + K2 \left(\frac{4pQ1Q3}{\sqrt{A2B1C1}} - \frac{2H5pQ1Q3}{\sqrt{A2B1C1^2}} - \frac{2H5pQ1Q3}{\sqrt{A2B1^2C1}} - \frac{H5pQ1Q3}{A2^{3/2}B1C1} + \frac{4pQ2Q3}{\sqrt{A4B2C1}} - \frac{2H6pQ2Q3}{\sqrt{A4B2C1^2}} - \right. \right. \right. \\
& \left. \left. \frac{2H6pQ2Q3}{\sqrt{A4B2^2C1}} - \frac{H6pQ2Q3}{A4^{3/2}B2C1} + \frac{2H7pQ1Q4}{\sqrt{A1B1S11^2}} + \frac{2H8pQ2Q4}{\sqrt{A3B2S11^2}} - \frac{4pQ1Q4}{\sqrt{A1B1S11}} + \frac{2H7pQ1Q4}{\sqrt{A1B1^2S11}} + \frac{H7pQ1Q4}{A1^{3/2}B1S11} - \frac{4pQ2Q4}{\sqrt{A3B2S11}} + \frac{2H8pQ2Q4}{\sqrt{A3B2^2S11}} + \right. \right. \\
& \left. \left. \frac{H8pQ2Q4}{A3^{3/2}B2S11} \right) - \frac{M2Q1Q3z}{A2^{3/2}} - \frac{M6pQ1Q3z}{A2^{3/2}} + \frac{3M2p^2Q1Q3z}{A2^{5/2}} - \frac{M3Q2Q3z}{A4^{3/2}} - \frac{M7pQ2Q3z}{A4^{3/2}} + \frac{3M3p^2Q2Q3z}{A4^{5/2}} + \frac{M4Q1Q4z}{A1^{3/2}} + \frac{M8pQ1Q4z}{A1^{3/2}} - \right. \\
& \left. \frac{3M4p^2Q1Q4z}{A1^{5/2}} + \frac{M1Q2Q4z}{A3^{3/2}} + \frac{M5pQ2Q4z}{A3^{3/2}} - \frac{3M1p^2Q2Q4z}{A3^{5/2}} \right) + \frac{1}{4K\pi} b_z c \left(-\frac{G2M10}{C1} + \frac{G2M12}{C2} + \frac{2G2M9Q3}{C1^2} - \frac{2G2M11Q4}{C2^2} + \right. \\
& \frac{6p^2Q1Q3z}{A2^{3/2}C1^2} + \frac{6p^2Q2Q3z}{A4^{3/2}C1^2} - \frac{6p^2Q1Q4z}{A1^{3/2}C2^2} - \frac{6p^2Q2Q4z}{A3^{3/2}C2^2} + \frac{4p^2Q1Q4S5z}{A1^{3/2}C2^3} + \frac{3p^2Q1Q4S5z}{A1^{5/2}C2^2} - \frac{4p^2Q1Q3S6z}{A2^{3/2}C1^3} - \frac{3p^2Q1Q3S6z}{A2^{5/2}C1^2} + \\
& \frac{4p^2Q2Q4S7z}{A3^{3/2}C2^3} + \frac{3p^2Q2Q4S7z}{A3^{5/2}C2^2} - \frac{4p^2Q2Q3S8z}{A4^{3/2}C1^3} - \frac{3p^2Q2Q3S8z}{A4^{5/2}C1^2} \left) + \frac{1}{4K\pi} b_z c \left(G2 \left(\frac{2Q1Q3}{\sqrt{A2B1^2}} + \frac{Q1Q3}{A2^{3/2}B1} + \frac{2Q2Q3}{\sqrt{A4B2^2}} + \frac{Q2Q3}{A4^{3/2}B2} - \right. \right. \right. \\
& \left. \frac{2Q1Q4}{\sqrt{A1B1^2}} - \frac{Q1Q4}{A1^{3/2}B1} - \frac{2Q2Q4}{\sqrt{A3B2^2}} - \frac{Q2Q4}{A3^{3/2}B2} \right) + \frac{6p^2Q1Q3z}{A2^{3/2}B1^2} + \frac{6p^2Q2Q3z}{A4^{3/2}B2^2} - \frac{6p^2Q1Q4z}{A1^{3/2}B1^2} - \frac{6p^2Q2Q4z}{A3^{3/2}B2^2} - \frac{4p^2Q1Q3S1z}{A2^{3/2}B1^3} - \\
& \frac{3p^2Q1Q3S1z}{A2^{5/2}B1^2} + \frac{4p^2Q2Q4S10z}{A3^{3/2}B2^3} + \frac{3p^2Q2Q4S10z}{A3^{5/2}B2^2} - \frac{4p^2Q2Q3S2z}{A4^{3/2}B2^3} - \frac{3p^2Q2Q3S2z}{A4^{5/2}B2^2} + \frac{4p^2Q1Q4S9z}{A1^{3/2}B1^3} + \frac{3p^2Q1Q4S9z}{A1^{5/2}B1^2} \left) \right) v; \\
\frac{\sigma_{xy}}{\mu} = & \frac{1}{4K\pi} b_z c \left(\frac{G2}{C2} \left(-\frac{1}{\sqrt{A1}} + \frac{1}{\sqrt{A3}} + \frac{Q1^2}{A1^{3/2}} - \frac{Q2^2}{A3^{3/2}} \right) - \frac{G2}{C1} \left(-\frac{1}{\sqrt{A2}} + \frac{1}{\sqrt{A4}} + \frac{Q1^2}{A2^{3/2}} - \frac{Q2^2}{A4^{3/2}} \right) - \frac{4p^2Q1^2z}{A2^{3/2}C1^2} + \frac{4p^2Q1^2z}{A1^{3/2}C2^2} + \right. \\
& \frac{4p^2Q2^2z}{A4^{3/2}C1^2} - \frac{4p^2Q2^2z}{A3^{3/2}C2^2} + \frac{p^2S5z}{A1^{3/2}C2^2} - \frac{3p^2Q1^2S5z}{A1^{5/2}C2^2} - \frac{p^2S6z}{A2^{3/2}C1^2} + \frac{3p^2Q1^2S6z}{A2^{5/2}C1^2} - \frac{p^2S7z}{A3^{3/2}C2^2} + \frac{3p^2Q2^2S7z}{A3^{5/2}C2^2} + \frac{p^2S8z}{A4^{3/2}C1^2} - \\
& \left. \frac{3p^2Q2^2S8z}{A4^{5/2}C1^2} \right) + \frac{1}{4K\pi} b_z c \left(G2 \left(-\frac{1}{\sqrt{A1B1}} + \frac{1}{\sqrt{A2B1}} + \frac{1}{\sqrt{A3B2}} - \frac{1}{\sqrt{A4B2}} - \frac{Q3^2}{A2^{3/2}B1} + \frac{Q3^2}{A4^{3/2}B2} + \frac{Q4^2}{A1^{3/2}B1} - \frac{Q4^2}{A3^{3/2}B2} \right) - \right. \\
& \frac{4p^2Q3^2z}{A2^{3/2}B1^2} + \frac{4p^2Q3^2z}{A4^{3/2}B2^2} + \frac{4p^2Q4^2z}{A1^{3/2}B1^2} - \frac{4p^2Q4^2z}{A3^{3/2}B2^2} - \frac{p^2S1z}{A2^{3/2}B1^2} + \frac{3p^2Q3^2S1z}{A2^{5/2}B1^2} - \frac{p^2S10z}{A3^{3/2}B2^2} + \frac{3p^2Q4^2S10z}{A3^{5/2}B2^2} + \frac{p^2S2z}{A4^{3/2}B2^2} - \\
& \left. \frac{3p^2Q3^2S2z}{A4^{5/2}B2^2} + \frac{p^2S9z}{A1^{3/2}B1^2} - \frac{3p^2Q4^2S9z}{A1^{5/2}B1^2} \right); \\
\frac{\sigma_{xz}}{\mu} = & \frac{1}{4K\pi} b_z c \left((1 + 2K) \left(\frac{Q3}{\sqrt{A2B1}} - \frac{Q3}{\sqrt{A4B2}} - \frac{Q4}{\sqrt{A1B1}} + \frac{Q4}{\sqrt{A3B2}} \right) + G2 \left(-\frac{2pQ3}{\sqrt{A2B1^2}} - \frac{pQ3}{A2^{3/2}B1} + \frac{2pQ3}{\sqrt{A4B2^2}} + \frac{pQ3}{A4^{3/2}B2} + \right. \right. \\
& \frac{2pQ4}{\sqrt{A1B1^2}} + \frac{pQ4}{A1^{3/2}B1} - \frac{2pQ4}{\sqrt{A3B2^2}} - \frac{pQ4}{A3^{3/2}B2} \left) - \frac{p^2Q3S1}{A2^{3/2}B1^2} - \frac{p^2Q4S10}{A3^{3/2}B2^2} + \frac{p^2Q3S2}{A4^{3/2}B2^2} + \frac{p^2Q4S9}{A1^{3/2}B1^2} - \frac{6p^3Q3z}{A2^{3/2}B1^2} + \frac{6p^3Q3z}{A4^{3/2}B2^2} - \right. \\
& \frac{6p^3Q4z}{A1^{3/2}B1^2} - \frac{6p^3Q4z}{A3^{3/2}B2^2} - \frac{2pQ3S1z}{A2^{3/2}B1^2} + \frac{4p^3Q3S1z}{A2^{3/2}B1^3} + \frac{3p^3Q3S1z}{A2^{5/2}B1^2} - \frac{2pQ4S10z}{A3^{3/2}B2^2} + \frac{4p^3Q4S10z}{A3^{3/2}B2^3} + \frac{3p^3Q4S10z}{A3^{5/2}B2^2} + \frac{2pQ3S2z}{A4^{3/2}B2^2} - \\
& \frac{4p^3Q3S2z}{A4^{3/2}B2^3} - \frac{3p^3Q3S2z}{A4^{5/2}B2^2} + \frac{2pQ4S9z}{A1^{3/2}B1^2} - \frac{4p^3Q4S9z}{A1^{3/2}B1^3} - \frac{3p^3Q4S9z}{A1^{5/2}B1^2} \left) + \frac{1}{4K\pi} b_z c \left(K2 \left(-\frac{H5Q3}{\sqrt{A2B1C1}} + \frac{H6Q3}{\sqrt{A4B2C1}} - \frac{2Q1^2Q3}{\sqrt{A2B1C1}} + \right. \right. \right. \\
& \frac{2H5Q1^2Q3}{\sqrt{A2B1^2C1}} + \frac{H5Q1^2Q3}{A2^{3/2}B1C1} + \frac{2Q2^2Q3}{\sqrt{A4B2C1}} - \frac{2H6Q2^2Q3}{\sqrt{A4B2^2C1}} - \frac{H6Q2^2Q3}{A4^{3/2}B2C1} + \frac{H7Q4}{\sqrt{A1B1S11}} - \frac{H8Q4}{\sqrt{A3B2S11}} + \frac{2Q1^2Q4}{\sqrt{A1B1S11}} - \frac{2H7Q1^2Q4}{\sqrt{A1B1^2S11}} - \\
& \frac{H7Q1^2Q4}{A1^{3/2}B1S11} - \frac{2Q2^2Q4}{\sqrt{A3B2S11}} + \frac{2H8Q2^2Q4}{\sqrt{A3B2^2S11}} + \frac{H8Q2^2Q4}{A3^{3/2}B2S11} \left) + \frac{M2pQ3z}{A2^{3/2}} - \frac{M3pQ3z}{A4^{3/2}} - \frac{3M2pQ1^2Q3z}{A2^{5/2}} + \frac{3M3pQ2^2Q3z}{A4^{5/2}} + \frac{M1pQ4z}{A3^{3/2}} - \\
& \frac{M4pQ4z}{A1^{3/2}} + \frac{3M4pQ1^2Q4z}{A1^{5/2}} - \frac{3M1pQ2^2Q4z}{A3^{5/2}} - \frac{pQ1Q3}{A2^{3/2}} \left(-\frac{6Q1}{B1^2} - \frac{4Q1}{C1^2} + \frac{4Q1S1}{B1^3} \right) z + \frac{pQ2Q4}{A3^{3/2}} \left(\frac{6Q2}{B2^2} - \frac{4Q2S10}{B2^3} + \frac{4Q2}{S11^2} \right) z - \\
& \frac{pQ2Q3}{A4^{3/2}} \left(\frac{6Q2}{B2^2} + \frac{4Q2}{C1^2} - \frac{4Q2S2}{B2^3} \right) z + \frac{pQ1Q4}{A1^{3/2}} \left(-\frac{6Q1}{B1^2} - \frac{4Q1}{S11^2} + \frac{4Q1S9}{B1^3} \right) z \left); \right.
\end{aligned}$$

$$\begin{aligned}
\frac{\sigma_{yz}}{\mu} = & \frac{1}{4K\pi} b_z c \left(\frac{(1+2K)M11}{C2} - \frac{(1+2K)M9}{C1} - \frac{2G2M11p}{C2^2} + \frac{2G2M9p}{C1^2} + \frac{G2}{C2} \left(-\frac{pQ1}{A1^{3/2}} - \frac{pQ2}{A3^{3/2}} \right) - \frac{G2}{C1} \left(-\frac{pQ1}{A2^{3/2}} - \frac{pQ2}{A4^{3/2}} \right) - \right. \\
& \frac{p^2Q1S5}{A1^{3/2}C2^2} + \frac{p^2Q1S6}{A2^{3/2}C1^2} - \frac{p^2Q2S7}{A3^{3/2}C2^2} + \frac{p^2Q2S8}{A4^{3/2}C1^2} + \frac{6p^3Q1z}{A2^{3/2}C1^2} - \frac{6p^3Q1z}{A1^{3/2}C2^2} + \frac{6p^3Q2z}{A4^{3/2}C1^2} - \frac{6p^3Q2z}{A3^{3/2}C2^2} - \frac{2pQ1S5z}{A1^{3/2}C2^2} + \frac{4p^3Q1S5z}{A1^{3/2}C2^3} + \\
& \left. \frac{3p^3Q1S5z}{A1^{5/2}C2^2} + \frac{2pQ1S6z}{A2^{3/2}C1^2} - \frac{4p^3Q1S6z}{A2^{3/2}C1^3} - \frac{3p^3Q1S6z}{A2^{5/2}C1^2} - \frac{2pQ2S7z}{A3^{3/2}C2^2} + \frac{4p^3Q2S7z}{A3^{3/2}C2^3} + \frac{3p^3Q2S7z}{A3^{5/2}C2^2} + \frac{2pQ2S8z}{A4^{3/2}C1^2} - \frac{4p^3Q2S8z}{A4^{3/2}C1^3} - \frac{3p^3Q2S8z}{A4^{5/2}C1^2} \right) + \\
& \frac{1}{4K\pi} b_z c \left(K2 \left(\frac{H5Q1}{\sqrt{A2B1C1}} + \frac{H6Q2}{\sqrt{A4B2C1}} + \frac{2Q1Q3^2}{\sqrt{A2B1C1}} - \frac{2H5Q1Q3^2}{\sqrt{A2B1C1^2}} - \frac{H5Q1Q3^2}{A2^{3/2}B1C1} + \frac{2Q2Q3^2}{\sqrt{A4B2C1}} - \frac{2H6Q2Q3^2}{\sqrt{A4B2C1^2}} - \frac{H6Q2Q3^2}{A4^{3/2}B2C1} + \right. \right. \\
& \left. \frac{2H7Q1Q4^2}{\sqrt{A1B1S11^2}} + \frac{2H8Q2Q4^2}{\sqrt{A3B2S11^2}} - \frac{H7Q1}{\sqrt{A1B1S11}} - \frac{H8Q2}{\sqrt{A3B2S11}} - \frac{2Q1Q4^2}{\sqrt{A1B1S11}} + \frac{H7Q1Q4^2}{A1^{3/2}B1S11} - \frac{2Q2Q4^2}{\sqrt{A3B2S11}} + \frac{H8Q2Q4^2}{A3^{3/2}B2S11} \right) - \frac{M2pQ1z}{A2^{3/2}} + \\
& \frac{M4pQ1z}{A1^{3/2}} + \frac{M1pQ2z}{A3^{3/2}} - \frac{M3pQ2z}{A4^{3/2}} + \frac{3M2pQ1Q3^2z}{A2^{5/2}} + \frac{3M3pQ2Q3^2z}{A4^{5/2}} - \frac{3M4pQ1Q4^2z}{A1^{5/2}} - \frac{3M1pQ2Q4^2z}{A3^{5/2}} + \frac{pQ1Q4}{A1^{3/2}} \left(\frac{4Q4}{B1^2} + \frac{6Q4}{S11^2} - \right. \\
& \left. \frac{4Q4(2Q1^2+3S11)}{S11^3} \right) z + \frac{pQ2Q4}{A3^{3/2}} \left(\frac{4Q4}{B2^2} + \frac{6Q4}{S11^2} - \frac{4Q4(2Q2^2+3S11)}{S11^3} \right) z - \frac{pQ1Q3}{A2^{3/2}} \left(\frac{4Q3}{B1^2} + \frac{6Q3}{C1^2} - \frac{4Q3S6}{C1^3} \right) z - \frac{pQ2Q3}{A4^{3/2}} \left(\frac{4Q3}{B2^2} + \frac{6Q3}{C1^2} - \right. \\
& \left. \frac{4Q3S8}{C1^3} \right) z);
\end{aligned}$$

$$\begin{aligned}
A1 &= (a-x)^2 + (b-y)^2 + (c+z)^2; & A2 &= (a-x)^2 + (b+y)^2 + (c+z)^2; \\
A3 &= (a+x)^2 + (b-y)^2 + (c+z)^2; & A4 &= (a+x)^2 + (b+y)^2 + (c+z)^2; \\
B1 &= (a-x)^2 + (c+z)^2; & B2 &= (a+x)^2 + (c+z)^2; & C1 &= (b+y)^2 + (c+z)^2; & C2 &= (b-y)^2 + \\
& (c+z)^2; & p &= c+z; & Q1 &= a-x; & Q2 &= a+x; \\
Q3 &= b+y; & Q4 &= -b+y; & K &= -1+v; & K2 &= -1+2v; & K3 &= 1+v; \\
K4 &= -2cK - zK2; & S1 &= 3A2 - Q3^2; & S2 &= 3A4 - Q3^2; & S3 &= 3A1 - Q5^2; \\
S4 &= 3A3 - Q5^2; & S5 &= 3A1 - Q1^2; & S6 &= 3A2 - Q1^2; & S7 &= 3A3 - Q2^2; \\
S8 &= 3A4 - Q2^2; & S9 &= 3A1 - Q4^2; & S10 &= 3A3 - Q4^2; & S11 &= p^2 + Q4^2; \\
G1 &= -z - 2pK; & G2 &= -G1; & H1 &= 3p^2 + 2Q1^2 + 3Q3^2; & H2 &= 3p^2 + 2Q2^2 + 3Q3^2; & H3 &= 3p^2 + \\
& 2Q1^2 + 3Q4^2; & H4 &= 3p^2 + 2Q2^2 + 3Q4^2; & H5 &= 2p^2 + Q1^2 + Q3^2; & H6 &= 2p^2 + Q2^2 + Q3^2; & H7 &= \\
& 2p^2 + Q1^2 + Q4^2; & H8 &= 2p^2 + Q2^2 + Q4^2; \\
M1 &= \frac{S10}{B2^2} + \frac{2Q2^2+3S11}{S11^2}; & M2 &= \frac{S1}{B1^2} + \frac{S6}{C1^2}; & M3 &= \frac{S2}{B2^2} + \frac{S8}{C1^2}; & M4 &= \frac{2Q1^2+3S11}{S11^2} + \frac{S9}{B1^2}; \\
M5 &= \frac{6p}{B2^2} - \frac{4pS10}{B2^3} + \frac{6p}{S11^2} - \frac{4p(2Q2^2+3S11)}{S11^3}; & M6 &= \frac{6p}{B1^2} + \frac{6p}{C1^2} - \frac{4pS1}{B1^3} - \frac{4pS6}{C1^3}; \\
M7 &= \frac{6p}{B2^2} + \frac{6p}{C1^2} - \frac{4pS2}{B2^3} - \frac{4pS8}{C1^3}; & M8 &= \frac{6p}{B1^2} + \frac{6p}{S11^2} - \frac{4p(2Q1^2+3S11)}{S11^3} - \frac{4pS9}{B1^3}; \\
M9 &= \frac{Q1}{\sqrt{A2}} + \frac{Q2}{\sqrt{A4}}; & M10 &= -\frac{Q1Q3}{A2^{3/2}} - \frac{Q2Q3}{A4^{3/2}}; & M11 &= \frac{Q1}{\sqrt{A1}} + \frac{Q2}{\sqrt{A3}}; \\
M12 &= -\frac{Q1Q4}{A1^{3/2}} - \frac{Q2Q4}{A3^{3/2}};
\end{aligned}$$

REFERENCES

1. Hull D, Bacon DJ. Introduction to Dislocations. University of Liverpool, UK; 2011.
2. Hirth JP, Lothe J. Theory of Dislocations. Krieger Publishing Company, Malabar, Florida; 1982.
3. Weertman J, Weertman JR. Elementary Dislocation Theory. Oxford University Press, Oxford; 1992.
4. Kroupa F. Circular edge dislocation loop. Czechoslovak Journal of Physics B. 1960; 10: 284–293.
5. Bullough R, Newman RC. The spacing of prismatic dislocation loops. Philosophical Magazine. 1960; 5(57): 921–926.
6. Keller JM. unpublished.; 1957.
7. Kröner E. Kontinuumstheorie Der Versetzungen Und Eigenspannungen. Springer-Verlag, Berlin; 1958.
8. Kroupa F. Interaction between prismatic dislocation loops and straight dislocations – 1. Philosophical Magazine. 1962; 7(77): 783–801.
9. Marcinkowski MJ, Sree Harsh KS. Properties of finite circular dislocation glide loops. Journal of Applied Physics. 1968; 39(3): 1775–1783.
10. Khraishi TA, Hirth JP, Zbib HM, Khaleel MA. The displacement, and strain-stress fields of a general circular Volterra dislocation loop. International Journal of Engineering Science. 2000; 38(3): 251–266.
11. Khraishi TA, Zbib HM, Hirth JP, de la Rubia TD. The stress field of a general circular volterra dislocation loop: analytical and numerical approaches. Philosophical Magazine Letters. 2000; 80(2): 95–105.
12. Khraishi TA, Zbib HM. The Displacement Field of a Rectangular Volterra Dislocation Loop. Philosophical Magazine Letters. 2002; 82(5): 265-277.
<https://doi.org/10.1080/09500830210125770>
13. Demir I, Hirth JP, Zbib HM. Extended stress field around a cylindrical crack using the theory of dislocation pile-ups. International Journal of Engineering Science. 1992; 30(7): 829–845.
14. Demir I, Hirth JP, Zbib HM. The Somigliana ring dislocation. Journal of Elasticity. 1992; 28: 223–246.

15. Demir I, Khraishi TA. The Torsional Dislocation Loop and Mode III Cylindrical Crack. *Journal of Mechanics*. 2005; 21(2): 115-122.
16. Yoffe EH. A dislocation at a free surface. *Philosophical Magazine*. 1961; 6(69): 1147–55.
17. Baštecká, J. Interaction of dislocation loop with free surface. *Czechoslovak Journal of Physics*. 1964; 14: 430-42.
18. Chou YT. Energy of circular dislocation loops in thin plates. *Acta Metall*. 1963; 11(8): 829–834.
19. Baštecká J, Kroupa F. Elastic interaction of dislocation loops and point defects. *Czechoslovak Journal of Physics*. 1964; 14: 443–453.
20. Bacon DJ, Groves PP. The dislocation in a semi-infinite isotropic Medium. In: Bacon DJ, Groves PP, Ed., *Fundamental Aspects of Dislocation Theory*, Witt R and Bullough R, Inc., Washington, DC, USA; 1970.
21. Groves PP, Bacon DJ. The dislocation loop near a free surface. *Philosophical Magazine*. 1970; 22: 83–91.
22. Jing P, Khraishi TA, Zepeda-Ruiz LA, Wirth BD. The elastic fields of sub-surface dislocation loops: a comparison between analytical continuum-theory solutions and atomistic calculations. *Int. J. Theoretical and Applied Multiscale Mechanics*. 2009; 1(1): 71-85.
23. Maurissen Y, Capella L. Stress field of a dislocation segment parallel to a free surface. *Philosophical Magazine*. 1974; 29(5): 1227–1225.
24. Maurissen, Y, Capella L. Stress field of a dislocation segment perpendicular to a free surface. *Philosophical Magazine*. 1974; 30(3): 679–683.
25. Comninou M, Dundurs J. The angular dislocation in a half space. *Journal of Elasticity*. 1975; 19, 203-16.
26. Lothe J, Indenbom VL, Chamrov VA. Elastic field and self-force of dislocations emerging at the free surfaces of an anisotropic half-space. *Physica Status Solidi(B)*. 1982; 5: 671–7.
27. Gosling TJ, Willis JR. A line-integral representation for the stresses due to an arbitrary dislocation in an isotropic half-space. *Journal of Mechanics and Physics of Solids*. 1994; 42(8): 1199-1221.
28. Khraishi TA, Zbib HM, de la Rubia, TD. The Treatment of Traction free Boundary Condition in Three-dimensional Dislocation Dynamics using Generalized Image Stress Analysis. *Materials Science and Engineering A*. 2001; 309-310: 283-287.

29. Khraishi TA, Zbib HM. Free Surface Effects in 3D Dislocation Dynamics: Formulation and Modeling. *Journal of Engineering Materials and Technology (JEMT)*. 2002; 124(3): 342-351.
30. Yan L, Khraishi TA, Shen YL, Horstemeyer MF. A Distributed Dislocation Method for Treating Free-Surface Image Stresses in 3D Dislocation Dynamics Simulations. *Modelling and Simulation in Materials Science and Engineering*. 2004; 12: 289-301.
31. Siddique AB, Khraishi TA. Numerical methodology for treating static and dynamic dislocation problems near a free surface. *Journal of Physics Communications*. 2020; 4 (5), 055005, DOI 10.1088/2399-6528/ab8ff9.
32. Lerma J, Khraishi TA, Shen YL. Elastic Fields of 2D and 3D Misfit Particles in an Infinite Medium. *Mechanics Research Communications*. 2007; 34(1): 31-43.
33. Lerma J, Khraishi TA, Kataria S, Shen YL. Distributed Dislocation Method for Determining Elastic Fields of 2D and 3D Volume Misfit Particles in Infinite Space and Extension of the Method for Particles in Half Space. *Journal of Mechanics*. 2015; 31(3): 249-260.
34. Khraishi TA, Shen YL. *Introductory Continuum Mechanics with Applications to Elasticity*. University Readers/Cognella, San Diego, California; 2011.

Chapter 4 Strain Field Development of a Rectangular Dislocation Loop in a Semi-Infinite Medium with Verification

ABSTRACT

This paper considers a rectangular Volterra dislocation loop lying beneath and parallel to a free surface in a semi-infinite material. The paper utilizes the displacement field of an infinitesimal dislocation loop to obtain the strain field and then integrate over a finite rectangular area. For the loop, it can have three non-zero Burgers vector components. The stress field is also obtained from Hooke's law for isotropic materials. Analytical and numerical verifications of the strain and stress fields are performed. In addition, the effect of the free surface on stresses is displayed versus depth from the surface. Verification includes satisfaction of the zero-traction boundary condition, the stress equilibrium equations and the strain compatibility equations.

Keywords: Rectangular dislocation loop; half medium; strain/stress field; numerical/analytical verification.

INTRODUCTION

Dislocation loops are defects in the material, associating the collapse of a large number of point defects into lower energy defect structures. A rectangular dislocation loop is a closed loop composed of four straight dislocation lines. Dislocation lines have to end on free surfaces, grain boundaries, or form a closed loop inside a material. They cannot end inside the crystal [1]. In this work, the development of the strain field of a Volterra-type rectangular dislocation loop parallel to the free surface of half medium, and having three non-zero Burgers vector components, is focused on.

Several dislocation problems in terms of material type, geometry and size have been developed for decades. In the early years, research on infinite isotropic materials was studied by different researchers. Development of the elastic fields of infinite screw and edge dislocations in an infinite isotropic medium were provided [2-4]. Furthermore, integral equations for finding the displacement field (the Burgers equation) and the stress field (the Peach-Koehler equation) of a closed dislocation loop (of any shape) in an *infinite* isotropic material have been provided by Hirth JP et al. [2].

A couple of researchers have studied different kinds of dislocation loop problems applying various techniques. Initially, [5-6] researched the prismatic circular loop. The circular glide loop was initially investigated by Keller JM [7] Kröner E [8], which was later corrected in [9-10]. Khraishi TA et al [11] Khraishi TA et al. [12] corrected some earlier work in a more recent study of the displacement and stress fields of glide and prismatic circular dislocation loops. The displacement field of a rectangular dislocation loop of the Volterra type in an infinite medium was obtained by Khraishi TA et al. [13], which contains a solid angle term. The above references in this paragraph all focused on an infinite material.

One application for dislocation loops is its use in the “collocation point” method that is used to resolve traction-free surface problems in a semi-infinite material simulated with the 3-D DDD method via a surface mesh of rectangular/triangular dislocation loops [14-18]. Siddique AB et al [19] extended the collocation-point method to deal with curved free surfaces. For circular dislocation loops, they were used for modeling pile-ups around rigid cylindrical particles [20] and for modeling Frank sessile loops which are caused by irradiation damage in some metals [21-23].

As for studies involving dislocations near a free surface, Yoffe EH et al [24] developed the elastic fields of a dislocation terminating on a free surface (for any Burgers vector). Groves PP et al. [25] studied the effects of free surfaces on a dislocation loop. Maurissen Y et al. [26] Maurissen Y et al [27] obtained the correction terms of the stress field of a dislocation half-line and segment parallel and perpendicular to a free surface in a semi-infinite elastic medium. Comninou M et al. [28] presented the formulations for the elastic fields of an angular dislocation in an isotropic half-space. Gosling TJ et al. [29] determined the stresses due to an arbitrary dislocation in a semi-infinite medium as a line integral along the dislocation. Jing et al. [30] found the displacement field of a rectangular dislocation loop parallel to a free surface.

In this paper, the strain components of a rectangular dislocation loop parallel to a free surface are obtained. Also, analytical and numerical verifications for the strain field are performed. The verification is to ensure that the Strain Compatibility Equations are satisfied. Then, the stress field, obtained via Hooke’s law using the strain developed herein, is verified using the Equilibrium Equations and the zero-traction condition on the free surface. Moreover, plots reflecting the effect of the free surface correction term are presented at different depths beneath the surface.

METHODOLOGY

Development of the strains of the sub-surface rectangular dislocation loop

The dislocation problem under consideration is shown in Fig. 1. The figure shows a rectangular dislocation loop (also described as a “finite-sized dislocation loop”) in a semi-infinite isotropic medium and which is below the free surface. This Volterra-type dislocation loop has three Burgers vector components b_x , b_y and b_z . Also, it has a dimension $2a$ in the x -direction and a dimension $2b$ in the y -direction. The line sense of the dislocation loop is shown by the arrow around the dislocation loop. The goal of this problem is to obtain the strain components at an arbitrary material field point P. Note that in this paper, x_1 and x are used interchangeably, so are x_2 and y , and so are x_3 and z . Analogously for x'_1 and x' , and so on.

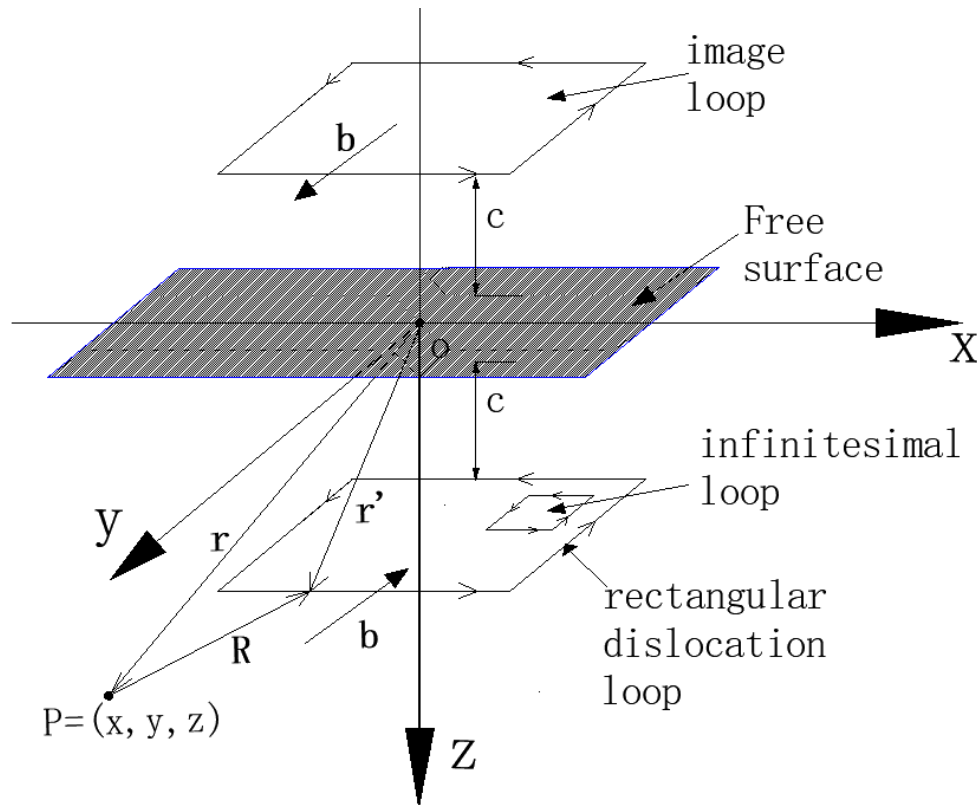


Fig. 1. A rectangular dislocation loop with an arbitrary Burgers vector, below a free surface. Also, an image dislocation loop with opposite Burgers vector is shown above the surface. An infinitesimal dislocation loop used in the integration is also shown.

To find the total strain field due to the subsurface rectangular dislocation loop, one can sum up the three contributions of the total strain field as in the following:

$$\epsilon = \epsilon^{inf} + \epsilon^{imag} + \epsilon^s \quad (1)$$

Where the superscript ‘*inf*’ refers to the strain solution of a rectangular dislocation loop in an infinite medium, not in a half medium as shown in Fig. 1. The superscript ‘*imag*’ refers to the strain solution of an image dislocation loop with an opposite Burgers vector laying above the surface. And the ‘*s*’ superscript refers to surface correction term which ensures the zero-traction condition on the free surface, i.e. the image loop by itself does not annul all the stress traction components on the surface.

Let’s focus on the correction term in the above equation first. Bacon and Grove provided an equation for the displacement surface correction term of a subsurface infinitesimal dislocation loop with area dS [25]:

$$du_i^s = -kx'_3(1 - 2\delta_{j3})\left[A_{i3}\left(\frac{1}{R}\right)_{,ij} - \left(\frac{x_3}{R}\right)_{,ij3}\right] \quad (2)$$

where, $k = b_j dS/4\pi(1 - \nu)$, $A_{ij} = 2\nu + 4(1 - \nu)\delta_{ij}$, $dS = dx'_1 dx'_2$, $R^2 = (x_1 - x'_1)^2 + (x_2 - x'_2)^2 + (x_3 + x'_3)^2$. δ_{ij} is the ij^{th} component of the Kronecker delta.

Equation (2) can be written explicitly as follows:

When

i=1:

j=1:

$$du_1^s = -\frac{x'_3 b_x dS}{4\pi(1-\nu)} \left[2\nu \left(\frac{1}{R}\right)_{,11} - \left(\frac{x_3}{R}\right)_{,113} \right] \quad (3)$$

i=1:

j=2:

$$du_1^s = -\frac{x'_3 b_y dS}{4\pi(1-\nu)} \left[2\nu \left(\frac{1}{R}\right)_{,12} - \left(\frac{x_3}{R}\right)_{,123} \right] \quad (4)$$

i=1:

j=3:

$$du_1^s = \frac{x'_3 b_z dS}{4\pi(1-\nu)} \left[2\nu \left(\frac{1}{R}\right)_{,13} - \left(\frac{x_3}{R}\right)_{,133} \right] \quad (5)$$

When

i=2:

j=1:

$$du_2^s = -\frac{x'_3 b_x dS}{4\pi(1-\nu)} \left[2\nu \left(\frac{1}{R}\right)_{,21} - \left(\frac{x_3}{R}\right)_{,213} \right] \quad (6)$$

i=2:

j=2:

$$du_2^s = -\frac{x'_3 b_y dS}{4\pi(1-\nu)} \left[2\nu \left(\frac{1}{R}\right)_{,22} - \left(\frac{x_3}{R}\right)_{,223} \right] \quad (7)$$

i=2:

j=3:

$$du_2^s = \frac{x'_3 b_z dS}{4\pi(1-\nu)} \left[2\nu \left(\frac{1}{R}\right)_{,23} - \left(\frac{x_3}{R}\right)_{,233} \right] \quad (8)$$

When

i=3:

j=1:

$$du_3^s = -\frac{x'_3 b_x dS}{4\pi(1-\nu)} \left[(2\nu + 4(1-\nu)) \left(\frac{1}{R}\right)_{,31} - \left(\frac{x_3}{R}\right)_{,313} \right] \quad (9)$$

i=3:

j=2:

$$du_3^s = -\frac{x_3' b_y dS}{4\pi(1-\nu)} \left[(2\nu + 4(1-\nu)) \left(\frac{1}{R}\right)_{,32} - \left(\frac{x_3}{R}\right)_{,323} \right] \quad (10)$$

i=3:

j=3:

$$du_3^s = \frac{x_3' b_z dS}{4\pi(1-\nu)} \left[(2\nu + 4(1-\nu)) \left(\frac{1}{R}\right)_{,33} - \left(\frac{x_3}{R}\right)_{,333} \right] \quad (11)$$

To find the strain field for the correction term of an infinitesimal loop, the tensorial small strain definition is applied:

$$d\epsilon_{ij}^s = \frac{1}{2} \left(\frac{\partial du_i^s}{\partial x_j} + \frac{\partial du_j^s}{\partial x_i} \right) \quad (12)$$

As for the strain surface *correction* term in equation (1) for the finite rectangular loop, it can be obtained with integration via:

$$\epsilon = \int_A d\epsilon^s \quad (13)$$

Where A is the area of integration. For the infinite term in equation (1), the elastic fields of a rectangular dislocation loop have been obtained in [31]. Hence, the development of the infinite term in equation (1) is not repeated here for brevity. If one has the solution for the *infinite* term in equation (1), one can easily obtain the *image* term which has an opposite Burgers vector and opposite 'z' value to infinite term. If one has the expressions for the three terms contributing to equation (1), then the *total* strain field can be easily determined from the sum of these terms.

RESULTS AND DISCUSSION

Based on the above, the strain field of a rectangular dislocation loop has been obtained with integrations and other manipulations all performed using the strong symbolic engine of the mathematical software Mathematica. Results of the correction term are provided in the Appendix. If one is interested in the stress field (which is not shown herein explicitly like the strains for brevity sake), one can use Hooke's law for isotropic materials:

$$\sigma_{ij} = \lambda \epsilon_{kk} \delta_{ij} + 2\mu \epsilon_{ij} \quad (14)$$

where $\lambda = \frac{E\nu}{(1+\nu)(1-2\nu)}$, $\mu = \frac{E}{2(1+\nu)}$ Here, δ_{ij} is the ij^{th} component of the Kronecker delta, μ is shear modulus, ϵ_{kk} is the dilatation or the volumetric strain, and E is Young's modulus.

Strain Compatibility Equations Verification

The equations of compatibility can be written in indicial notation as [32]:

$$\epsilon_{ij,kl} - \epsilon_{jl,ik} - \epsilon_{ik,jl} + \epsilon_{kl,ij} = 0 \quad (15)$$

This equation can be expanded over the repeated indices and written explicitly as six different/unique equations:

$$\frac{\partial^2 \epsilon_{xx}}{\partial y^2} + \frac{\partial^2 \epsilon_{yy}}{\partial x^2} = 2 \frac{\partial^2 \epsilon_{xy}}{\partial x \partial y} \quad (16)$$

$$\frac{\partial^2 \epsilon_{xx}}{\partial z^2} + \frac{\partial^2 \epsilon_{zz}}{\partial x^2} = 2 \frac{\partial^2 \epsilon_{xz}}{\partial x \partial z} \quad (17)$$

$$\frac{\partial^2 \epsilon_{zz}}{\partial y^2} + \frac{\partial^2 \epsilon_{yy}}{\partial z^2} = 2 \frac{\partial^2 \epsilon_{zy}}{\partial z \partial y} \quad (18)$$

$$\frac{\partial^2 \epsilon_{xx}}{\partial y \partial z} + \frac{\partial^2 \epsilon_{yz}}{\partial x^2} = \frac{\partial^2 \epsilon_{xz}}{\partial x \partial y} + \frac{\partial^2 \epsilon_{xy}}{\partial x \partial z} \quad (19)$$

$$\frac{\partial^2 \epsilon_{yy}}{\partial x \partial z} + \frac{\partial^2 \epsilon_{xz}}{\partial y^2} = \frac{\partial^2 \epsilon_{xy}}{\partial y \partial z} + \frac{\partial^2 \epsilon_{yz}}{\partial x \partial y} \quad (20)$$

$$\frac{\partial^2 \epsilon_{zz}}{\partial x \partial y} + \frac{\partial^2 \epsilon_{xy}}{\partial z^2} = \frac{\partial^2 \epsilon_{xz}}{\partial y \partial z} + \frac{\partial^2 \epsilon_{yz}}{\partial x \partial z} \quad (21)$$

These equations should be satisfied at every material point in the solid. To verify the developed strain solution, one can see if equations (16-21) are identically zero using either analytical or numerical methods. For the analytical method, the equations are so humongous that Mathematica is not able to reduce them to 0. However, for any given line in space along the x -, y - or z -directions, Mathematica identically converts the compatibility equations to zero. Hence analytical verification of the compatibility equations is feasible.

Alternatively, numerical verifications can also be shown by plotting equations (16-21) along any plane in the material to see if the equations give a zero result. Fig. 2 shows such plotting for $b_z \neq 0$. The figure shows that the compatibility equations are satisfied. Note that given the combination of Burgers vector components and compatibility equations a total of eighteen plots are minimally generated. Therefore, only three plots for one of the Burgers vector components are shown here for brevity.

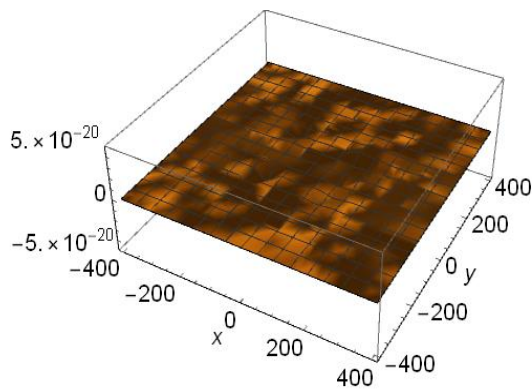


Fig. 2.1 Plot of equation (16)

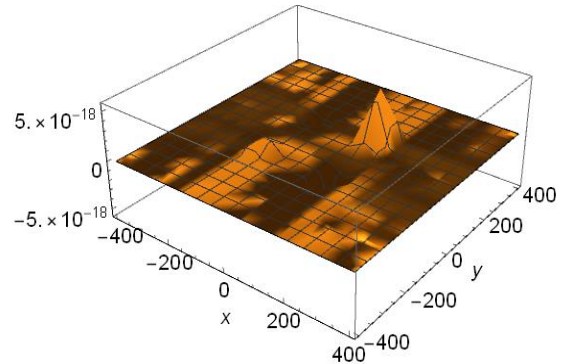


Fig. 2.2 Plot of equation (19)

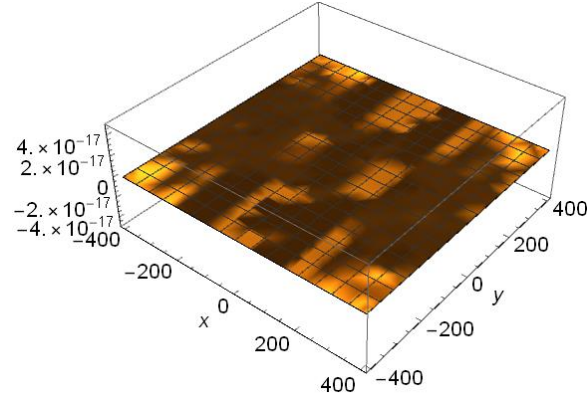


Fig. 2.3 Plot of equation (20)

For these plots, the following values were chosen: $a = b = 100b_z$, $z' = c = 10b_z$, $b_x = b_y = 0$, $b_z = 1$, $\nu = 0.3$, $\mu = G = 100$, $z = 11b_z$, $-4a \leq x \leq 4a$, $-4b \leq y \leq 4b$

Equilibrium Equations Verification

To verify the strain field developed in this paper, one can use equation (14) to obtain the stress field and see if the obtained stress field can satisfy the equilibrium equations. The partial differential equations of static equilibrium in a solid material can be written in indicial notation as:

$$\sigma_{ij,j} = \frac{\partial \sigma_{ij}}{\partial x_j} = 0 \quad (22)$$

If the last equation is expanded on the repeated indices then the resulting three equations are:

$$\frac{\partial \sigma_{xx}}{\partial x} + \frac{\partial \sigma_{xy}}{\partial y} + \frac{\partial \sigma_{xz}}{\partial z} = 0 \quad (23)$$

$$\frac{\partial \sigma_{yx}}{\partial x} + \frac{\partial \sigma_{yy}}{\partial y} + \frac{\partial \sigma_{yz}}{\partial z} = 0 \quad (24)$$

$$\frac{\partial \sigma_{zx}}{\partial x} + \frac{\partial \sigma_{zy}}{\partial y} + \frac{\partial \sigma_{zz}}{\partial z} = 0 \quad (25)$$

This is keeping in mind the symmetry of the stress tensor, i.e. $\sigma_{ij} = \sigma_{ji}$. These equations should be satisfied at every material point of a solid in equilibrium. To verify the stress solution given by equation (14), one can see if equations (23-25) are identically satisfied

either using analytical or numerical methods. For the analytical method, the equations are all reduced to zero by utilizing Mathematica. Analogously, if one considers any line in space, the three equilibrium equations also equate analytically to zero. Hence, analytical verification of the equilibrium equations is feasible.

Alternatively, numerical verification can also be made by plotting equations (23-25) along any plane in the material to see if the equations show a zero result. Fig. 3 shows such plotting for $b_y \neq 0$. The figure shows that the equilibrium equations are satisfied. Note that given the combination of Burgers vector components and equilibrium equations a total of nine plots are minimally generated. Therefore, only three plots for one of the Burgers vector components are shown here for brevity.

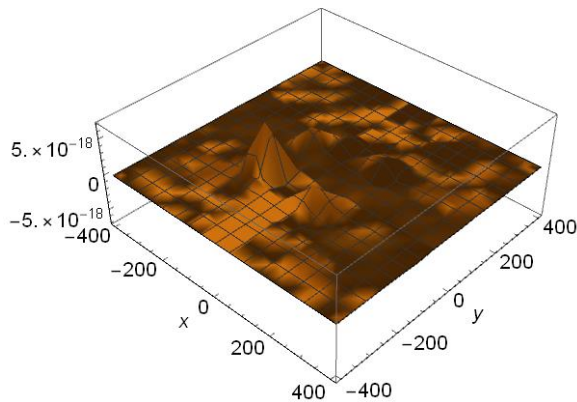


Fig. 3.1 Plot of equation (23)

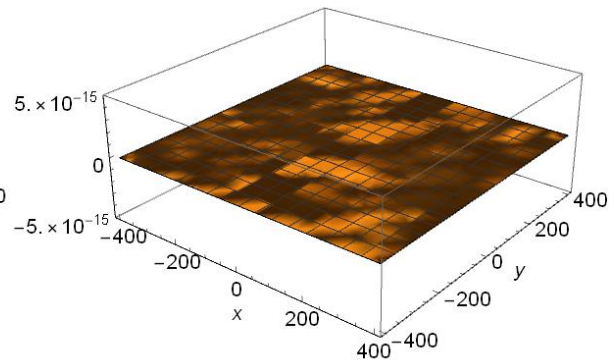


Fig. 3.2 Plot of equation (24)

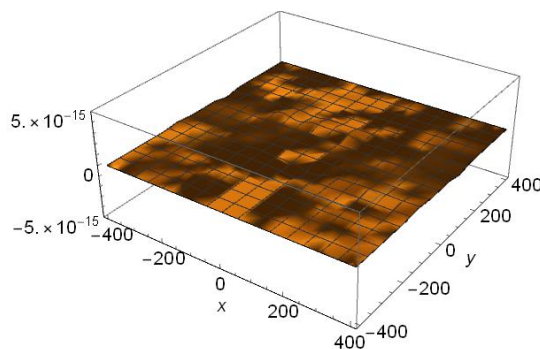


Fig. 3.3 Plot of equation (25)

For these plots, the following values were chosen: $a = b = 100b_y$, $z' = c = 10b_y$, $b_x = b_z = 0$, $b_y = 1$, $\nu = 0.3$, $\mu = 100$, $z = 11b_y$, $-4a \leq x \leq 4a$, $-4b \leq y \leq 4b$

Free-Traction Condition on the Free Surface

Another way to verify the strain field developed herein is to plug the obtained strain field solution into equation (14) to get the stress solution and check if the stress solution satisfies the free-traction condition on the free surface. The stress traction \vec{T} at the free surface can be written as:

$$\vec{T} = \boldsymbol{\sigma}\vec{n} \quad (26)$$

Which should be $\vec{0}$ at the free surface. Here, $\boldsymbol{\sigma}$ is given by equation (14). The unit normal vector at the free surface is $\{0 \ 0 \ -1\}$, see Fig. 1. In this case, σ_{xz} σ_{yz} and σ_{zz} components should all be zero at the free surface. To make sure that these three stress components are zero on the surface, one could use equation (14) and specify $z = 0$ in it and see if it reduces to 0 for each of the three stress components. Unfortunately, since the final solutions of stress field obtained by equation (14) are too long, Mathematica was not able to analytically simplify these stress components at $z = 0$ down to 0 value even if one waited more than 24 hours for the simplification result. Alternatively, if one considers arbitrary lines along the x and y directions on the free surface, these stress components did reduce to zero identically. In addition to the analytical verification, surface plots of the three stress field components on the free surface were generated. This is a numerical verification as all such three stress values should be zero. The plots in Fig. 4 are done for $b_x \neq 0$.

Normalized Plots for the Stress Field of a Subsurface Rectangular Dislocation Loop

Note that by taking the developed total strain solution (the three parts of it) and substituting them into equation (14), one can then separate the stresses into three parts and write an equation similar to equation (1):

$$\sigma = \sigma^{inf} + \sigma^{imag} + \sigma^s \quad (27)$$

As equation (27) shows, total stress field for the subsurface rectangular dislocation loop involves three terms which are the infinite term, the image term and the surface correction term.

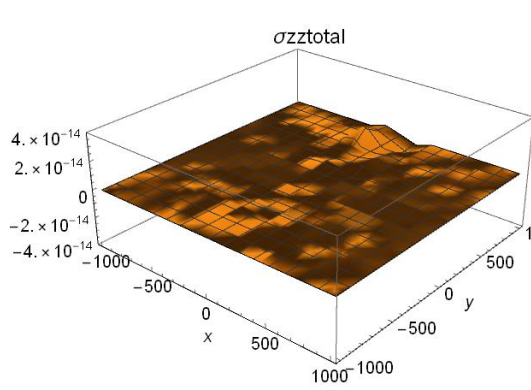


Fig. 4.1 Plot of the equation for σ_{zz}

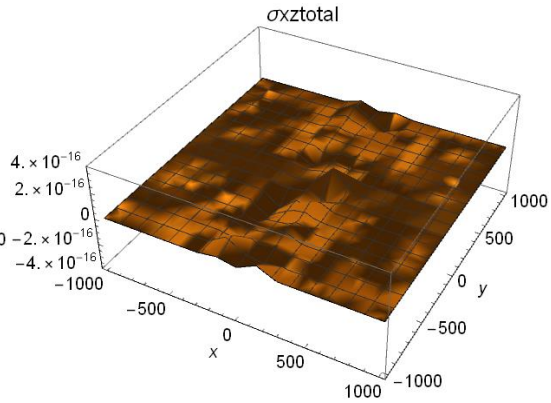


Fig. 4.2 Plot of the equation for σ_{xz}

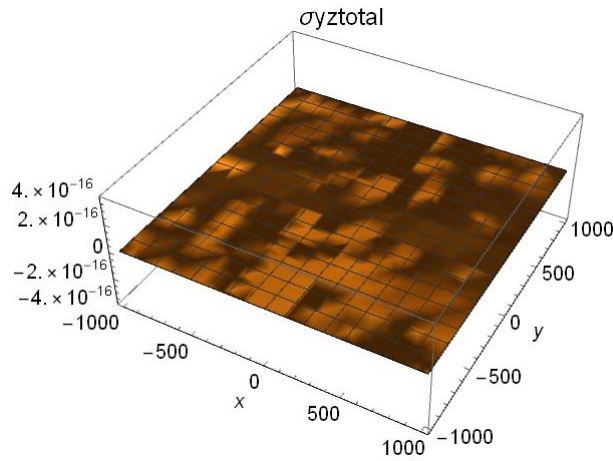


Fig. 4.3 Plot of the equation for σ_{yz}

For these plots, the following values were chosen: $a = b = 100b_x$, $z' = c = 10b_x$, $b_y = b_z = 0$, $b_x = 1$, $\nu = 0.3$, $\mu = 100$, $z = 0$, $-10a \leq x \leq 10a$, $-10b \leq y \leq 10b$

To investigate the stress field of a rectangular dislocation loop in an isotropic half medium at different z depths, one can plot separately the total stress and its parts along the x and y directions. Fig. 5 shows the effect of depth on the different stresses

(total stress, infinite term, image term and stress correction term). Fig. 6 shows the effect of depth on the stress correction term. For the plots in Figs. 5 and 6, the following values were chosen: $a = b = 100b_x$, $z' = c = 400b_x$, $b_y = b_z = 0$, $b_x = 1$, $\nu = 0.3$, $\mu = 1$, $-10a \leq x \leq 10a$, $y = 0$.

For the plots in Fig. 7, the following values were chosen: $a = b = 100b_z$, $z' = c = 400b_z$, $b_y = b_x = 0$, $b_z = 1$, $\nu = 0.3$, $\mu = 1$, $-10b \leq y \leq 10b$, $x = 0$. Similar to Figs. 5 and 6, these figures also show the effect of depth on the stress correction term but for $b_z \neq 0$.

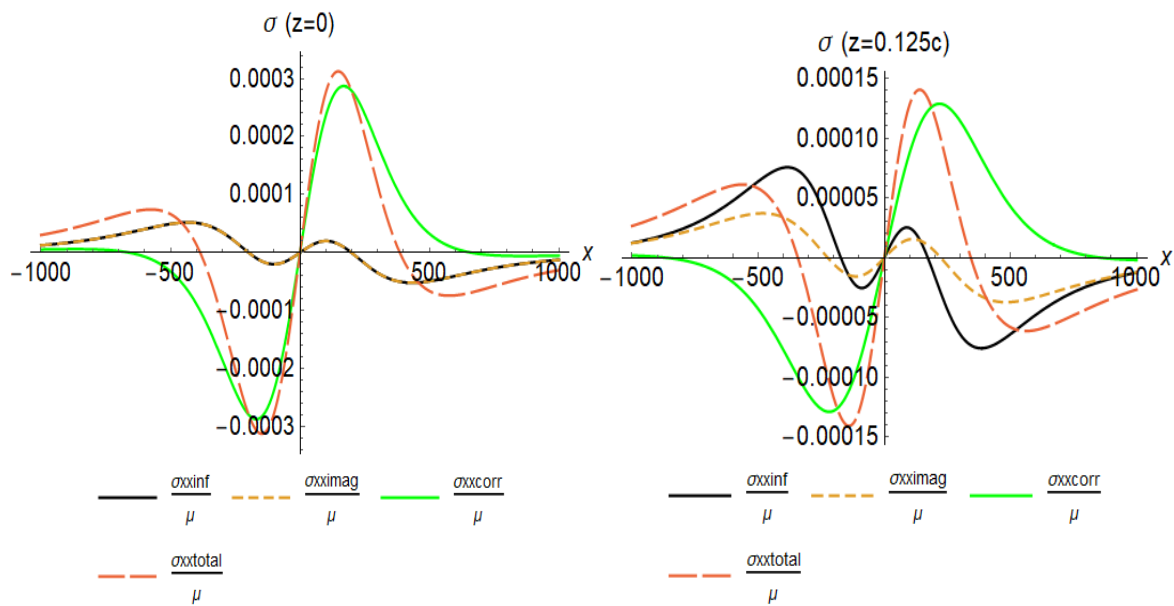


Fig. 5.1 σ_{xx} for $z/c=0$

Fig. 5.2 σ_{xx} for $z/c=0.125$

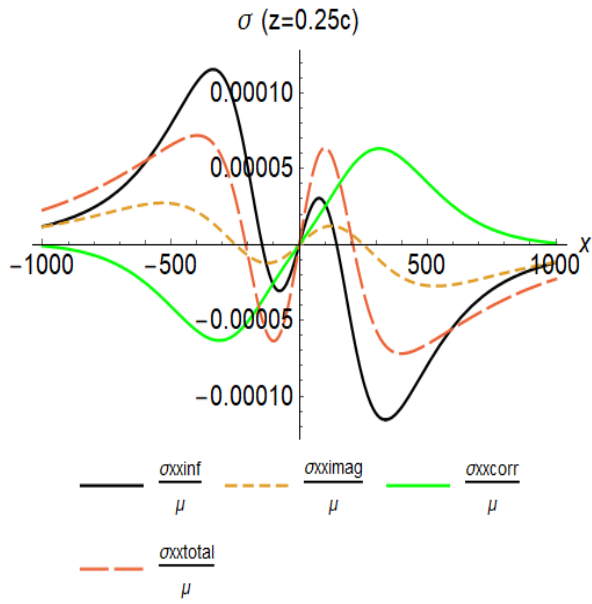


Fig. 5.3 σ_{xx} with $z/c=0.25$

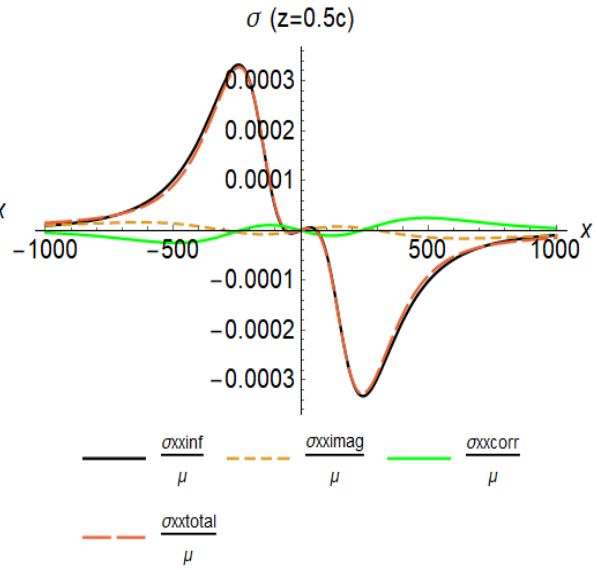


Fig. 5.4 σ_{xx} for $z/c=0.5$

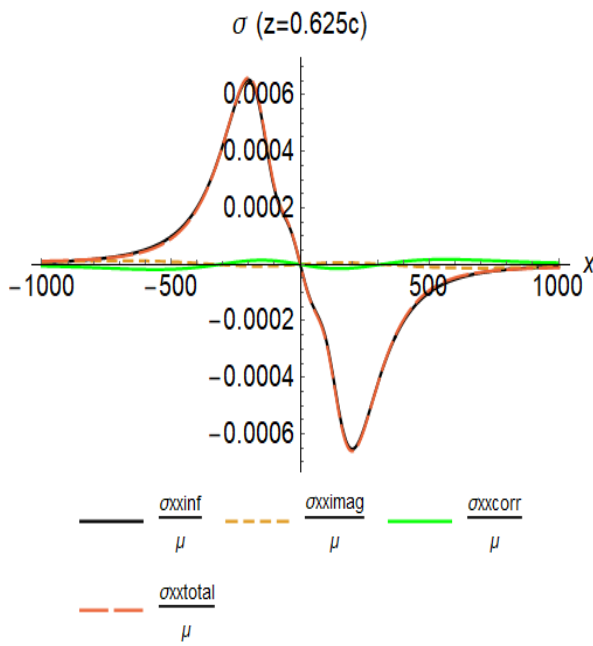


Fig. 5.5 σ_{xx} for $z/c=0.625$

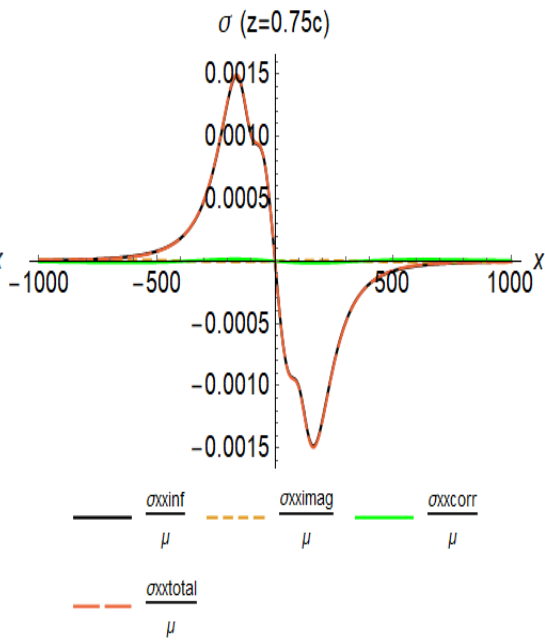


Fig. 5.6 σ_{xx} for $z/c=0.75$

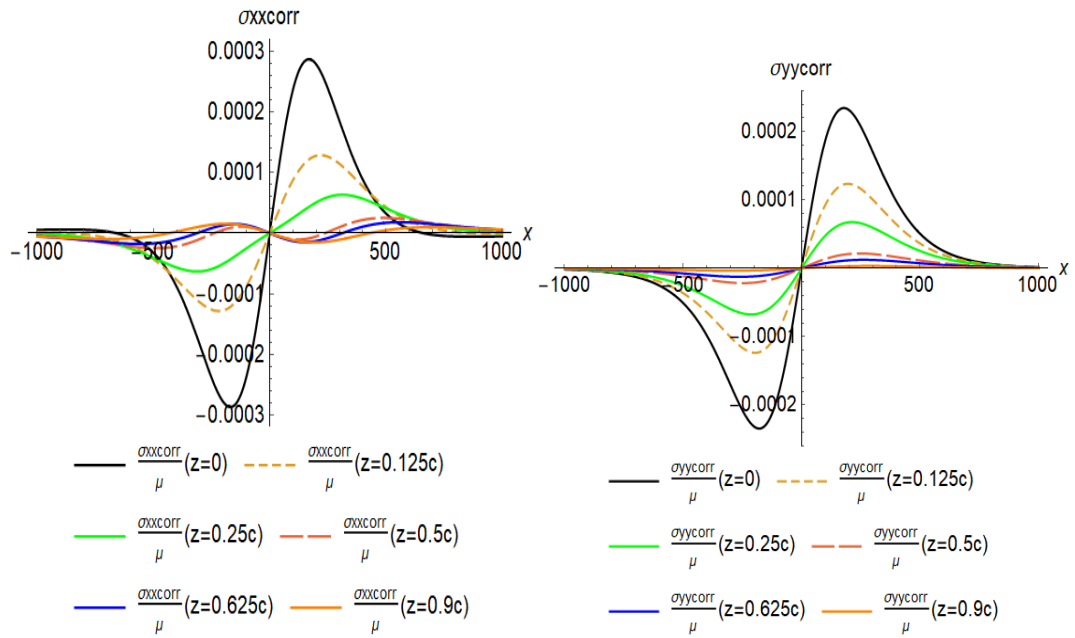


Fig. 6.1 σ_{xx} surface correction (varying z), $b_x \neq 0$

Fig. 6.2 σ_{yy} surface correction (varying z), $b_x \neq 0$

As the plots in Fig. 5 show, the correction term nearly dominates the total stress value of a dislocation loop at the surface, while the effect of the infinite term is much lesser. However, as the material point in question gets further away from the free surface, the infinite term gradually dominates the total stress value while the effect of the surface correction term on the total stress gets weaker. Indeed, at high depths closer to the dislocation loop in the half medium, the total stress value is almost all due to the infinite term. Fig. 6, which focuses on the stress correction term only, shows a similar trend for this term as it is usually highest on the surface and diminishes close the dislocation loop. Note that some stress components are not drawn here since they are identically equal to zero along a line parallel to x with $y=0$ and $b_x \neq 0$. Fig. 7 is similar to Figs. 5 and 6 but is done along a line parallel to the y -axis with $x=0$ and $b_z \neq 0$. This figure also shows that the stress correction term diminishes fast from the free surface. In Fig. 7, the stress correction terms for σ_{xy} and σ_{xz} are identically zero along a line parallel to the y -axis with $x=0$ and $b_z \neq 0$ and hence are not plotted here. Moreover, the plots of stress components for b_y are not shown here for brevity since the plots are similar to the ones of stress components for b_x .

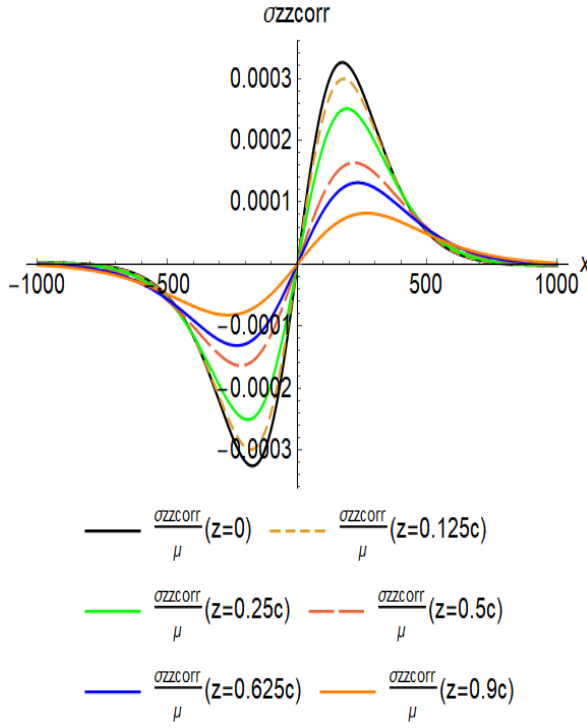


Fig. 6.3 σ_{zz} surface correction (varying z), $b_x \neq 0$

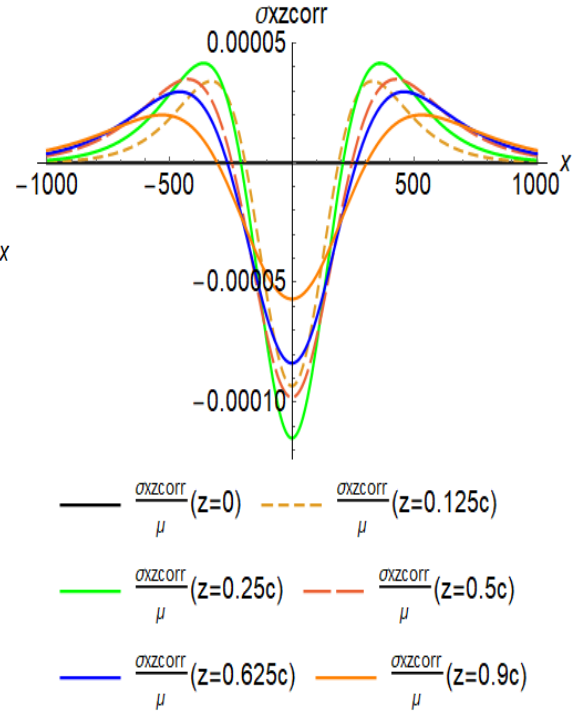


Fig.6.4 σ_{xz} surface correction (varying z), $b_x \neq 0$

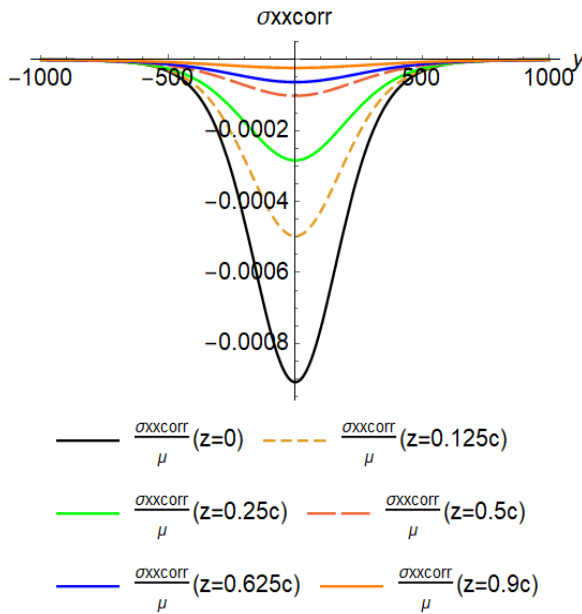


Fig. 7.1 σ_{xx} surface correction (varying z), $b_z \neq 0$

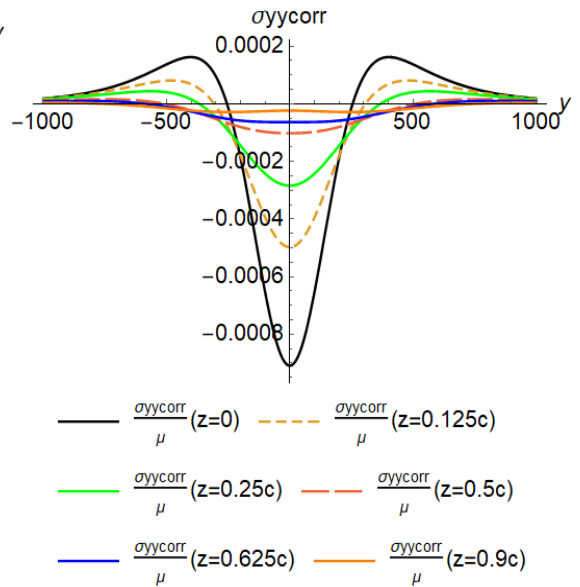


Fig. 7.2 σ_{yy} surface correction (varying z), $b_z \neq 0$

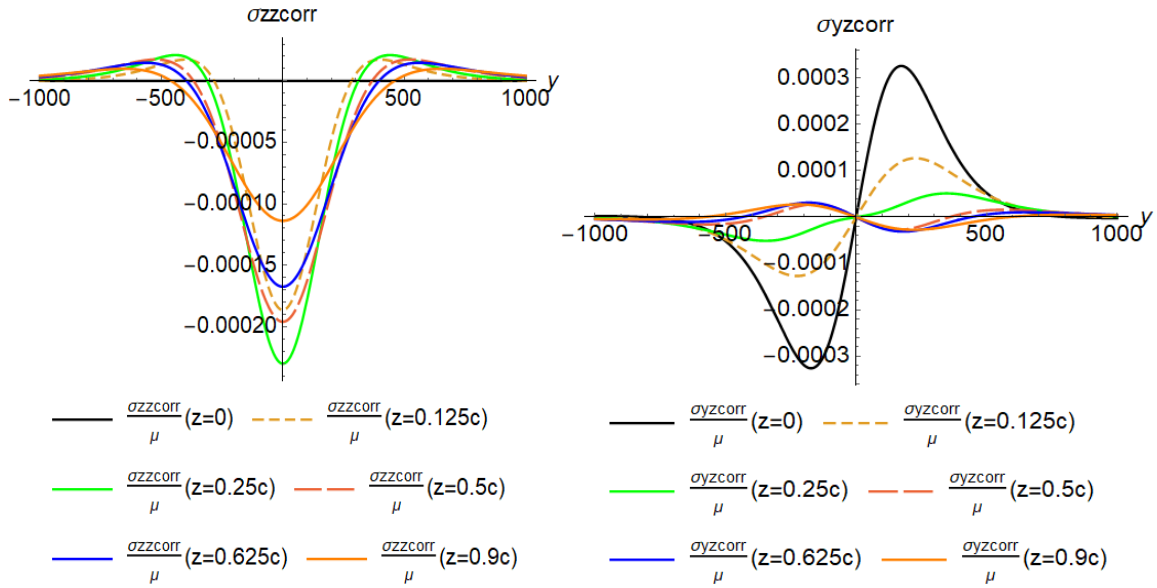


Fig. 7.3 σ_{zz} surface correction (varying z), $b_z \neq 0$ Fig. 7.4 σ_{yz} surface correction (varying z), $b_z \neq 0$

CONCLUSIONS

In conclusion, the strain field of a subsurface rectangular dislocation loop parallel to the free surface in a half medium has been obtained in this paper. The developed strain field is verified using different fundamental equations of continuum mechanics. Firstly, the strain solution is verified using the Strain Compatibility Equations, which are the equations relating the different strain components' spatial distribution. As the results show, the strain solution developed herein satisfies the Compatibility Equations. Secondly, one can also verify the strain field by plugging the strain solution into Hooke's Law to obtain the stress field. Then, one can check if this stress field satisfies the Equilibrium Equations

and the zero-traction condition on the free surface. As the results show, the stress field obtained in this manner does indeed satisfy the Equilibrium Equations and the free-traction condition. The last conclusion from this work regards the decay rate of the surface effects on the total stress. The surface effects diminish quickly away from the surface as one gets closer and closer to the subsurface dislocation loop.

APPENDIX

Considering the Burgers vector component b_x :

$$\begin{aligned}
\epsilon_{xx} = & \frac{1}{4K_1\pi} b_x c \left(-3 p_1 \left(\frac{Q_1^2}{A_2^{5/2} B_1} - \frac{Q_2^2}{A_4^{5/2} B_2} \right) Q_3 z + 3 p_1 \left(\frac{Q_1^2}{A_1^{5/2} B_1} - \frac{Q_2^2}{A_3^{5/2} B_2} \right) Q_4 z + \right. \\
& \frac{Q_3(Q_1^4 + p_1(p_1^2 p_2 - 6Q_1^2 z))}{\sqrt{A_2} B_1^3} - \frac{Q_4(Q_1^4 + p_1(p_1^2 p_2 - 6Q_1^2 z))}{\sqrt{A_1} B_1^3} - \frac{Q_3(Q_2^4 - p_1(-p_1^2 p_2 + 6Q_2^2 z))}{\sqrt{A_4} B_2^3} + \\
& \frac{Q_4(Q_2^4 - p_1(-p_1^2 p_2 + 6Q_2^2 z))}{\sqrt{A_3} B_2^3} - \frac{Q_3(-c^3 z + cz(Q_1^2 - 3z^2) - (Q_1^2 - z^2)^2 - c^2(Q_1^2 + 3z^2))}{A_2^{3/2} B_1^2} + \\
& \frac{Q_4(-c^3 z + cz(Q_1^2 - 3z^2) - (Q_1^2 - z^2)^2 - c^2(Q_1^2 + 3z^2))}{A_1^{3/2} B_1^2} - \frac{Q_3(c^3 z - cz(Q_2^2 - 3z^2) + (Q_2^2 - z^2)^2 + c^2(Q_2^2 + 3z^2))}{A_4^{3/2} B_2^2} + \\
& \left. \frac{Q_4(c^3 z - cz(Q_2^2 - 3z^2) + (Q_2^2 - z^2)^2 + c^2(Q_2^2 + 3z^2))}{A_3^{3/2} B_2^2} \right) + \frac{b_x c v}{2K_1\pi} \left(\frac{Q_1^2}{B_1} \left(-\frac{Q_3}{A_2^{3/2}} + \frac{Q_4}{A_1^{3/2}} \right) + \right. \\
& \left. \frac{(-p_1^2 + Q_1^2)}{B_1^2} \left(-\frac{Q_3}{\sqrt{A_2}} + \frac{Q_4}{\sqrt{A_1}} \right) + \frac{Q_2^2}{B_2} \left(\frac{Q_3}{A_4^{3/2}} - \frac{Q_4}{A_3^{3/2}} \right) + \frac{(-p_1^2 + Q_2^2)}{B_2^2} \left(\frac{Q_3}{\sqrt{A_4}} - \frac{Q_4}{\sqrt{A_3}} \right) \right); \\
\epsilon_{yy} = & -\frac{b_x c K_2}{4K_1\pi} \left(-\frac{Q_3}{A_2^{3/2}} + \frac{Q_3}{A_4^{3/2}} \right) + \frac{b_x c K_2}{4K_1\pi} \left(-\frac{Q_4}{A_1^{3/2}} + \frac{Q_4}{A_3^{3/2}} \right) - \frac{3b_x c p_1 z}{4K_1\pi} \left(-\frac{Q_3}{A_2^{5/2}} + \frac{Q_3}{A_4^{5/2}} \right) + \\
& \frac{3b_x c p_1 z}{4K_1\pi} \left(-\frac{Q_4}{A_1^{5/2}} + \frac{Q_4}{A_3^{5/2}} \right);
\end{aligned}$$

$$\begin{aligned}
\epsilon_{zz} &= \frac{b_x c K_3 p_1^2 Q_3}{2A_2^{3/2} B_1 K_1 \pi} - \frac{b_x c K_3 p_1^2 Q_3}{2A_4^{3/2} B_2 K_1 \pi} - \frac{b_x c K_3 (-p_1^2 + Q_1^2) Q_3}{2\sqrt{A_2} B_1^2 K_1 \pi} + \frac{b_x c K_3 (-p_1^2 + Q_2^2) Q_3}{2\sqrt{A_4} B_2^2 K_1 \pi} - \\
&\frac{b_x c p_1 (p_1^2 p_3 + p_4 Q_2^2) Q_3}{4A_4^{3/2} B_2^2 K_1 \pi} - \frac{b_x c K_3 p_1^2 Q_4}{2A_1^{3/2} B_1 K_1 \pi} + \frac{b_x c K_3 p_1^2 Q_4}{2A_3^{3/2} B_2 K_1 \pi} + \frac{b_x c K_3 (-p_1^2 + Q_1^2) Q_4}{2\sqrt{A_1} B_1^2 K_1 \pi} - \\
&\frac{b_x c K_3 (-p_1^2 + Q_2^2) Q_4}{2\sqrt{A_3} B_2^2 K_1 \pi} + \frac{b_x c p_1 (p_1^2 p_3 + p_4 Q_2^2) Q_4}{4A_3^{3/2} B_2^2 K_1 \pi} + \frac{b_x c p_1 Q_3 (p_1^2 p_3 + 3Q_1^2 (c + 2z))}{4A_2^{3/2} B_1^2 K_1 \pi} - \\
&\frac{b_x c p_1 Q_4 (p_1^2 p_3 + 3Q_1^2 (c + 2z))}{4A_1^{3/2} B_1^2 K_1 \pi} + \frac{b_x c Q_3 (-3Q_1^4 + p_1 (p_1^2 p_5 + 6Q_1^2 z))}{4\sqrt{A_2} B_1^3 K_1 \pi} - \\
&\frac{b_x c Q_4 (-3Q_1^4 + p_1 (p_1^2 p_5 + 6Q_1^2 z))}{4\sqrt{A_1} B_1^3 K_1 \pi} - \frac{b_x c Q_3 (-3Q_2^4 + p_1 (p_1^2 p_5 + 6Q_2^2 z))}{4\sqrt{A_4} B_2^3 K_1 \pi} + \\
&\frac{b_x c Q_4 (-3Q_2^4 + p_1 (p_1^2 p_5 + 6Q_2^2 z))}{4\sqrt{A_3} B_2^3 K_1 \pi} - \frac{3b_x c p_1^3 Q_3 z}{4(\pi - \pi\nu)} \left(-\frac{1}{A_2^{5/2} B_1} + \frac{1}{A_4^{5/2} B_2} \right) + \\
&\frac{3b_x c p_1^3 Q_4 z}{4(\pi - \pi\nu)} \left(-\frac{1}{A_1^{5/2} B_1} + \frac{1}{A_3^{5/2} B_2} \right); \\
\epsilon_{xy} &= \frac{b_x c}{4K_1 \pi} \left(-\frac{Q_1}{A_1^{3/2}} - \frac{Q_2}{A_3^{3/2}} + \frac{3p_1 Q_1 z}{A_1^{5/2}} + \frac{3p_1 Q_2 z}{A_3^{5/2}} \right) - \frac{b_x c}{4K_1 \pi} \left(-\frac{Q_1}{A_2^{3/2}} - \frac{Q_2}{A_4^{3/2}} + \frac{3p_1 Q_1 z}{A_2^{5/2}} + \right. \\
&\left. \frac{3p_1 Q_2 z}{A_4^{5/2}} \right) + \frac{b_x c \nu}{2K_1 \pi} \left(\frac{Q_1}{A_1^{3/2}} + \frac{Q_2}{A_3^{3/2}} \right) - \frac{b_x c \nu}{2K_1 \pi} \left(\frac{Q_1}{A_2^{3/2}} + \frac{Q_2}{A_4^{3/2}} \right); \\
\epsilon_{xz} &= \frac{b_x c p_1 Q_1 Q_3 (3A_2 - Q_3^2)}{2A_2^{3/2} B_1^2 K_1 \pi} + \frac{b_x c p_1 Q_2 Q_3 (3A_4 - Q_3^2)}{2A_4^{3/2} B_2^2 K_1 \pi} - \frac{b_x c p_1 Q_1 Q_4 (3A_1 - Q_4^2)}{2A_1^{3/2} B_1^2 K_1 \pi} - \\
&\frac{b_x c p_1 Q_2 Q_4 (3A_3 - Q_4^2)}{2A_3^{3/2} B_2^2 K_1 \pi} + \frac{3a b_x c p_1^2 Q_3 z}{4A_4^{5/2} B_1 K_1 \pi} + \frac{3a b_x c p_1^2 Q_3 z}{4A_4^{5/2} B_2 K_1 \pi} - \frac{3a b_x c p_1^2 Q_4 z}{4A_1^{5/2} B_1 K_1 \pi} - \frac{3a b_x c p_1^2 Q_4 z}{4A_3^{5/2} B_2 K_1 \pi} - \\
&\frac{3b_x c p_1^2 Q_3 x z}{4A_2^{5/2} B_1 K_1 \pi} + \frac{3b_x c p_1^2 Q_3 x z}{4A_4^{5/2} B_2 K_1 \pi} + \frac{3b_x c p_1^2 Q_4 x z}{4A_1^{5/2} B_1 K_1 \pi} - \frac{3b_x c p_1^2 Q_4 x z}{4A_3^{5/2} B_2 K_1 \pi} - \\
&\frac{a b_x c Q_3 (3A_2 - Q_3^2) (p_6 (c^2 + Q_1^2) - z^3)}{4A_2^{3/2} B_1^3 K_1 \pi} + \frac{a b_x c Q_4 (3A_1 - Q_4^2) (p_6 (c^2 + Q_1^2) - z^3)}{4A_1^{3/2} B_1^3 K_1 \pi} + \\
&\frac{b_x c Q_3 (3A_2 - Q_3^2) x (p_6 (c^2 + Q_1^2) - z^3)}{4A_2^{3/2} B_1^3 K_1 \pi} - \frac{b_x c Q_4 (3A_1 - Q_4^2) x (p_6 (c^2 + Q_1^2) - z^3)}{4A_1^{3/2} B_1^3 K_1 \pi} - \\
&\frac{a b_x c Q_3 (3A_4 - Q_3^2) (p_6 (c^2 + Q_2^2) - z^3)}{4A_4^{3/2} B_2^3 K_1 \pi} + \frac{a b_x c Q_4 (3A_3 - Q_4^2) (p_6 (c^2 + Q_2^2) - z^3)}{4A_3^{3/2} B_2^3 K_1 \pi} - \\
&\frac{b_x c Q_3 (3A_4 - Q_3^2) x (p_6 (c^2 + Q_2^2) - z^3)}{4A_4^{3/2} B_2^3 K_1 \pi} + \frac{b_x c Q_4 (3A_3 - Q_4^2) x (p_6 (c^2 + Q_2^2) - z^3)}{4A_3^{3/2} B_2^3 K_1 \pi}; \\
\epsilon_{yz} &= \frac{3b_x c p_1}{2K_1 \pi} \left(\frac{1}{3A_3^{3/2}} - \frac{1}{3(A_3 - 4ax)^{3/2}} \right) - \frac{3b_x c p_1}{2K_1 \pi} \left(\frac{1}{3A_4^{3/2}} - \frac{1}{3(A_4 - 4ax)^{3/2}} \right) + \frac{b_x c}{4K_1 \pi} \left(\frac{p_6}{A_1^{3/2}} + \right. \\
&\left. \frac{-2c - 3z}{A_3^{3/2}} - \frac{3p_1^2 z}{A_1^{5/2}} + \frac{3p_1^2 z}{A_3^{5/2}} \right) - \frac{b_x c}{4K_1 \pi} \left(\frac{p_6}{A_2^{3/2}} + \frac{-2c - 3z}{A_4^{3/2}} - \frac{3p_1^2 z}{A_2^{5/2}} + \frac{3p_1^2 z}{A_4^{5/2}} \right);
\end{aligned}$$

Considering the Burgers vector component b_y :

$$\epsilon_{xx} = \frac{3b_y c}{4K_1\pi} \left(\frac{K_2 Q_1}{3A_1^{3/2}} + \frac{K_2 Q_2}{3A_3^{3/2}} + \frac{p_1 Q_1 z}{A_1^{5/2}} + \frac{p_1 Q_2 z}{A_3^{5/2}} \right) - \frac{3b_y c}{4K_1\pi} \left(\frac{K_2 Q_1}{3A_2^{3/2}} + \frac{K_2 Q_2}{3A_4^{3/2}} + \frac{p_1 Q_1 z}{A_2^{5/2}} + \frac{p_1 Q_2 z}{A_4^{5/2}} \right);$$

$$\begin{aligned} \epsilon_{yy} = & -\frac{b_y c Q_1 (Q_3^4 - p_1 (-p_1^2 p_2 + 6Q_3^2 z))}{4C_1^3 K_1 \pi \sqrt{C_1 + Q_1^2}} - \frac{b_y c Q_2 (Q_3^4 - p_1 (-p_1^2 p_2 + 6Q_3^2 z))}{4\sqrt{A_4} C_1^3 K_1 \pi} + \\ & \frac{b_y c Q_1 (Q_4^4 + p_1 (p_1^2 p_2 - 6Q_4^2 z))}{4C_2^3 K_1 \pi \sqrt{C_2 + Q_1^2}} + \frac{b_y c Q_2 (Q_4^4 + p_1 (p_1^2 p_2 - 6Q_4^2 z))}{4\sqrt{A_3} C_2^3 K_1 \pi} - \\ & \frac{b_y c Q_1 (c^3 z - cz(Q_3^2 - 3z^2) + (Q_3^2 - z^2)^2 + c^2(Q_3^2 + 3z^2))}{4C_1^2 K_1 \pi (C_1 + Q_1^2)^{3/2}} - \\ & \frac{b_y c Q_2 (c^3 z - cz(Q_3^2 - 3z^2) + (Q_3^2 - z^2)^2 + c^2(Q_3^2 + 3z^2))}{4A_4^{3/2} C_1^2 K_1 \pi} - \\ & \frac{b_y c Q_1 (-c^3 z + cz(Q_4^2 - 3z^2) - (Q_4^2 - z^2)^2 - c^2(Q_4^2 + 3z^2))}{4C_2^2 K_1 \pi (C_2 + Q_1^2)^{3/2}} - \\ & \frac{b_y c Q_2 (-c^3 z + cz(Q_4^2 - 3z^2) - (Q_4^2 - z^2)^2 - c^2(Q_4^2 + 3z^2))}{4A_3^{3/2} C_2^2 K_1 \pi} + \frac{b_y c v}{2K_1 \pi} \left(\frac{Q_1 Q_3^2}{A_2^{3/2} C_1} + \frac{Q_2 Q_3^2}{A_4^{3/2} C_1} - \frac{Q_1 (p_1^2 - Q_3^2)}{\sqrt{A_2} C_1^2} - \right. \\ & \left. \frac{Q_2 (p_1^2 - Q_3^2)}{\sqrt{A_4} C_1^2} - \frac{Q_1 Q_4^2}{A_1^{3/2} C_2} - \frac{Q_2 Q_4^2}{A_3^{3/2} C_2} + \frac{Q_1 (p_1^2 - Q_4^2)}{\sqrt{A_1} C_2^2} + \frac{Q_2 (p_1^2 - Q_4^2)}{\sqrt{A_3} C_2^2} \right) - \frac{3b_y c p_1 Q_2 z}{4(\pi - \pi v)} \left(\frac{Q_3^2}{A_4^{5/2} C_1} - \right. \\ & \left. \frac{Q_4^2}{A_3^{5/2} C_2} \right) - \frac{3b_y c p_1 Q_1 z}{4(\pi - \pi v)} \left(\frac{Q_3^2}{C_1 (C_1 + Q_1^2)^{5/2}} - \frac{Q_4^2}{C_2 (C_2 + Q_1^2)^{5/2}} \right); \end{aligned}$$

$$\begin{aligned} \epsilon_{zz} = & -\frac{b_y c K_3 p_1^2 Q_1}{2C_1 K_1 \pi (C_1 + Q_1^2)^{3/2}} + \frac{b_y c K_3 p_1^2 Q_1}{2C_2 K_1 \pi (C_2 + Q_1^2)^{3/2}} - \frac{b_y c K_3 p_1^2 Q_2}{2A_4^{3/2} C_1 K_1 \pi} + \frac{b_y c K_3 p_1^2 Q_2}{2A_3^{3/2} C_2 K_1 \pi} + \\ & \frac{b_y c K_3 Q_1 (-p_1^2 + Q_3^2)}{2C_1^2 K_1 \pi \sqrt{C_1 + Q_1^2}} + \frac{b_y c K_3 Q_2 (-p_1^2 + Q_3^2)}{2\sqrt{A_4} C_1^2 K_1 \pi} - \frac{b_y c p_1 Q_1 (p_1^2 p_3 + p_4 Q_3^2)}{4C_1^2 K_1 \pi (C_1 + Q_1^2)^{3/2}} - \frac{b_y c p_1 Q_2 (p_1^2 p_3 + p_4 Q_3^2)}{4A_4^{3/2} C_1^2 K_1 \pi} - \\ & \frac{b_y c K_3 Q_1 (-p_1^2 + Q_4^2)}{2C_2^2 K_1 \pi \sqrt{C_2 + Q_1^2}} - \frac{b_y c K_3 Q_2 (-p_1^2 + Q_4^2)}{2\sqrt{A_3} C_2^2 K_1 \pi} + \frac{b_y c p_1 Q_1 (p_1^2 p_3 + 3Q_4^2 (c + 2z))}{4C_2^2 K_1 \pi (C_2 + Q_1^2)^{3/2}} + \\ & \frac{b_y c p_1 Q_2 (p_1^2 p_3 + 3Q_4^2 (c + 2z))}{4A_3^{3/2} C_2^2 K_1 \pi} - \frac{b_y c Q_1 (-3Q_3^4 + p_1 (p_1^2 p_5 + 6Q_3^2 z))}{4C_1^3 K_1 \pi \sqrt{C_1 + Q_1^2}} - \\ & \frac{b_y c Q_2 (-3Q_3^4 + p_1 (p_1^2 p_5 + 6Q_3^2 z))}{4\sqrt{A_4} C_1^3 K_1 \pi} + \frac{b_y c Q_1 (-3Q_4^4 + p_1 (p_1^2 p_5 + 6Q_4^2 z))}{4C_2^3 K_1 \pi \sqrt{C_2 + Q_1^2}} + \\ & \frac{b_y c Q_2 (-3Q_4^4 + p_1 (p_1^2 p_5 + 6Q_4^2 z))}{4\sqrt{A_3} C_2^3 K_1 \pi} - \frac{3b_y c p_1^3 Q_1 z}{4(\pi - \pi v)} \left(\frac{1}{C_1 (C_1 + Q_1^2)^{5/2}} - \frac{1}{C_2 (C_2 + Q_1^2)^{5/2}} \right) - \\ & \frac{3b_y c p_1^3 Q_2 z}{4(\pi - \pi v)} \left(\frac{1}{A_4^{5/2} C_1} - \frac{1}{A_3^{5/2} C_2} \right); \end{aligned}$$

$$\begin{aligned}
\epsilon_{xy} &= -\frac{b_{yc} Q3(Q1^2+Q3^2-p1(-c+2z))}{4A2^{5/2}K1\pi} + \frac{b_{yc} Q3(Q2^2+Q3^2-p1(-c+2z))}{4A4^{5/2}K1\pi} + \\
&\frac{b_{yc} Q4(Q1^2+Q4^2-p1(-c+2z))}{4A1^{5/2}K1\pi} - \frac{b_{yc} Q4(Q2^2+Q4^2-p1(-c+2z))}{4A3^{5/2}K1\pi} - \frac{b_{yc} v}{2K1\pi} \left(-\frac{Q3}{A2^{3/2}} + \frac{Q3}{A4^{3/2}}\right) + \\
&\frac{b_{yc} v}{2K1\pi} \left(-\frac{Q4}{A1^{3/2}} + \frac{Q4}{A3^{3/2}}\right); \\
\epsilon_{xz} &= \frac{b_{yc} p1}{2K1\pi} \left(-\frac{1}{A1^{3/2}} + \frac{1}{A3^{3/2}}\right) - \frac{b_{yc} p1}{2K1\pi} \left(-\frac{1}{A2^{3/2}} + \frac{1}{A4^{3/2}}\right) + \frac{b_{yc}}{4K1\pi} \left(\frac{p6}{A1^{3/2}} + \frac{p7}{A3^{3/2}} - \frac{3p1^2z}{A1^{5/2}} + \right. \\
&\left. \frac{3p1^2z}{A3^{5/2}}\right) - \frac{b_{yc}}{4K1\pi} \left(\frac{p6}{A2^{3/2}} + \frac{p7}{A4^{3/2}} - \frac{3p1^2z}{A2^{5/2}} + \frac{3p1^2z}{A4^{5/2}}\right); \\
\epsilon_{yz} &= \frac{b_{yc} p1Q1(3p1^2+2Q1^2+3Q3^2)}{2C1^2K1\pi(C1+Q1^2)^{3/2}} + \frac{b_{yc} p1Q2(3p1^2+2Q2^2+3Q3^2)}{2A4^{3/2}C1^2K1\pi} + \\
&\frac{b_{yc} p1Q1(3p1^2+2Q1^2+3Q4^2)}{2C2^2K1\pi(C2+Q1^2)^{3/2}} + \frac{b_{yc} p1Q2(3p1^2+2Q2^2+3Q4^2)}{2A3^{3/2}C2^2K1\pi} + \frac{b_{yc} p1Q1(3p1^2+2Q1^2+3Q3^2)y}{2C1^2K1\pi(C1+Q1^2)^{3/2}} + \\
&\frac{b_{yc} p1Q2(3p1^2+2Q2^2+3Q3^2)y}{2A4^{3/2}C1^2K1\pi} - \frac{b_{yc} p1Q1(3p1^2+2Q1^2+3Q4^2)y}{2C2^2K1\pi(C2+Q1^2)^{3/2}} - \frac{b_{yc} p1Q2(3p1^2+2Q2^2+3Q4^2)y}{2A3^{3/2}C2^2K1\pi} + \\
&\frac{3b_{yc} p1^2Q1z}{4C1K1\pi(C1+Q1^2)^{5/2}} + \frac{3b_{yc} p1^2Q1z}{4C2K1\pi(C2+Q1^2)^{5/2}} + \frac{3b_{yc} p1^2Q2z}{4A4^{5/2}C1K1\pi} + \frac{3b_{yc} p1^2Q2z}{4A3^{5/2}C2K1\pi} + \\
&\frac{3b_{yc} p1^2Q1yz}{4C1K1\pi(C1+Q1^2)^{5/2}} - \frac{3b_{yc} p1^2Q1yz}{4C2K1\pi(C2+Q1^2)^{5/2}} + \frac{3b_{yc} p1^2Q2yz}{4A4^{5/2}C1K1\pi} - \frac{3b_{yc} p1^2Q2yz}{4A3^{5/2}C2K1\pi} - \\
&\frac{b_{yc} Q1(3p1^2+2Q1^2+3Q3^2)(p6(c^2+Q3^2)-z^3)}{4C1^3K1\pi(C1+Q1^2)^{3/2}} - \frac{b_{yc} Q2(3p1^2+2Q2^2+3Q3^2)(p6(c^2+Q3^2)-z^3)}{4A4^{3/2}C1^3K1\pi} - \\
&\frac{b_{yc} Q1(3p1^2+2Q1^2+3Q4^2)(p6(c^2+Q3^2)-z^3)}{4C1^3K1\pi(C1+Q1^2)^{3/2}} - \frac{b_{yc} Q2(3p1^2+2Q2^2+3Q4^2)(p6(c^2+Q3^2)-z^3)}{4A4^{3/2}C1^3K1\pi} - \\
&\frac{b_{yc} Q1(3p1^2+2Q1^2+3Q4^2)(p6(c^2+Q4^2)-z^3)}{4C2^3K1\pi(C2+Q1^2)^{3/2}} - \frac{b_{yc} Q2(3p1^2+2Q2^2+3Q4^2)(p6(c^2+Q4^2)-z^3)}{4A3^{3/2}C2^3K1\pi} + \\
&\frac{b_{yc} Q1(3p1^2+2Q1^2+3Q4^2)y(p6(c^2+Q4^2)-z^3)}{4C2^3K1\pi(C2+Q1^2)^{3/2}} + \frac{b_{yc} Q2(3p1^2+2Q2^2+3Q4^2)y(p6(c^2+Q4^2)-z^3)}{4A3^{3/2}C2^3K1\pi},
\end{aligned}$$

Considering the Burgers vector component b_z :

$$\begin{aligned}
\epsilon_{xx} = & -\frac{3a b_z c p^2 Q_3 z}{4A2^{5/2}B1K1\pi} - \frac{3a b_z c p^2 Q_3 z}{4A4^{5/2}B2K1\pi} + \frac{3a b_z c p^2 Q_4 z}{4A1^{5/2}B1K1\pi} + \frac{3a b_z c p^2 Q_4 z}{4A3^{5/2}B2K1\pi} + \frac{3 b_z c p^2 Q_3 x z}{4A2^{5/2}B1K1\pi} - \\
& \frac{3 b_z c p^2 Q_3 x z}{4A4^{5/2}B2K1\pi} - \frac{3 b_z c p^2 Q_4 x z}{4A1^{5/2}B1K1\pi} + \frac{3 b_z c p^2 Q_4 x z}{4A3^{5/2}B2K1\pi} + \frac{a b_z c Q_3(p_8+2cQ_1^2+3Q_1^2 z)}{2\sqrt{A}2B1^3K1\pi} + \\
& \frac{a b_z c Q_3(p_8+2cQ_1^2+3Q_1^2 z)}{4A2^{3/2}B1^2K1\pi} - \frac{a b_z c Q_4(p_8+2cQ_1^2+3Q_1^2 z)}{2\sqrt{A}1B1^3K1\pi} - \frac{a b_z c Q_4(p_8+2cQ_1^2+3Q_1^2 z)}{4A1^{3/2}B1^2K1\pi} - \\
& \frac{b_z c Q_3 x(p_8+2cQ_1^2+3Q_1^2 z)}{2\sqrt{A}2B1^3K1\pi} - \frac{b_z c Q_3 x(p_8+2cQ_1^2+3Q_1^2 z)}{4A2^{3/2}B1^2K1\pi} + \frac{b_z c Q_4 x(p_8+2cQ_1^2+3Q_1^2 z)}{2\sqrt{A}1B1^3K1\pi} + \\
& \frac{b_z c Q_4 x(p_8+2cQ_1^2+3Q_1^2 z)}{4A1^{3/2}B1^2K1\pi} + \frac{a b_z c Q_3(p_8+2cQ_2^2+3Q_2^2 z)}{2\sqrt{A}4B2^3K1\pi} + \frac{a b_z c Q_3(p_8+2cQ_2^2+3Q_2^2 z)}{4A4^{3/2}B2^2K1\pi} - \\
& \frac{a b_z c Q_4(p_8+2cQ_2^2+3Q_2^2 z)}{2\sqrt{A}3B2^3K1\pi} - \frac{a b_z c Q_4(p_8+2cQ_2^2+3Q_2^2 z)}{4A3^{3/2}B2^2K1\pi} + \frac{b_z c Q_3 x(p_8+2cQ_2^2+3Q_2^2 z)}{2\sqrt{A}4B2^3K1\pi} + \\
& \frac{b_z c Q_3 x(p_8+2cQ_2^2+3Q_2^2 z)}{4A4^{3/2}B2^2K1\pi} - \frac{b_z c Q_4 x(p_8+2cQ_2^2+3Q_2^2 z)}{2\sqrt{A}3B2^3K1\pi} - \frac{b_z c Q_4 x(p_8+2cQ_2^2+3Q_2^2 z)}{4A3^{3/2}B2^2K1\pi} - \\
& \frac{a b_z c p_1 Q_3(3A_2-Q_3^2)v}{2A2^{3/2}B1^2K1\pi} - \frac{a b_z c p_1 Q_3(3A_4-Q_3^2)v}{2A4^{3/2}B2^2K1\pi} + \frac{a b_z c p_1 Q_4(3A_1-Q_4^2)v}{2A1^{3/2}B1^2K1\pi} + \\
& \frac{a b_z c p_1 Q_4(3A_3-Q_4^2)v}{2A3^{3/2}B2^2K1\pi} + \frac{b_z c p_1 Q_3(3A_2-Q_3^2)xv}{2A2^{3/2}B1^2K1\pi} - \frac{b_z c p_1 Q_3(3A_4-Q_3^2)xv}{2A4^{3/2}B2^2K1\pi} - \frac{b_z c p_1 Q_4(3A_1-Q_4^2)xv}{2A1^{3/2}B1^2K1\pi} + \\
& \frac{b_z c p_1 Q_4(3A_3-Q_4^2)xv}{2A3^{3/2}B2^2K1\pi};
\end{aligned}$$

$$\begin{aligned}
\epsilon_{yy} = & -\frac{3b b_z c p^2 Q_1 z}{4C1K1\pi(C1+Q1^2)^{5/2}} - \frac{3b b_z c p^2 Q_1 z}{4C2K1\pi(C2+Q1^2)^{5/2}} - \frac{3b b_z c p^2 Q_2 z}{4A4^{5/2}C1K1\pi} - \frac{3b b_z c p^2 Q_2 z}{4A3^{5/2}C2K1\pi} - \\
& \frac{3 b_z c p^2 Q_1 y z}{4C1K1\pi(C1+Q1^2)^{5/2}} + \frac{3 b_z c p^2 Q_1 y z}{4C2K1\pi(C2+Q1^2)^{5/2}} - \frac{3 b_z c p^2 Q_2 y z}{4A4^{5/2}C1K1\pi} + \frac{3 b_z c p^2 Q_2 y z}{4A3^{5/2}C2K1\pi} + \\
& \frac{b b_z c Q_1(p_8+2cQ_3^2+3Q_3^2 z)}{4C1^2K1\pi(C1+Q1^2)^{3/2}} + \frac{b b_z c Q_1(p_8+2cQ_3^2+3Q_3^2 z)}{2C1^3K1\pi\sqrt{C1+Q1^2}} + \frac{b b_z c Q_2(p_8+2cQ_3^2+3Q_3^2 z)}{2\sqrt{A}4C1^3K1\pi} + \\
& \frac{b b_z c Q_2(p_8+2cQ_3^2+3Q_3^2 z)}{4A4^{3/2}C1^2K1\pi} + \frac{b_z c Q_1 y(p_8+2cQ_3^2+3Q_3^2 z)}{4C1^2K1\pi(C1+Q1^2)^{3/2}} + \frac{b_z c Q_1 y(p_8+2cQ_3^2+3Q_3^2 z)}{2C1^3K1\pi\sqrt{C1+Q1^2}} + \\
& \frac{b_z c Q_2 y(p_8+2cQ_3^2+3Q_3^2 z)}{2\sqrt{A}4C1^3K1\pi} + \frac{b_z c Q_2 y(p_8+2cQ_3^2+3Q_3^2 z)}{4A4^{3/2}C1^2K1\pi} + \frac{b b_z c Q_1(p_8+2cQ_4^2+3Q_4^2 z)}{4C2^2K1\pi(C2+Q1^2)^{3/2}} + \\
& \frac{b b_z c Q_1(p_8+2cQ_4^2+3Q_4^2 z)}{2C2^3K1\pi\sqrt{C2+Q1^2}} + \frac{b b_z c Q_2(p_8+2cQ_4^2+3Q_4^2 z)}{2\sqrt{A}3C2^3K1\pi} + \frac{b b_z c Q_2(p_8+2cQ_4^2+3Q_4^2 z)}{4A3^{3/2}C2^2K1\pi} - \\
& \frac{b_z c Q_1 y(p_8+2cQ_4^2+3Q_4^2 z)}{4C2^2K1\pi(C2+Q1^2)^{3/2}} - \frac{b_z c Q_1 y(p_8+2cQ_4^2+3Q_4^2 z)}{2C2^3K1\pi\sqrt{C2+Q1^2}} - \frac{b_z c Q_2 y(p_8+2cQ_4^2+3Q_4^2 z)}{2\sqrt{A}3C2^3K1\pi} - \\
& \frac{b_z c Q_2 y(p_8+2cQ_4^2+3Q_4^2 z)}{4A3^{3/2}C2^2K1\pi} - \frac{b b_z c p_1 Q_1(3p^2+2Q_1^2+3Q_3^2)v}{2C1^2K1\pi(C1+Q1^2)^{3/2}} - \frac{b b_z c p_1 Q_2(3p^2+2Q_2^2+3Q_3^2)v}{2A4^{3/2}C1^2K1\pi} -
\end{aligned}$$

$$\begin{aligned}
& \frac{b b_z c p_1 Q_1 (3p_1^2 + 2Q_1^2 + 3Q_4^2) \nu}{2C_2^2 K_1 \pi (C_2 + Q_1^2)^{3/2}} - \frac{b b_z c p_1 Q_2 (3p_1^2 + 2Q_2^2 + 3Q_4^2) \nu}{2A_3^{3/2} C_2^2 K_1 \pi} - \frac{b_z c p_1 Q_1 (3p_1^2 + 2Q_1^2 + 3Q_3^2) y \nu}{2C_1^2 K_1 \pi (C_1 + Q_1^2)^{3/2}} \\
& \frac{b_z c p_1 Q_2 (3p_1^2 + 2Q_2^2 + 3Q_3^2) y \nu}{2A_4^{3/2} C_1^2 K_1 \pi} + \frac{b_z c p_1 Q_1 (3p_1^2 + 2Q_1^2 + 3Q_4^2) y \nu}{2C_2^2 K_1 \pi (C_2 + Q_1^2)^{3/2}} + \frac{b_z c p_1 Q_2 (3p_1^2 + 2Q_2^2 + 3Q_4^2) y \nu}{2A_3^{3/2} C_2^2 K_1 \pi}, \\
\epsilon_{zz} = & \frac{1}{4\pi Q_1^5 (1-\nu)} b_z c \sqrt{C_1 + Q_1^2} Q_3 \left(-\frac{8p_1^2 Q_1^4 z}{C_1^3} + \frac{3p_1^4 Q_1^4 z}{(C_1 + Q_1^2)^3 (p_1^2 + Q_1^2)} + \right. \\
& \frac{2p_1^6 p_9 Q_1^2 + 20p_1^3 Q_1^6 + 3p_0 Q_1^8 + 3p_1^8 z + 12p_1^4 Q_1^4 (c + 2z)}{(C_1 + Q_1^2)(p_1^2 + Q_1^2)^3} - \\
& \frac{p_1^2 Q_1^2 (p_1^4 z + 2Q_1^4 (2c + 5z) + p_1^2 Q_1^2 (4c + 7z))}{(C_1 + Q_1^2)^2 (p_1^2 + Q_1^2)^2} + \frac{2Q_1^2 (2c^2 z + 5Q_1^2 z + 2z^3 + 4c(Q_1^2 + z^2))}{C_1^2} - \\
& \left. \frac{3c^2 z + 5Q_1^2 z + 3z^3 + 2c(2Q_1^2 + 3z^2)}{C_1} \right) - \frac{1}{4\pi Q_1^5 (1-\nu)} b_z c Q_4 \sqrt{p_1^2 + Q_1^2 + Q_4^2} \left(-\frac{8p_1^2 Q_1^4 z}{(p_1^2 + Q_4^2)^3} + \right. \\
& \frac{3p_1^4 Q_1^4 z}{(p_1^2 + Q_1^2)(p_1^2 + Q_1^2 + Q_4^2)^3} + \frac{2p_1^6 p_9 Q_1^2 + 20p_1^3 Q_1^6 + 3p_0 Q_1^8 + 3p_1^8 z + 12p_1^4 Q_1^4 (c + 2z)}{(p_1^2 + Q_1^2)^3 (p_1^2 + Q_1^2 + Q_4^2)} - \\
& \frac{p_1^2 Q_1^2 (p_1^4 z + 2Q_1^4 (2c + 5z) + p_1^2 Q_1^2 (4c + 7z))}{(p_1^2 + Q_1^2)^2 (p_1^2 + Q_1^2 + Q_4^2)^2} + \frac{2Q_1^2 (2c^2 z + 5Q_1^2 z + 2z^3 + 4c(Q_1^2 + z^2))}{(p_1^2 + Q_4^2)^2} - \\
& \left. \frac{3c^2 z + 5Q_1^2 z + 3z^3 + 2c(2Q_1^2 + 3z^2)}{p_1^2 + Q_4^2} \right) + \frac{1}{4\pi Q_2^5 (1-\nu)} \sqrt{A_4} b_z c Q_3 \left(-\frac{8p_1^2 Q_2^4 z}{C_1^3} + \frac{3p_1^4 Q_2^4 z}{A_4^3 B_2} + \right. \\
& \frac{2p_1^6 p_9 Q_2^2 + 20p_1^3 Q_2^6 + 3p_0 Q_2^8 + 3p_1^8 z + 12p_1^4 Q_2^4 (c + 2z)}{A_4 B_2^3} - \\
& \frac{p_1^2 Q_2^2 (p_1^4 z + 2Q_2^4 (2c + 5z) + p_1^2 Q_2^2 (4c + 7z))}{A_4^2 B_2^2} + \frac{2Q_2^2 (2c^2 z + 5Q_2^2 z + 2z^3 + 4c(Q_2^2 + z^2))}{C_1^2} - \\
& \left. \frac{3c^2 z + 5Q_2^2 z + 3z^3 + 2c(2Q_2^2 + 3z^2)}{C_1} \right) - \frac{1}{4\pi Q_2^5 (1-\nu)} \sqrt{A_3} b_z c Q_4 \left(\frac{3p_1^4 Q_2^4 z}{A_3^3 B_2} - \frac{8p_1^2 Q_2^4 z}{(p_1^2 + Q_4^2)^3} + \right. \\
& \frac{2p_1^6 p_9 Q_2^2 + 20p_1^3 Q_2^6 + 3p_0 Q_2^8 + 3p_1^8 z + 12p_1^4 Q_2^4 (c + 2z)}{A_3 B_2^3} - \\
& \frac{p_1^2 Q_2^2 (p_1^4 z + 2Q_2^4 (2c + 5z) + p_1^2 Q_2^2 (4c + 7z))}{A_3^2 B_2^2} + \frac{2Q_2^2 (2c^2 z + 5Q_2^2 z + 2z^3 + 4c(Q_2^2 + z^2))}{(p_1^2 + Q_4^2)^2} - \\
& \left. \frac{3c^2 z + 5Q_2^2 z + 3z^3 + 2c(2Q_2^2 + 3z^2)}{p_1^2 + Q_4^2} \right) + \frac{1}{2\pi (1-\nu)} b_z c \left(\frac{p_1 \sqrt{C_1 + Q_1^2} Q_3}{Q_1^3} \left(\frac{1}{C_1} - \frac{2Q_1^2}{C_1^2} + \right. \right. \\
& \frac{p_1^2 Q_1^2}{(C_1 + Q_1^2)^2 (p_1^2 + Q_1^2)} - \frac{p_1^4 + 2p_1^2 Q_1^2 + 3Q_1^4}{(C_1 + Q_1^2)(p_1^2 + Q_1^2)^2} \left. \right) + \frac{\sqrt{A_4} p_1 Q_3}{Q_2^3} \left(\frac{1}{C_1} - \frac{2Q_2^2}{C_1^2} + \frac{p_1^2 Q_2^2}{A_4^2 B_2} - \right. \\
& \left. \frac{p_1^4 + 2p_1^2 Q_2^2 + 3Q_2^4}{A_4 B_2^2} \right) - \frac{\sqrt{A_3} p_1 Q_4}{Q_2^3} \left(\frac{p_1^2 Q_2^2}{A_3^2 B_2} - \frac{p_1^4 + 2p_1^2 Q_2^2 + 3Q_2^4}{A_3 B_2^2} - \frac{2Q_2^2}{(p_1^2 + Q_4^2)^2} + \frac{1}{p_1^2 + Q_4^2} \right) - \\
& \frac{p_1 Q_4 \sqrt{p_1^2 + Q_1^2 + Q_4^2}}{Q_1^3} \left(-\frac{2Q_1^2}{(p_1^2 + Q_4^2)^2} + \frac{1}{p_1^2 + Q_4^2} + \frac{p_1^2 Q_1^2}{(p_1^2 + Q_1^2)(p_1^2 + Q_1^2 + Q_4^2)^2} - \right. \\
& \left. \frac{p_1^4 + 2p_1^2 Q_1^2 + 3Q_1^4}{(p_1^2 + Q_1^2)^2 (p_1^2 + Q_1^2 + Q_4^2)} \right) (2(1 - \nu) + \nu);
\end{aligned}$$

$$\epsilon_{xy} = \frac{b_z c}{4K_1\pi} \left(\frac{-2c-3z}{A_1^{3/2}} + \frac{3p_1^2 z}{A_1^{5/2}} - \frac{3p_1^2 z}{A_3^{5/2}} + \frac{2c+3z}{A_3^{3/2}} \right) - \frac{b_z c}{4K_1\pi} \left(\frac{-2c-3z}{A_2^{3/2}} + \frac{3p_1^2 z}{A_2^{5/2}} - \frac{3p_1^2 z}{A_4^{5/2}} + \frac{2c+3z}{A_4^{3/2}} \right) +$$

$$\frac{b_z c p_1 v}{2K_1\pi} \left(\frac{1}{A_1^{3/2}} - \frac{1}{A_3^{3/2}} \right) - \frac{b_z c p_1 v}{2K_1\pi} \left(\frac{1}{A_2^{3/2}} - \frac{1}{A_4^{3/2}} \right);$$

$$\epsilon_{xz} = \frac{b_z c p_1^2 Q_3}{2A_2^{3/2} B_1 K_1 \pi} - \frac{b_z c p_1^2 Q_3}{2A_4^{3/2} B_2 K_1 \pi} - \frac{b_z c p_1^2 Q_4}{2A_1^{3/2} B_1 K_1 \pi} + \frac{b_z c p_1^2 Q_4}{2A_3^{3/2} B_2 K_1 \pi} - \frac{b_z c Q_3(Q_1^2 - p_1^2)}{2\sqrt{A_2} B_1^2 K_1 \pi} +$$

$$\frac{b_z c Q_4(Q_1^2 - p_1^2)}{2\sqrt{A_1} B_1^2 K_1 \pi} + \frac{b_z c Q_3(Q_2^2 - p_1^2)}{2\sqrt{A_4} B_2^2 K_1 \pi} - \frac{b_z c Q_4(Q_2^2 - p_1^2)}{2\sqrt{A_3} B_2^2 K_1 \pi} + \frac{3b_z c p_1^3 Q_3 z}{4A_2^{5/2} B_1 K_1 \pi} - \frac{3b_z c p_1^3 Q_3 z}{4A_4^{5/2} B_2 K_1 \pi} -$$

$$\frac{3b_z c p_1^3 Q_4 z}{4A_1^{5/2} B_1 K_1 \pi} + \frac{3b_z c p_1^3 Q_4 z}{4A_3^{5/2} B_2 K_1 \pi} - \frac{b_z c p_1 Q_3(p_1^2 p_3 + 3a^2(c+2z) - 6ax(c+2z) + 3x^2(c+2z))}{4A_2^{3/2} B_1^2 K_1 \pi} +$$

$$\frac{b_z c p_1 Q_4(p_1^2 p_3 + 3a^2(c+2z) - 6ax(c+2z) + 3x^2(c+2z))}{4A_1^{3/2} B_1^2 K_1 \pi} -$$

$$\frac{b_z c Q_3(-3a^4 + p_1^3 p_5 + 12a^3 x - 3x^4 + 6p_1 x^2 z + 12ax(x^2 - p_1 z) + 6a^2(-3x^2 + p_1 z))}{4\sqrt{A_2} B_1^3 K_1 \pi} +$$

$$\frac{b_z c Q_4(-3a^4 + p_1^3 p_5 + 12a^3 x - 3x^4 + 6p_1 x^2 z + 12ax(x^2 - p_1 z) + 6a^2(-3x^2 + p_1 z))}{4\sqrt{A_1} B_1^3 K_1 \pi} +$$

$$\frac{b_z c Q_3(-3a^4 + p_1^3 p_5 - 12a^3 x - 3x^4 + 6p_1 x^2 z + 6a^2(-3x^2 + p_1 z) + 12ax(-x^2 + p_1 z))}{4\sqrt{A_4} B_2^3 K_1 \pi} -$$

$$\frac{b_z c Q_4(-3a^4 + p_1^3 p_5 - 12a^3 x - 3x^4 + 6p_1 x^2 z + 6a^2(-3x^2 + p_1 z) + 12ax(-x^2 + p_1 z))}{4\sqrt{A_3} B_2^3 K_1 \pi} +$$

$$\frac{b_z c p_1 Q_3(3c^3 + 8c^2 z + 6Q_2^2 z + 2z^3 + c(3Q_2^2 + 7z^2))}{4A_4^{3/2} B_2^2 K_1 \pi} - \frac{b_z c p_1 Q_4(3c^3 + 8c^2 z + 6Q_2^2 z + 2z^3 + c(3Q_2^2 + 7z^2))}{4A_3^{3/2} B_2^2 K_1 \pi},$$

$$\epsilon_{yz} = -\frac{b_z c p_1^2 Q_1}{2C_1 K_1 \pi (C_1 + Q_1^2)^{3/2}} + \frac{b_z c p_1^2 Q_1}{2C_2 K_1 \pi (C_2 + Q_1^2)^{3/2}} - \frac{b_z c p_1^2 Q_2}{2A_4^{3/2} C_1 K_1 \pi} + \frac{b_z c p_1^2 Q_2}{2A_3^{3/2} C_2 K_1 \pi} +$$

$$\frac{b_z c Q_1(Q_3^2 - p_1^2)}{2C_1^2 K_1 \pi \sqrt{C_1 + Q_1^2}} + \frac{b_z c Q_2(Q_3^2 - p_1^2)}{2\sqrt{A_4} C_1^2 K_1 \pi} - \frac{b_z c Q_1(Q_4^2 - p_1^2)}{2C_2^2 K_1 \pi \sqrt{C_2 + Q_1^2}} - \frac{b_z c Q_2(Q_4^2 - p_1^2)}{2\sqrt{A_3} C_2^2 K_1 \pi} -$$

$$\frac{3b_z c p_1^3 Q_1 z}{4C_1 K_1 \pi (C_1 + Q_1^2)^{5/2}} + \frac{3b_z c p_1^3 Q_1 z}{4C_2 K_1 \pi (C_2 + Q_1^2)^{5/2}} - \frac{3b_z c p_1^3 Q_2 z}{4A_4^{5/2} C_1 K_1 \pi} + \frac{3b_z c p_1^3 Q_2 z}{4A_3^{5/2} C_2 K_1 \pi} -$$

$$\frac{b_z c p_1 Q_1(p_1^2 p_3 + 3b^2(c+2z) - 6by(c+2z) + 3y^2(c+2z))}{4C_2^2 K_1 \pi (C_2 + Q_1^2)^{3/2}} -$$

$$\frac{b_z c p_1 Q_2(p_1^2 p_3 + 3b^2(c+2z) - 6by(c+2z) + 3y^2(c+2z))}{4A_3^{3/2} C_2^2 K_1 \pi} -$$

$$\frac{b_z c Q_1(-3b^4 + p_1^3 p_5 + 12b^3 y - 3y^4 + 6p_1 y^2 z + 12by(y^2 - p_1 z) + 6b^2(-3y^2 + p_1 z))}{4C_2^3 K_1 \pi \sqrt{C_2 + Q_1^2}} -$$

$$\frac{b_z c Q_2(-3b^4 + p_1^3 p_5 + 12b^3 y - 3y^4 + 6p_1 y^2 z + 12by(y^2 - p_1 z) + 6b^2(-3y^2 + p_1 z))}{4\sqrt{A_3} C_2^3 K_1 \pi} +$$

$$\frac{b_z c Q_1(-3b^4 + p_1^3 p_5 - 12b^3 y - 3y^4 + 6p_1 y^2 z + 6b^2(-3y^2 + p_1 z) + 12by(-y^2 + p_1 z))}{4C_1^3 K_1 \pi \sqrt{C_1 + Q_1^2}} +$$

$$\frac{b_2 c Q 2(-3b^4 + p1^3 p5 - 12b^3 y - 3y^4 + 6p1 y^2 z + 6b^2(-3y^2 + p1 z) + 12b y(-y^2 + p1 z))}{4\sqrt{A} 4C1^3 K1 \pi} +$$

$$\frac{b_2 c p1 Q1(3c^3 + 8c^2 z + 6Q3^2 z + 2z^3 + c(3Q3^2 + 7z^2))}{4C1^2 K1 \pi (C1 + Q1^2)^{3/2}} + \frac{b_2 c p1 Q2(3c^3 + 8c^2 z + 6Q3^2 z + 2z^3 + c(3Q3^2 + 7z^2))}{4A4^{3/2} C1^2 K1 \pi},$$

$$p1 = zp + z = c + z;$$

$$p2 = z - zp = z - c;$$

$$p3 = 2z + 3zp = 2z + 3c;$$

$$p4 = 6z + 3zp = 6z + 3c;$$

$$p5 = z + 3zp = z + 3c;$$

$$p6 = 3z + 2zp = 3z + 2c;$$

$$p7 = -3z - 2zp = -3z - 2c;$$

$$p8 = -z^3 + 3zzp^2 + 2zp^3 = -z^3 + 3zc^2 + 2c^3;$$

$$p9 = 7z + 2zp = 7z + 2c;$$

$$p0 = 5z + 4zp = 5z + 4c;$$

$$A1 = p1^2 + (a - x)^2 + (b - y)^2;$$

$$A2 = p1^2 + (a - x)^2 + (b + y)^2;$$

$$A3 = p1^2 + (a + x)^2 + (b - y)^2;$$

$$A4 = p1^2 + (a + x)^2 + (b + y)^2;$$

$$B1 = p1^2 + (a - x)^2;$$

$$B2 = p1^2 + (a + x)^2;$$

$$C1 = p1^2 + (b + y)^2;$$

$$C2 = p1^2 + (b - y)^2;$$

$$K1 = -1 + v;$$

$$K2 = -1 + 2v;$$

$$K3 = -2 + v;$$

$$Q1 = a - x;$$

$$Q2 = a + x;$$

$$Q3 = b + y;$$

$$Q4 = -b + y;$$

REFERENCES

1. Meyers MA, Chawla KK. Mechanical Behavior of Materials. 2nd edition. University of Cambridge, UK; 2009.
2. Hirth JP, Lothe J. Theory of dislocations. 5th edition. Krieger Publishing Company, Malabar, Florida; 1982.
3. Hull D, Bacon DJ. Introduction to Dislocations. University of Liverpool, UK; 2011.
4. Weertman J, Weertman JR. Elementary Dislocation Theory. Oxford University Press, Oxford; 1992.
5. Kroupa F. Circular edge dislocation loop. Czechoslovak Journal of Physics B. 1960; 10:284–293.
6. Bullough R, Newman RC. The spacing of prismatic dislocation loops. Philosophical Magazine. 1960;5(57):921–926.
7. Keller JM. Unpublished; 1957.
8. Kröner E. Kontinuumstheorie Der Versetzungen Und Eigenspannungen. Springer-Verlag, Berlin; 1958.
9. Kroupa F. Interaction between prismatic dislocation loops and straight dislocations 1. Philosophical Magazine. 1962;7(77):783–801.
10. Marcinkowski MJ, Sree Harsha KS. Properties of finite circular dislocation glide loops. Journal of Applied Physics. 1968;39(3):1775–1783.

11. Khraishi TA, Hirth JP, Zbib HM, Khaleel MA. The displacement, and strain-stress fields of a general circular Volterra dislocation loop. *International Journal of Engineering Science*. 2000;38(3):251–266.
12. Khraishi TA, Zbib HM, Hirth JP, De La Rubia TD. The stress field of a general circular Volterra dislocation loop: analytical and numerical approaches. *Philosophical Magazine Letters*. 2000;80(2):95–105.
13. Khraishi TA, Zbib HM. The displacement field of a rectangular Volterra dislocation loop. *Philosophical Magazine Letters*. 2002;82(5):265–277.
14. Khraishi TA, Zbib HM, De La Rubia TD. The treatment of traction-free boundary condition in three-dimensional dislocation dynamics using generalized image stress analysis. *Materials Science and Engineering A*. 2001;309-310:283-87.
15. Khraishi TA, Zbib HM. Free surface effects in 3d dislocation dynamics: Formulation and Modeling. *Journal of Engineering Materials and Technology (JEMT)*. 2002;124(3):342-51.
16. Yan L, Khraishi TA, Shen Y-L, Horstemeyer MF. A distributed-dislocation method for treating free-surface image stresses in 3D dislocation dynamics simulations. *Modelling and Simulation in Materials Science and Engineering*. 2004;12(4):289-301.
17. Siddique AB, Khraishi T. Numerical methodology for treating static and dynamic dislocation problems near a free surface. *Journal of Physics Communications*. 2020;4(5):055005.
DOI:10.1088/2399-6528/ab8ff9.
18. Siddique AB, Khraishi T. A mesh-independent brute-force approach for traction-free corrections in dislocation problems. *Modeling and Numerical Simulation of Material Science*. 2021;11(1):1-18, DOI: 10.4236/mnsms.2021.111001.
19. Siddique AB, Khraishi T. Screw dislocations around voids of any shape: A Generalized Numerical approach. *Forces in Mechanics*. 2021; 3:100014.
DOI: <https://doi.org/10.1016/j.finmec.2021.100014>.

20. Khraishi TA, Zbib HM. Dislocation dynamics simulations of the interaction between a short rigid fiber and a glide circular dislocation pile-up. *Computational Materials Science*. 2002;24(3):310-22.
21. De La Rubia TD, Zbib HM, Khraishi TA, Wirth BD, Victoria M, Caturla MJ. Multiscale Modelling of Plastic Flow Localization in Irradiated Materials. *Nature*. 2000;406(6798):871-74.
22. Khraishi TA, Zbib HM, De La Rubia TD, Victoria M. Modeling of irradiation-induced hardening in metals using dislocation dynamics. *Philosophical Magazine Letters*. 2001;81(9):583-93.
23. Khraishi TA, Zbib HM, De La Rubia TD, Victoria M. Localized deformation and hardening in irradiated metals: Three-dimensional discrete dislocation dynamics simulations. *Metallurgical and Materials Transactions B*. 2002;33(2):285-96.
24. Yoffe, EH. A dislocation at a free surface. *The Philosophical Magazine*. 1961;69(6):1147-55.
25. Groves PP, Bacon DJ. The dislocation loop near a free surface. *Philosophical Magazine*. 1970;22(175):83-91.
26. Maurissen Y, Capella L. Stress field of a dislocation segment parallel to a free surface. *Philosophical Magazine*. 1974;29(5):1227-29.
27. Maurissen Y, Capella L. Stress field of a dislocation segment perpendicular to a free surface. *Philosophical Magazine*. 1974;30(3):679-83.
28. Comninou M, Dundurs J. The angular dislocation in a half space. *Journal of Elasticity*. 1975; 5:203-16.
29. Gosling TJ, Willis JR. A line-integral representation for the stresses due to an arbitrary dislocation in an isotropic half-space. *Journal of Mechanics and Physics of Solids*. 1994;42(8):1199-1221.
30. Jing P, Khraishi TA. The elastic fields of sub-surface dislocation loops: a comparison between analytical continuum-theory solutions and atomistic calculations. *Int. J. Theoretical and Applied Multiscale Mechanics*. 2009;1(1):71-85.

31. Li L, Khraishi TA. The stress field of a rectangular dislocation loop in an infinite medium: analytical solution with verification. *Journal of Materials Science Research and Reviews*. 2021;7(1):47-59.
Available: <https://www.journaljmsrr.com/index.php/JMSRR/article/view/30172>
32. Khraishi TA, Shen, YL. *Introductory continuum mechanics with applications to elasticity*. University Readers/Cognella, San Diego, California; 2011.

